DEPARTAMENTO DE CIÊNCIAS DA VIDA

FACULDADE DE CIÊNCIAS E TECNOLOGIA
UNIVERSIDADE DE COIMBRA

Contribution of Proteolytic Pathways in the development of Age-related Macular Degeneration (AMD)

Dissertação apresentada à Universidade de Coimbra para cumprimento dos requisitos necessários à obtenção do grau de Mestre em Bioquímica, realizada sob a orientação científica do Professor Doutor Henrique Girão (Universidade de Coimbra) e da Professora Doutora Paula Veríssimo (Universidade de Coimbra)

Lídia Maria Jordão Grilo

2014

group of ubiquitin-dependent proteolysis and intercellular communication

This work was developed in the following institution:

Group of ubiquitin-dependent proteolysis and intercellular communication,
Institute for Biomedical Imaging and Life Sciences, Faculty of Medicine,
University of Coimbra, Coimbra

Agradecimentos

Chegada ao final de mais uma etapa da minha vida, gostaria de agradecer todos os que me acompanharam neste percurso. Sem vocês, este trabalho não teria sido possível.

Em primeiro lugar, quero agradecer ao Doutor Henrique Girão por me ter dado a oportunidade de trabalhar no seu laboratório. Agradeço a confiança que em mim depositou e a liberdade que me deu na execução do trabalho prático.

Em segundo lugar, quero agradecer à Doutora Rosa Fernandes. Estou profundamente grata por todo o seu apoio ao longo deste trabalho, quer na coordenação do trabalho prático, como na escrita da tese. Agradeço a disponibilidade, paciência e compreensão que sempre teve comigo, apesar dos meus erros e limitações.

Do mesmo modo, quero deixar o meu agradecimento a todo o grupo G(U)IC pela assistência fornecida e por todo o conhecimento obtido. Agradeço em especial à Ana Soares por me ter guiado no início do meu percurso no laboratório, bem como por estar sempre lá para ajudar. Um especial obrigado à Vanessa, pela companhia e pelas conversas que tivemos.

Quero também deixar umas palavras de agradecimento à Professora Doutora Paula Veríssimo, por ter aceitado ser minha orientadora interna. Agradeço a competência, dedicação e apoio que sempre teve para com os alunos de Bioquímica.

Um grande obrigado a todos os meus amigos, que me proporcionaram os melhores momentos nestes cinco anos de faculdade. Agradeço à Filipa, ao Amarante, à MJ, à Raquel e à Sofia pela amizade. Por todos os jantares e cafezinhos depois de um dia longo no laboratório, por me ensinarem a descontrair e viver a vida. Sem vocês, Coimbra não teria metade da piada. À Sara e à Raquel Fernandes, pela amizade inabalável, mesmo quando estamos distantes. Obrigada pelas longas conversas e pelos momentos bem passados. Às minhas colegas da RUP III, por todo o carinho e compreensão. Agradeço a todos os que comigo partilharam as experiências memoráveis que vivi nesta maravilhosa cidade, que levo comigo pra vida.

Por fim, um obrigado de coração à minha família. Aos meus pais, que apesar de alguns sacrifícios, me encorajaram e tudo fizeram para que eu pudesse continuar os meus estudos. Aos meus irmãos, por todas as brincadeiras e disparates. Aos meus avós, apesar de fisicamente ausentes, sinto que me acompanharam e acompanharão toda a minha vida. Sempre.

Muito Obrigada!

Index

Abbreviations

Akt/PKB	Protein kinase B
AGEs	Advanced-glycation end products
AMD	Age-related macular degeneration
AMP	Adenosine 5'-monophosphate
AMPK	AMP-activated protein kinase
ANOVA	Analysis of variance
ARNT	Aryl hydrocarbon receptor nuclear translocator
ARPE-19	Spontaneously arising human retinal pigment epithelium cell line
Atg	Autophagy-related gene
ATP	Adenosise-5'-triphosphate
BafA1	Bafilomycin A1
BRB	Blood-retinal barrier
BrMb	Bruch's membrane
BSA	Bovine serum albumin
CatD	Cathepsin D
CC	Choriocapillaris
CD63	CD63 antigen
CD68	CD68 antigen
CDKN1A	Cyclin-dependent kinase inhibitor 1A
CH	Choroid
CHX	Cycloheximide
CIP1	CDK-interacting protein 1
CMA	Chaperone-mediated autophagy
CNV	Choroidal neovascularization
CP	Core particle
CQ	Chloroquine
DAPI	4',6-diamidino-2-phenylindole
DMEM-F12	Dulbecco's Modified Eagle's Medium/ Nutrient Mixture F-12 Ham
DMSO	Dimethyl sulfoxide
DNA	Deoxyribonucleic acid
E1	Ubiquitin-activating enzyme
E2	Ubiquitin-conjugating enzyme

E3	Ubiquitin protein ligase
ECL	Enhanced chemiluminescence
EDTA	Ethylenediaminetetraacetic acid
FBS	Fetal bovine serum
FGF	Fibroblast growth factor
FIP200	Focal adhesion kinase interacting protein of 200 kD
FKBP12	FK-binding protein 12
FRB	FKBP12-Rapamycin Binding
GAPDH	Glyceraldehyde 3-phosphate dehydrogenase
GCL	Ganglion cell layer
GFP	Green fluorescent protein
H2O2	Hydrogen peroxide
HCl	Hydrochloric acid
HCQ	Hydroxychloroquine
HIF-1	Hypoxia-Inducible Factor 1
HIF-1α	Hypoxia-Inducible Factor 1 alpha
HRP	Horseradish peroxidase
HSPA8/HSC70	Heat shock 70 kDa protein 8
IAM	Iodoacetamide
IGF-I	Insulin-like growth factor I
IgG	Immunoglobulin G
IL-8	Interleukin-8
ILVs	Intraluminal vesicles INL Inner nuclear layer
IPL	Inner plexiform layer
LAMP2	Lysosomal-associated membrane protein 2
LAMP2A	Lysosomal-associated membrane protein 2A
LC3	Light chain of the microtubule- associated protein 1
MAPK	Mitogen-activated protein kinase
MBVs	Multivesicular bodies
MCP-1	Monocyte chemotactic protein-1
MG-132	Carbobenzoxy-L-Leucil-Leucil-L-Leucinal
mTOR	mammalian target of rapamycin
mTORC1	mammalian target of rapamycin complex 1
mTORC2	mammalian target of rapamycin complex 2

MTT	3-(4,5-dimethylthiazol-2-yl)-2,5-diphenyltetrazolium bromide
NF-κB	Nuclear factor κB
ONL	Outer nuclear layer
OPL	Outer plexiform layer
OS	Outer segments
PAS	Pre-autophagosomal structures
PBS	Phosphate-buffered saline
PDPK1	3-phosphoinositide dependent protein kinase-1
PEDF	Pigmented epithelium derived factor
PI3K	Phosphatidylinositol-3-kinase
PMSF	Phenylmethylsulfonyl fluoride
POS	Photoreceptor outer segments
PUFA	Polyunsaturated fatty acids
RIPA	Radioimmunoprecipitation assay buffer
RNA	Ribonucleic acid
ROS	Reactive oxygen species
RP	Regulatory particle
RPE	Retinal pigment epithelium
SDS	Sodium dodecyl sulfate
SDS-PAGE	Sodium dodecyl sulfate-polyacrylamide gel electrophoresis
SEM	Standard errors of the mean
SQSTM1	Sequestosome 1
TBS	Tris-buffered saline
TGF-β	Transforming growth factor β
ULK1	Uncoordinated 51-like kinase 1
UPP	Ubiquitin-proteasome pathway
UPS	Ubiquitin-proteasome system
VEGF	Vascular endothelial growth factor
VEGFR	Vascular endothelial growth factor receptor
VHL	von Hippel-Lindau
Vps34	Vacuolar protein sorting 34

List of Figures and Tables

FIGURE INDEX

TABLE INDEX

CHAPTER 2 – MATERIALS and METHODS 31

Resumo

A degenerescência macular relacionada com a idade (DMRI) é a principal causa de cegueira na população idosa no mundo ocidental. Uma das principais características da DMRI é a formação de drusen, agregados de proteínas danificadas provocados por uma digestão incompleta dos segmentos externos dos fotorreceptores. Nas últimas décadas tem sido feito um grande esforço de forma a compreender os mecanismos que levam à formação dos drusen e o papel do epitélio pigmentado da retina (EPR) na sua formação; contudo, os processos que levam à formação dos drusen continuam desconhecidos.

Os resultados obtidos anteriormente sugerem uma relação entre a autofagia e a via ubiquitin proteassoma (VUP). As vias proteolíticas estão interligadas, de modo a assegurar a homeostase celular, e parecem ter um papel importante no desenvolvimento da DMRI. Estudos indicam uma diminuição na VUP na DMRI, provavelmente induzida pelo stress oxidativo. Apesar da actividade autofágica basal das células diminuir com a idade, estudos recentes apontam para um aumento no fluxo autofágico nas células do EPR envelhecidas. A nossa hipótese é de que na DMRI proteínas danificadas não são degradadas pela VUP, sendo exocitadas e agregando-se, formando os drusen. Este trabalho pretende clarificar os mecanismos moleculares e principais agentes ligados à disfunção do EPR, bem como avaliar a relação entre a VUP e a autofagia na DMRI.

Numa primeira abordagem, o proteassoma foi cronicamente inibido ao adicionar MG-132 a células ARPE-19, uma linha celular usada como modelo para o EPR humano. O tratamento com 0.20μM MG-132 durante 48h, apesar de não ter induzido citotoxicidade, levou à inibição do proteassoma, como concluído pela acumulação de conjugados de ubiquitina e diminuição da degradação da CDKN1A/p21, um substrato do proteassoma.

O efeito da inibição do proteassoma na macroautofagia também foi investigado. Células do EPR incubadas com o inibidor do proteassoma apresentaram actividade autofágica aumentada, verificada pelo aumento nos níveis proteicos de LC3-II. Esta observação sugere uma autofagia induzida pelo MG-132, que foi confirmada pelo aumento do fluxo autofágico, avaliado pelos valores de LC3-II na presença e na ausência de BafA1, um inibidor de proteases lisossomais. Além disso, os níveis protéicos de HIF-1α também foram analisados, uma vez que o nosso grupo recentemente demonstrou que o HIF-1α pode ser degradado por autofagia mediada por chaperonas (AMC). Foram encontrados níveis proteicos de HIF-1α reduzidos nas células do EPR sob inibição proteasomal, mais uma prova de que MG-132 induz autofagia. Curiosamente, apesar de induzir acumulação da LC3-II, o MG-132 aumenta o substrato autofágico SQSTM1/p62 nas células do EPR, como verificado por Western blotting e imunofluorescência. Os níveis proteicos de SQSTM1/p62 foram restaurados com a adição de CHX às células, indicando que o aumento de SQSTM1/p62 foi causado por estimulação da síntese proteica. A actividade lisossomal das células do EPR incubadas com MG-132 foi

investigada, através da medição dos níveis proteicos de CatD, a protéase lisossomal mais abundante. Após exposição a 0.20μM MG-132, os níveis de catD tanto nas formas percursoras como na madura estão aumentados, o que sugere um esforço da célula para formar catD activa e assim aumentar a actividade lisossomal. Estes dados indicam que a inibição do proteassoma com MG-132 estimula a autofagia nas células do EPR.

Por imunocitoquímica, verificou-se que o MG-132 induz um aumento na imunoreactividade para proteínas ubiquitinadas, principalmente na zona nuclear/ perinuclear. Com MG-132, SQSTM1/p62 e proteínas ubiquitinadas apresentam uma co-localização quase completa, o que sugere que a SQSTM1/p62 liga-se às proteínas ubiquitinadas, formando agressomas como descrito para várias doenças relacionadas com a idade. Com o proteassoma inibido SQSTM1/p62 actua como um adaptador para as proteínas ubiquitinadas, entregando-as aos lisossomas para degradação autofágica.

Na DMRI, em simultâneo com inibição do proteassoma ocorre a activação da autofagia nas células do EPR. A autofagia foi estimulada por starvation ou por rapamicina, um inhibidor do mTOR. Através da LC3-II e da SQSTM1/p62, verificámos que 6h é o tempo ao qual a autophagy modelada pela starvation é máxima. Células do EPR tratadas com os activadores de autofagia apresentaram fluxo autofágico aumentado, uma vez que tanto a starvation como a rapamicina aumentaram a LC3-II e diminuíram a acumulação de SQSTM1/p62 induzida pela BafA1.

De forma a estabelecer um modelo para a AMD, células ARPE-19 foram expostas simultaneamente a MG-132 e um dos activadores da autofagia. Starvation foi o indutor mais eficaz. Tratamento concomitante das células do EPR com MG-132 e starvation estimulou fortemente a autofagia. Os resultados sugerem que, apesar de ser um substrato autofágico, SQSTM1/p62 não é degradada quando o proteassoma está inibido, mesmo quando temos em paralelo autofagia estimulada.

Em suma, nós propomos um modelo in vitro para a DMRI, em que a ligação entre as vias proteolíticas é analisada. Na DMRI, a diminuição da actividade proteolítica resulta na acumulação de proteínas poliubiquitinadas, em agressomas. A inibição do proteassoma induz autofagia, através da SQSTM1/p62, que entrega as proteínas poliubiquitinadas para degradação autofágica no lisossoma. Porém, com o tempo o lisossoma atinge a sua capacidade máxima e acaba por não degradar todas as proteínas danificadas. A nossa hipótese é de que o EPR envelhecido liberta as proteínas intracelulares via exossomas, o que contribui para a formação e acumulação dos drusen. Estudos futuros são necessários a fim de percebermos os mecanismos por detrás da libertação dos exossomas e acumulação dos drusen, em particular quando o proteassoma está inibido e a autofagia estimulada, como usado neste trabalho.

Palavras-chave: Degenerescência macular relacionada com a idade, via ubiquitin proteassoma, autofagia, SQSTM1/p62.

Abstract

Age-related macular degeneration (AMD) is the main cause of blindness in the western world in elderly population. One of the principal features of AMD is the formation of drusen, damaged protein aggregates caused by incomplete photoreceptor outer segments digestion. Over the past decades a significant effort has been made to understand the mechanisms underlying drusen biogenesis and the involvement of RPE in their formation; however, the processes that lead to drusens formation remain unknown.

Accumulated evidence suggests a crosstalk between autophagy and the ubiquitin proteasome pathway (UPP). The proteolytic pathways are not compartmentalized, working together to ensure the cell homeostasis. Proteolytic pathways may have a key role in the development of AMD. The evidence clearly indicates an impairment of UPP in AMD, probably induced by oxidative stress. Although basal autophagic activity of living cells decreases with age, recent studies reported enhanced autophagy flux in aged RPE cells. We hypothesize that in AMD the misfolded/damaged proteins are not degraded by UPP, so they are exocytosed and aggregate, forming the drusen. This study aims to clarify the molecular mechanisms and key players intrinsically linked to RPE dysfunction and to evaluate the crosstalk between UPP and autophagy in AMD.

As a first approach, chronic proteasome inhibition was performed by adding MG-132 to ARPE-19 cells, a cell line commonly used as human RPE model. Treatment with 0.20μM MG-132 for 48h did not induce any significant cytotoxic effect and was able to successfully inhibit the proteasome, as conclude by accumulation of ubiquitin conjugates and impaired degradation of CDKN1A/p21, a known proteasome substrate.

The effect of proteasomal impairment in macroautophagy was also investigated. We found enhanced autophagy activity in RPE cells incubated with the proteasome inhibitor, verified by the increase in LC3-II protein levels. This finding suggests an MG-132-induced autophagy, which was confirmed by the enhanced autophagic flux, assessed by measuring LC3-II in the presence and absence of BafA1, a lysosomal protease inhibitor. Moreover, the HIF-1α protein levels were also analyzed, since recently our group shown that HIF-1α can be degraded by CMA. Accordingly, we found reduced HIF-1α protein levels in RPE cells due proteasomal inhibition, further evidence of MG-132-induced autophagy. Interestingly, although the MG-132 induced accumulation of LC3-II, we found that it significantly increased autophagy-specific substrate SQSTM1/p62 in RPE cells in a concentration-dependent manner, as verified by both Western blotting and immunofluorescence. SQSTM1/p62 protein levels were restored when CHX was added to the cells, indicating that this increase in SQSTM1/p62 protein content was caused by an enhanced protein synthesis. The lysosomal activity of RPE cells incubated with MG-132 was also investigated, by measuring the protein levels of CatD, the most abundant lysosomal protease. We found increased levels of catD at both precursors and mature forms after exposure to 0.20μM of MG-132, suggesting an effort of the cell to enhance

active catD formation and thus improve lysosomal activity. Taken together, this data strongly indicate that MG-132-induced proteasomal inhibition stimulates autophagy lysosomal pathway in RPE cells.

By Immunocytochemistry, we observed that MG-132 induced an increased immunoreactivity for ubiquitinated proteins mainly in the nuclear/perinuclear compartment. With MG-132, SQSTM1/p62 and ubiquitinated proteins co-localize almost completely and the immunoreactive puncta were very intense, suggesting that SQSTM1/p62 binds to ubiquitinated proteins, constituting SQSTM1-ubiquitin aggresomes as described to several age-related diseases. Our data indicate that upon proteasomal inhibition SQSTM1/p62 acts as a cargo adaptor for ubiquitinated proteins, shuttling them to lysosomes for autophagocytic degradation.

In AMD, in parallel with proteasome impairment occurs the activation of autophagy in RPE cells. Autophagy was stimulated by starvation or with rapamycin, an mTOR inhibitor. By LC3-II and SQSTM1/p62 protein levels, we verify that 6h was the time point in which RPE cells exhibits maximal serum starvation-triggered autophagy activation. RPE cells treated with autophagy activators exhibited an increase in the autophagic flux, as both starvation and rapamycin increased LC3-II protein content and decreased the BafA1-induced SQSTM1/p62 accumulation.

In order to establish an accurate cell model of AMD, ARPE-19 cells were exposed simultaneously to both MG-132 and one of the tested autophagy inducers. Starvation was the most effective autophagy inducer. Concomitant treatment of RPE cells with MG-132 and starvation strongly stimulated autophagy. Our data suggest that although SQSTM1/p62 is an autophagic substrate, this protein is not degraded upon proteasome inhibition, even when autophagy is stimulated.

Overall, we proposed an in vitro model for AMD, in which the crosstalk between the two major proteolytic pathways was analyzed. In AMD, impairment of proteasomal activity results in accumulated polyubiquitinated proteins in SQSTM1/p62-ubiquitin aggresomes. Proteasomal inhibition induces autophagy activation, through the action of SQSTM1/p62, which triggers polyubiquitinated proteins to autophagy clearance in the lysosome. However, with time lysosome becomes overloaded and thus damaged proteins cannot be degraded. We hypothesize that aged RPE releases intracellular proteins via exosomes and, therefore, this event contributes to formation and accumulation of drusen in AMD. Further studies investigating the mechanisms underlying exosomes release and accumulation of drusen, in particular in conditions of proteasome inhibition and autophagy activation that were used in this work, should aim at clarifying this issue.

Key words: Age-related macular degeneration, ubiquitin-proteasome pathway, autophagy, SQSTM1/p62

CHAPTER 1

INTRODUCTION and AIMS

1. The human retina

The ocular globe is constituted by six muscles involved in the ocular movements and three concentric layers working together to provide vision, nutrition and protection to the eye.

The exterior layer is constituted by the cornea and sclera. The medium or vascular layer is formed by the iris, choroid, corium and uvea. The interior layer is composed by the retina (Figure 1.1) (Parier and Soubrane, 2008, Bhutto and Lutty, 2012).

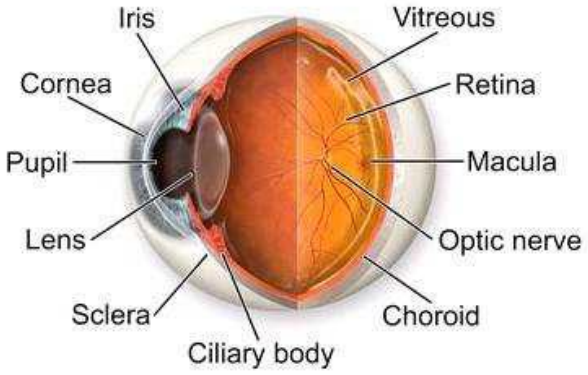

Figure 1.1 – The structure of human eye. From http://emeraldeye.com/images/illustrations/eye.jpg

The retina is the component of the eye responsible for image formation. It converts the visual image to electric impulses which are sent to the brain via the optic nerve. The retinal supply and oxygenation are sparse compared with the rate of oxygen consumption. Phototransduction and neural signaling are energy-consuming processes. The anatomy of the human retina assure high transparency and photoreceptor density (Bhutto and Lutty, 2012; Handa, 2012).

The human retina is approximately 0.2 mm thick, and has an area of approximately 1100 mm^2. Each retina possesses about 200 million neurons. The only area of the retina that is "blind" as it lacks photoreceptors is the optic disc, where neuronal cells merge to form the optic nerve. Temporal to the optic disc is the macula, the central posterior portion of the retina. The macula has the highest concentration of photoreceptors, which facilitate central vision and provides high-resolution visual acuity (Chopdar, Chakravarthy and Verma, 2003; Jager, Mieler and Miller, 2008). It has about 1.5mm of diameter and is composed by two or more layers of ganglion cells. In the center of the macula lays the fovea, a depression with high concentration of cone cells, responsible for the central vision (Chopdar, Chakravarthy and Verma, 2003).

The whole retina is frequently described as having ten layers, constituted of three major types of cells: neurons, glial cells and blood vessels. The majority of these cell types are affected to some degree in many retinal diseases including age-related macular degeneration (AMD). Retina is primarily a neuronal tissue. The glial cells of the retina, Müller cells and astrocytes, serve as support cells for the neurons and blood vessels.

Although its multilayered structure, the retina can be functionally divided in two parts: the neuronal retina, composed by the photoreceptors (cones and rods) and their neuronal connections, is responsible for the phototransduction process; the retinal pigment epithelium (RPE) and its basal lamina known as Bruch's membrane (BrMb) maintain the integrity between retina and choroid (Figure 1.2) (Chopdar, Chakravarthy and Verma, 2003; Rattner and Nathans, 2006).

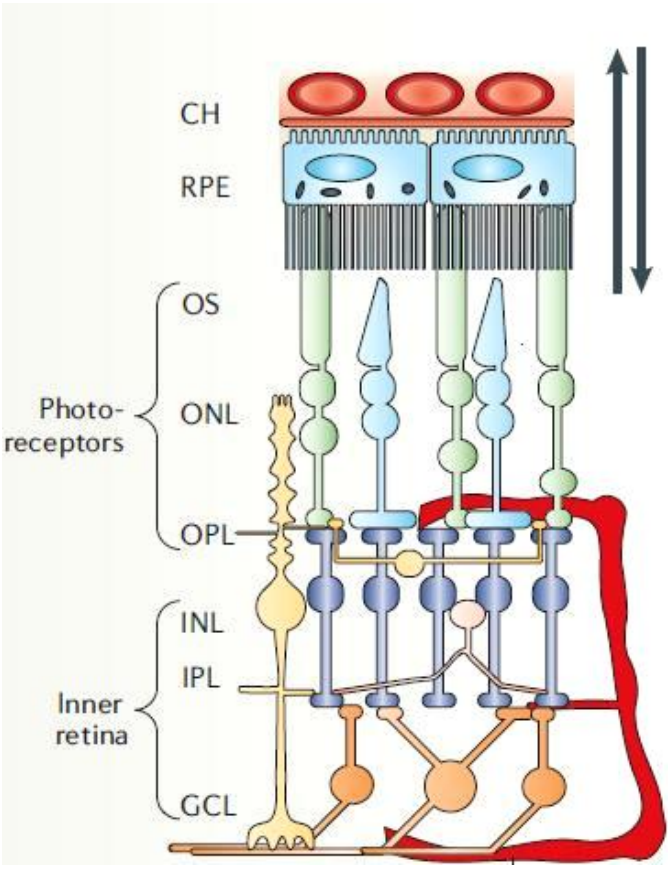

Figure 1.2 – Schematic diagram of the retina and choroid, showing the retinal layers. The choroidal vasculature is at the top and the inner retina is at the bottom. The vasculature of the inner retina is shown on the lower right. Arrows indicate the local diffusion of oxygen, nutrients and waste products between choroidal vasculature and the outer retina. CH, choroid; GCL, ganglion cell layer; INL, inner nuclear layer; IPL, inner plexiform layer; ONL, outer nuclear layer; OPL, outer plexiform layer; OS, outer segments; RPE, retinal pigment epithelium. Adapted from Rattner and Nathans, 2006.

1.1. Photoreceptor cells

The photoreceptors are neurons located in posterior retina which are responsible of phototransduction, a process by which light is converted in electrical signals that stimulate the neural impulse transmission to the brain through alterations in the membrane potential.

Histologically, the photoreceptors are classified into two types: cones and rods. The cones are present predominantly in the foveal region, whereas the rods are more common at the periphery of the retina. Rods are responsible for sensing motion, contrast and brightness, while cones are necessary for color vision, fine detail perception and spatial resolution. In humans there are three types of cones: red, green and blue cones, according with their response to different wavelengths (Bhutto and Lutty, 2012).

The photoreceptor cells are the primary neurons in the visual pathway. They differentiate longitudinally into two major divisions that extend from their cell body: the inner and outer segments. The inner segment contains the metabolic apparatus, namely a high level of mitochondrias needed to produce energy, since photoreceptors are cells metabolically very active. Photoreceptors consume more oxygen per gram of tissue than any other cell of human body and their oxygen levels are approximately zero in the absence of light (Wangsa-Wirawan and Linsenmeier, 2003). In its turn, the outer segment's major function is the conversion of light into neuroelectrical energy (Young, 1967).

In order to maintain the photoreceptor excitability, the outer segments are shed from the photoreceptors, allowing a constant renewal of photoreceptor outer segments (POS) (Young, 1967; Strauss, 2005; Bhutto and Lutty, 2012; Handa, 2012).

1.2. The retinal pigment epithelium (RPE)

The RPE is a monolayer of pigmented cells and forms part of the blood-retinal barrier (BRB) (Burke and Hjelmeland, 2005; Rattner and Nathans, 2006; Strauss, 2005). The apical membrane of the RPE faces the photoreceptor outer segments, whereas its basolateral membrane faces BrMb, a semi-permeable exchange barrier that separates the RPE from the choroid (Strauss, 2005). RPE cells receive their name from the melanin pigment granules (melanosomes) located in the apical cytoplasm (Burke and Hjelmeland,

2005). These pigments are responsible for absorbing the light focused by the lens in the retina (Rattner and Nathans, 2006; Handa, 2012; Strauss, 2005).

In fact, together the RPE and photoreceptors form a functional unit. Mutations in genes that are expressed in the RPE, such as MerTK or RPE65, can lead to photoreceptor degeneration (Gu et al., 1997; Thompson et al., 2002). On the other hand, mutations in genes expressed in photoreceptors, such as ABCR, can lead to degenerations of the RPE (Strauss, 2005).

In addition to supporting normal photoreceptor action, the RPE is essential for visual function. The RPE transports ions, water, and metabolic end products from the subretinal space to the blood and takes up nutrients such as glucose, retinol and fatty acids omega-3 from the blood, providing to POS the nutrients required to maintain their function (Ambati and Fowler, 2012; Strauss, 2005).

Another RPE function in the maintenance of photoreceptor excitability is the phagocytosis of shed photoreceptor outer segments (Strauss, 2005). Photoreceptors are exposed to intense levels of light. This leads to accumulation of photo-damaged proteins and lipids. To maintain the photoreceptor excitability, the POS undergo a constant renewal process. The POS are digested daily by the RPE and essential substances, such as retinal, are recycled and returned to photoreceptors to rebuild light-sensitive outer segments from the base of the photoreceptors (Bhutto and Lutty, 2012; Rattner and Nathans, 2006).

The RPE also plays an important role in the visual cycle, by participating in the light-dependent cycling and reisomerization of retinal (the vitamin A derivative that serves as the chromophore for the visual pigments). Photoreceptors are unable to reisomerize all-*trans*-retinal, formed after photon absorption, back into 11-*cis*-retinal. Thus retinal is transported to the RPE, reisomerized to 11-*cis*retinal and transported back to photoreceptors. This process is known as the visual cycle of retinal (Rattner and Nathans, 2006; Strauss, 2005).

In addition to these functions, the RPE is able to produce and to secrete a variety of growth factors, as fibroblastic (FGF-1, FGF-2 and FGF-5) and transforming growth factor beta (TGF-β) (Dunn et al., 1998; Matsumoto et al., 1994; Sternfeld et al., 1989; Tanihara et al., 1993 ; Bhutto and Lutty, 2012), as well as insulin-like growth factor I (IGF-I) (Martin, Yee and Feldman, 1992), vascular endothelial growth factor (VEGF) (Adamis et al., 1993), the pigmented epithelium derived factor (PEDF) (Streilein et al., 2002) and some interleukins (Streilein et al., 2002; Bhutto and Lutty, 2012).

Altogether, RPE cells perform a variety of complex functions in the retina. Therefore, it is not surprising that deregulation of the RPE has a critical impact on retinal function and may lead to loss of visual function and blindness.

1.3. Bruch's membrane (BrMb)

The BrMb is a thin connective tissue layer located between the RPE and the choriocapillaris. It is an elastin- and collagen-rich extracellular matrix with a penta-laminar structure. The main components of BrMb are collagens type I, II, IV, V and VI, fibronectin and laminin (Bhutto and Lutty, 2012).

BrMb principal role is to functions as a physical as well as biochemical barrier. It regulates the reciprocal diffusion of biomolecules, minerals, antioxidants and serum constituents between the choroid and the RPE (Bhutto and Lutty, 2012). Moreover, this membrane provides physical support for RPE cell adhesion (Del Priore et al., 2002) and a surface for migration and differentiation of RPE cells (Gong et al., 2008), as well as a preponderant function in wound healing (Bhutto and Lutty, 2012; Tezel et al., 2004).

The BrMb is unique to each human individual. Any alteration in the structure or composition of this membrane influences its diffusion properties and, ultimately, the function of the RPE and outer retina. Accumulating evidence suggests that the molecular, structural, and functional properties of BrMb are dependent on age, genetics, environmental factors, retinal location, and disease state (Bhutto and Lutty, 2012).

1.4. Choriocapillaris (CC)

Posterior to BrMB lies the choriocapillaris (CC), the capillary component of the choroidal vasculature. Whereas retinal vasculature supplies oxygen to the inner retina, the choroidal vasculature supplies oxygen to outer retina. The CC is composed by a single layer restricted to the inner portion of the choroid with feeding arterioles and draining venules entering the capillary plexus from below (Handa, 2012).

CC provides nutrients to RPE cells, so they can be metabolically active. The nutrients are transported by the CC, diffuse through the BrMb and are delivered to the RPE. RPE cells then are responsible for transporting nutrients into the photoreceptors from the CC and also the removal of waste from the photoreceptors by either recycling it, completely degrading or exocytosing the remains for CC to remove from the retina.

Photoreceptors/RPE/BrMB/CC form an active complex, being each component directly dependent of the others and any alterations in one component will influence the whole complex (Figure 1.3) (Bhutto and Lutty, 2012; Rattner and Nathans, 2006).

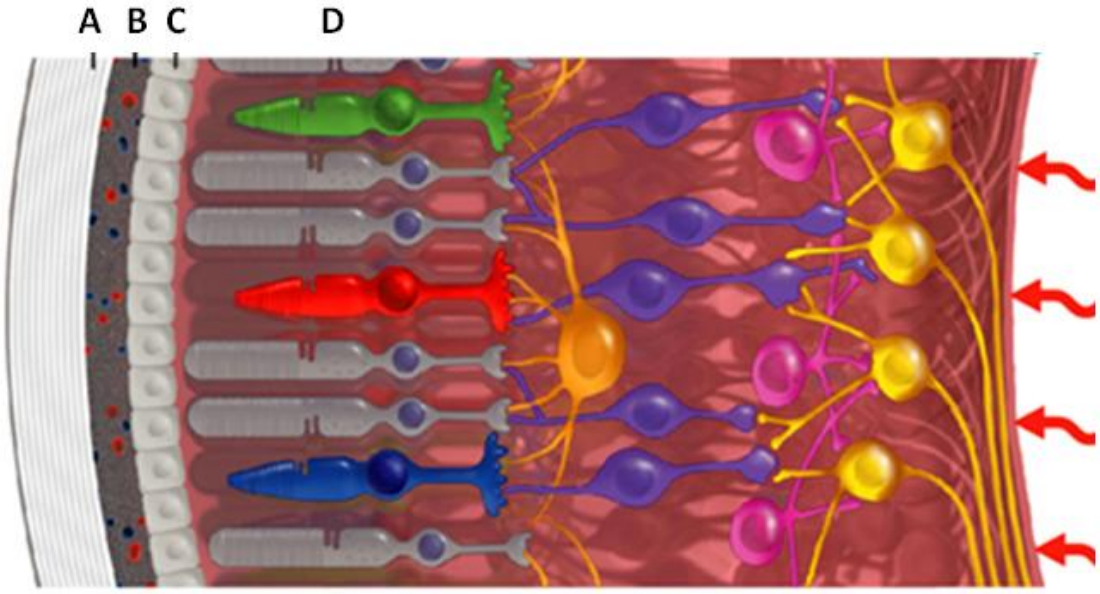

Figure 1.3 – Schematic representation of the Photoreceptors/RPE/BrMB/CC complex. A human retinal transversal cross section showing the photoreceptors/RPE/BrMB/CC complex and the major cell types**. A**- CC; **B**- BrMb; **C**- RPE; **D**- Photoreceptors. Adapted from http://www2.ibb.unesp.br/Museu_Escola/2_qualidade_vida_humana.html

2. Age-related macular degeneration

Age-related macular degeneration (AMD) is the leading cause of blindness among older adults in industrialized countries and its prevalence is rising as a consequence of increasing longevity (Rattner and Nathans, 2006).

Firstly described in 1885 by Otto Haab, this chronic disease is characterized by progressive changes that occur in the pigmented, neural and vascular layers of the macula, the central region of the retina bearing the highest concentration of photoreceptors. Accordingly, AMD can lead to severe impairment or loss of central vision (Ambati and Fowler, 2012).

It is estimated that AMD affects 10 millions in United States (Friedman et al., 2004), and its prevalence increases drastically with age, rising from 2% in people with 40 years old to 25% in people with the double of age (Friedman et al., 2004). More recently, a study from United Kingdom estimate that approximately 700 000 people will suffer from advanced AMD in 2020, which corresponds to 2.5% of the population with more than 50 years old (Owen et al., 2012). The data also indicates that this pathology is more abundant in Caucasians and Asians, and more frequent in women than in men (Friedman et al., 2004; Owen et al., 2012).

The earliest clinical manifestation and pathological feature of AMD is the formation of drusen, extracellular deposits of glycoproteins, lipids, and cellular debris located between Bruch's membrane and the RPE (Ambati et al., 2003a; Rattner and Nathans, 2006; Cook, Patel and Tufail, 2008). A few small drusens can be found in healthy individuals over the age of 50, but the presence of large or numerous drusen confers significant risk for AMD (Bhutto and Lutty, 2012; Klein et al., 1997).

Clinically, AMD is divided into two subtypes: the atrophic AMD ("dry" form) and the exudative AMD ("wet" form) (Figure 1.4). Atrophic AMD is more common, affecting 85% to 90% of the patients. Generally this type is less severe, develops slowly and it can lead to partial blindness. Atrophic AMD manifests with drusen, geographic atrophy of RPE and photoreceptor dysfunction and degeneration. The patients have distorted vision, reading difficulties, limited vision at night or in conditions of reduced light.

In this turn, exudative AMD is more debilitating and quickly leads to blindness if not treated (Guyer et al., 1986; Ambati and Fowler, 2012). It is very frequent AMD patients develop the atrophic form first and then the exudative, what makes that atrophic form is

considered as a risk factor or even a precursor of exudative form. The principal feature of exudative AMD is the choroid neovascularisation (CNV), the growth of new immature blood vessels from the choroid to the region underlying the RPE. The blood vessels may also extend through the RPE toward the subretinal space and retina. CNV can lead to blood and protein leakage in the subretinal space which, along with RPE atrophy and photoreceptor degeneration leads to vision loss (Ambati et al., 2003; Rattner and Nathans, 2006; Cook, Patel and Tufail, 2008).

Figure 1.4 – Fundus photographs in health and in AMD. (A) The ocular fundus of a healthy eye, showing normal pigmentation and retinal blood vessels. **(B)** The late-stage dry form of AMD, known as geographic atrophy with the characteristic large regions of depigmentation, especially in the macula (at the center of the image). **(C)** Wet AMD, where leaky blood vessels from the choroid invade the overlying retina. (Ambati and Fowler, 2012).

As a multifactorial disease, the exact etiology and pathogenesis of the disease remain largely unclear (Ambati et al., 2003; Bhutto and Lutty, 2012; Handa, 2012). However, several risk factors have been identified. Besides age, some of these include smoking, light exposure, genetics, diet, obesity, hypertension and asteriosclerosis (Clemons et al., 2005; Kaarniranta et al., 2013; Vingerling et al., 1995). The cigarette smoke is the factor which confers the major risk for AMD: smokers have about the triple of probability than the non-smokers to develop the disease (Chen et al., 2011; Wang et al., 2009). People who stopped smoking more than 20 years earlier were not at increased risk of AMD causing visual loss (Clemons et al., 2005; Thornton et al, 2005).

A diet lacking antioxidants is also associated with an increased risk of AMD since the retina is the tissue with the bigger oxygen consumption level in human body. RPE cells are rapidly damaged when exposed to oxidants (Beatty et al., 2000; Liang and Godley, 2003) and therefore oxidative stress has been widely implicated in the development of AMD (Winkler et al., 1999; Handa, J.T., 2012).

In the past decade, several genetic variants were associated to AMD, including variants in chromosome 1q32 (in *CFH region*) and 10q26 (*LOC387715/ARMS2*), as well

as in APOE and C2/BF genes (Yang et al., 2010). The link between genetics and AMD was reviewed by Swaroop and collaborators (Swaroop et al., 2007).

Currently, there is not an established therapy to the early stages of AMD. Antioxidants are commonly recommended, although some studies had concluded that the use of antioxidants does not prevent the development of the disease (Evans, 2008). Although geographic atrophy remains without treatment, in cases where CNV is present photodynamic therapy with Verteporfin has been applied. VEGF was identified as a key mediator of CNV and in increased vascular permeability (Leung et al., 1989). Thus several inhibitors of VEGF have been used in AMD, being at this moment the more common treatment to prevent the disease progression (Wong et al., 2007).

2.1. The retina in age-related macular degeneration

As mentioned before, AMD is characterized by visual function loss. The photoreceptors number diminishes a lot, and some studies indicate a bigger decrease in rods than in cones (Curcio et al., 2001). The photoreceptor degeneration seems to occur in the RPE/BrMB complex before the development of AMD (Curcio et al., 2001) and it is directly related to RPE degeneration, suggesting an important role of RPE in photoreceptors viability (Maeda et al., 1998; Bhutto and Lutty, 2012).

In AMD, besides the drusen, it was verified the formation of laminar basal deposits located between the RPE and the BrMb, and also linear basal deposits within the BrMb (Bhutto and Lutty, 2012). These deposits are constituted by lipoproteins and other hydrophobic compounds resultant from incomplete degradation of photoreceptor metabolic end products and the debris of RPE metabolism. In addition, it was verified an increase in collagen fibers, resulting in a thicker BrMb. This affects the materials transport capacity of the membrane, which can contribute to AMD pathology (Bhutto and Lutty, 2012).

With ageing, the RPE suffers several alterations, namely in the pigmentation and reduction of melanosomes. There is also an increase of lipofuscin levels and a decrease in RPE cell density (Delori et al., 2001), probably resultant from apoptosis caused by the accumulation of toxic substances (Figure 1.5). Lipofuscin is a mixture of non-degradable protein-lipid aggregates derived from the phagocytosis of POS (Sparrow and Boulton, 2005). This generates reactive oxygen species (ROS) when exposed to light, which

increases RPE cells oxidative stress, contributing to the pathogenesis of AMD (Strauss, 2005; Handa, 2012).

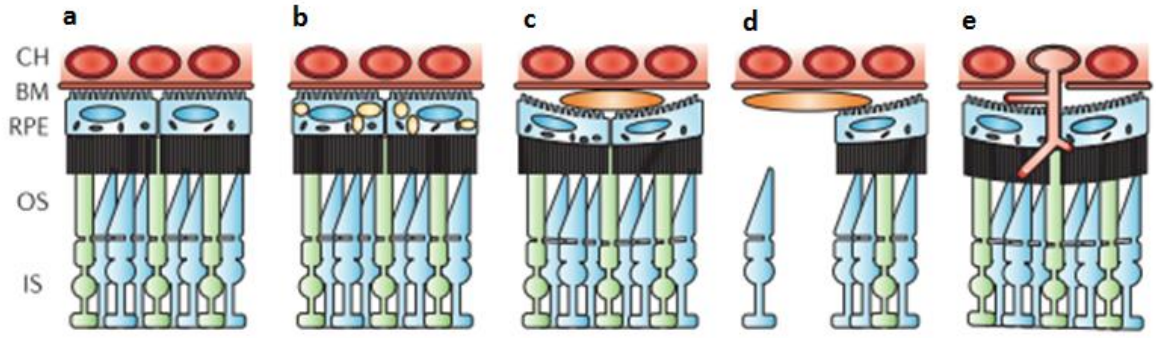

Figure 5 - Schematic illustration of the RPE and BrMb histopathology associated with various macular degenerative processes. (a) normal retina and RPE; **(b)** the RPE with lipofuscin accumulation; **(c)** a drusen sandwiched between the RPE and BrMb; **(d)** a drusen with adjacent geographic RPE atrophy and loss of overlying photoreceptors; **(e)** choroidal neovascularization. OS, outer segments; IS, inner segments. Adapted from Rattner and Nathans, 2006.

2.1.1. Oxidative stress and Age-related macular degeneration

Oxidative stress, which refers to cellular injury caused by reactive oxygen species (ROS), has been proposed to play a causative or contributing role in a large number of diseases, such as heart disease, certain types of cancers, neurodegenerative disorders, cataract and AMD (Fernandes and Pereira, 2007; Olinski et al., 2007; Qin, 2007). In fact, a progressive increase of the oxidative cellular environment, due to the altered redox homeostasis, appears to be one of the hallmarks of the aging process.

The retina is an ideal environment for the generation of ROS for several reasons. The oxygen consumption by the retina is much higher than any other tissue (Wangsa-Wirawan and Linsenmeier, 2003). Moreover the phagocytosis and digestion of POS by RPE provides an additional burden since the shed outer segments are extremely rich in polyunsaturated fatty acids (PUFA), which can be readily oxidized, initiating a cytotoxic chain-reaction which produces ROS (Beatty et al., 2000; Liang and Godley, 2003).

Consistent with a role of oxidative stress in the development of AMD, several studies indicate that exposure of RPE cells to oxidative stress results in an increase of angiogenic cytokines and growth factors, as well as in phenotypes associated with development of AMD (Kannan *et al.*, 2006; Schlingemann, 2004; Zhou *et al.*, 2005).

In the last several years, it has been admitted that oxidative stress can be due to the accumulation of Advanced-Glycation End products (AGEs) in the RPE and Bruch's membrane (Uchiki et al., 2011; Weikel et al., 2011). The drusen also contains AGEs

(Crabb et al., 2002). At this moment it is considered that AGEs may be involved in the development of choroid neovascularization in the wet AMD (Bhutto and Lutty, 2012).

To combat these toxic ROS, the RPE contains a complex composition of various pigments that are specialized to absorb the different wavelengths, such as carotenoids lutein and zeaxanthin (Beatty et al., 2000). RPE is also rich in antioxidants, namely superoxide dismutase and catalase (Miceli et al., 1994). In addition, RPE cells contain glutathione and melanin, which itself can function as an antioxidant. The third line of defense is the cell's physiological ability to repair damaged DNA, lipids and proteins (Strauss, 2005). However, with increasing age, the RPE antioxidant capability diminishes and thus aged RPE cells are more susceptible to oxidative damage (Liang and Godley, 2003; Wang et al., 2009).

2.1.2. Inflammation and Age-related macular degeneration

Emerging evidence indicates a key role of inflammation in many age-related diseases, such as AMD (Fernandes and Pereira, 2007; McGeer, Klegeris and McGeer, 2005; Donoso et al., 2006). Several studies have suggested a role for the complement system in AMD. The complement system is a central part of innate immunity, responsible of recognizing and eliminating invading microorganisms. Components of the complement pathway have been identified in drusen from eyes of patients with AMD (Mullins et al., 2000). Moreover, immune complexes and complement regulatory proteins are present in drusen and RPE (Crabb et al., 2002; Johnson et al., 2001; Nozaki et al., 2006), which fits well with earlier observations of chronic inflammatory cells associated with atrophic RPE and with neovascular lesions (Ding, Patel and Chan, 2009; Hageman et al., 1999; Johnson et al., 2001). Taken together, these data strongly suggest that AMD pathogenesis has a chronic inflammatory component (Penfold et al., 2001; Rattner and Nathans, 2006).

Interestingly, oxidative stress has been implicated in the inflammatory component of AMD (Zhou et al., 2006). The activation of redox-sensitive transcription factors may be involved in triggering the expression of pro-inflammatory cytokines, thus providing a link between oxidative stress and inflammation upon ageing (Chung et al., 2009; Handa, 2012). Accordingly, previous studies carried out in our lab demonstrated that oxidative stress inactivates the proteasome in human retinal pigment epithelial cells (Fernandes et al., 2006) and this results in an overexpression of interleukin (IL)-8 (Fernandes et al.,

2008). Moreover, the results from our group strongly indicate that increased IL-8 production is regulated by several oxysterols, namely 25-OH (Catarino et al., 2012). Upon proteasome inhibition, this increase in IL-8 levels in RPE cells occurs by a mechanism involving p38 Mitogen-activated Protein Kinase (MAPK) and Phosphatidylinositol 3-kinase (PI3K) activation (Fernandes, 2009).

3. Proteolytic pathways

As mentioned above, the RPE has been recognized as a primary site of pathology in AMD (Ambati, 2003; deJong, 2006). In AMD the RPE is not able to phagocytize the POS and scavenge the photoreceptors debris, which in healthy individuals occurs through proteolytic pathways (Young, 1967).

Proteins are degraded via two main pathways in eukaryotic cells. Short-lived proteins are degraded by the proteasome, whereas long-lived proteins are degraded by autophagy. Protein aggregates that form during oxidative stress and other conditions, leading to misfolding and aggregation of proteins are degraded by autophagy (Ravikumar et al., 2002, 2004).

3.1. Ubiquitin Proteasome Pathway (UPP)

The ubiquitin proteasome pathway (UPP) is the major proteolytic pathway within cells (Ciechanover, 2003). It is present in every eukaryotic cells, where it regulates vital biological processes, including cell division, differentiation, signal transduction, apoptosis, quality control and protein trafficking (Glickman and Ciechanover, 2002; Ciechanover, 2003; Shang and Taylor, 2004). This ATP-dependent pathway is also involved in the regulation of immune response and inflammation (Kloetzel, 2004; Qureshi et al., 2005).

Degradation of a protein by the UPP requires two separate and sucessive steps: first, the substrate is tagged by covalent attachment of multiple ubiquitin molecules. Ubiquitin is a small peptide of 76 amino acids, which is highly conserved from yeast to humans, being the most highly conserved protein identified in eukaryotes (Ozkaynak et al., 1984). In a second stage, the polyubiquitinated protein is degraded by the 26S proteasome complex with the release of free ubiquitin that can be used in subsequent ubiquitination cycles (Glickman and Ciechanover, 2002; Shang and Taylor, 2012).

The first step of UPP degradation, ubiquitin conjugation or ubiquitination, is a highly ordered process and involves three different classes of enzymes (Figure 1.6). Initially, an ubiquitin-activating enzyme (E1) activates ubiquitin in an ATP-dependent reaction to generate a high-energy thiol ester intermediate **(Fig. 1.6 step 1)**. Then, ubiquitin is transferred to one of a number of ubiquitin-conjugating enzymes (E2) also via formation of a thiol-ester bond **(Fig. 1.6 step 2)**. In the last step the activated ubiquitin is transferred

from the E2 enzyme to the substrate **(Fig. 1.6 step 3),** which can be either directly or through one member of the large family of ubiquitin protein ligases (E3). The ubiquitin molecule is normally transferred to an –NH2 group of an internal lysine in the substrate, though in a few cases ubiquitin can also be conjugated to the NH2-terminal amino group of the substrate (Fernandes, Ramalho & Pereira, 2006; Fernandes et al., 2008; Zhang et al., 2008). This sequence of reactions is repeated until a chain of at least four ubiquitin moieties is covalently attached to the substrate **(Fig. 1.6 step 4)**, which is required for substrate recognition by a large protease complex called the proteasome **(Fig. 1.6 step 5)** (Fernandes and Pereira, 2007; Glickman and Ciechanover, 2002).

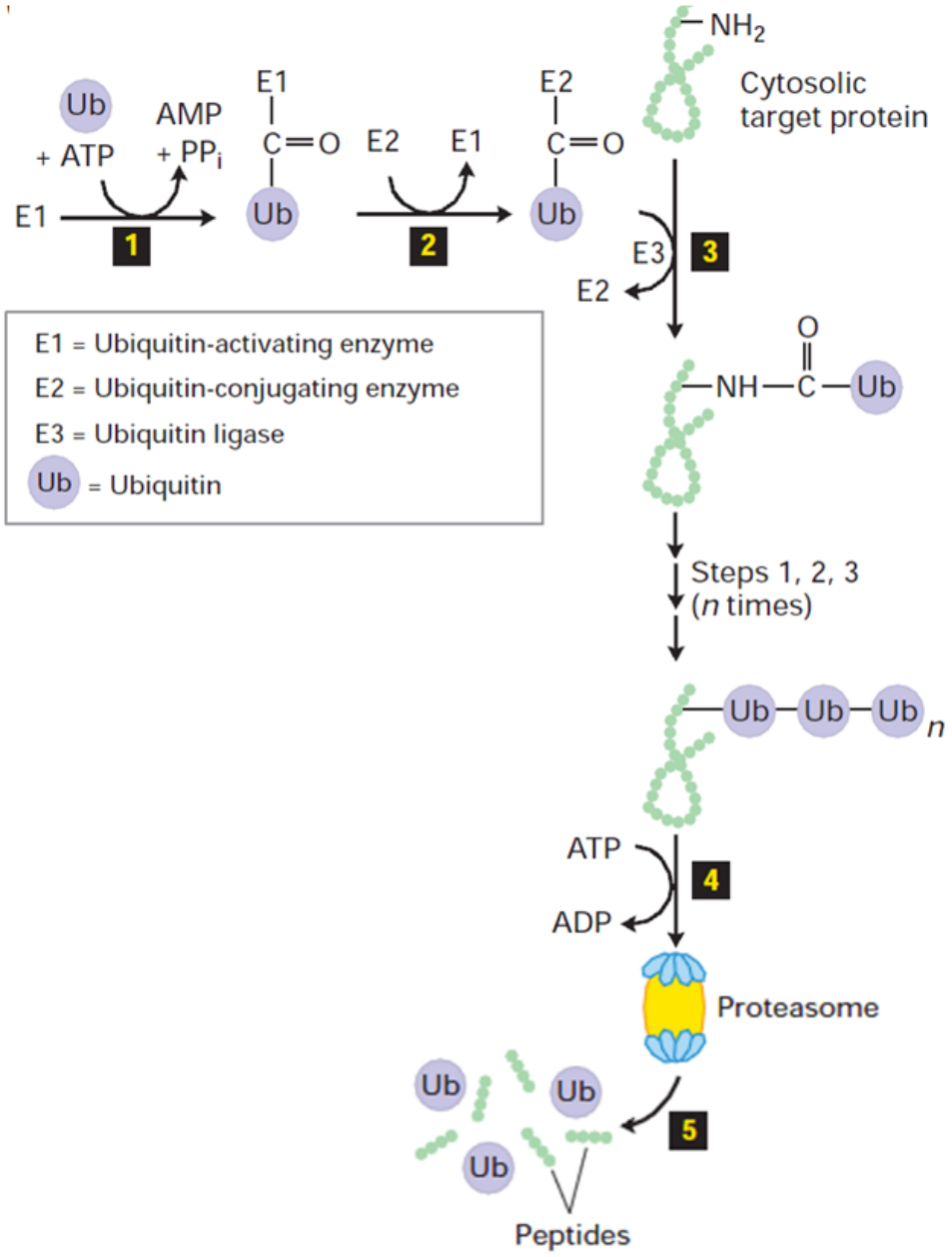

Figure 1.6 - The ubiquitin–proteasome pathway (UPP). A cascade of enzymatic reactions leads to ubiquitination of lysine residues of the substrate. Adaptad from Lodish, Molecular Cell Biology 5th Ed.

The most common and best characterized fate of a poly-ubiquitinated protein is its translocation to a large proteolytic complex, the 26S proteasome, where it is degraded. However, sometimes only one ubiquitin is attached to the target protein in one or more amino acid residues, which results in the production of a mono-ubiquitinated protein. Proteins can be mono-ubiquitinated in different residues resulting in the formation of a multi-mono-ubiquitinated protein (Hicke and Dunn, 2003; Haglund and Dikic, 2005). In most cases the final destination of such proteins is not degradation but rather targeting to specific subcellular compartments, including the endocytic pathway (Haglund and Dikic, 2005).

The proteasome is a 2.5 MDa complex that functions primarily to degrade proteins that have been ubiquitinated. It works through a multi-step process in which ubiquitinated substrates are first recognized by the proteasome complex, followed by substrate unfolding, translocation into the catalytic pore and deubiquitination, finally ending with the cleavage of peptide bonds. The proteasome exists in various forms, the most commonly described being the 26S proteasome (Figure 1.7).

The 26S proteasome complex consists of a 20S catalytic core or core particle (CP) and a regulatory particle (RP) consisting of two regulatory 19S caps (Ciechanover, 2003). The 20S particle is comprised of four heptameric rings arranged coaxially. The subunits of the 20S core are classified into α and β, with the noncatalytic α-heptameric rings forming each of the two outer rings and the catalytic β- heptamers forming the two inner rings (Bulteau et al., 2001; Ethen et al., 2007). The β-subunits contain three pairs of active sites that perform distinct proteolytic activities. The active sites have been classified as caspase-like, trypsin-like and chymotrypsin-like for cleavage of acid, basic and hydrophobic amino acids, respectively (Bulteau et al., 2001; Ethen et al., 2007). The 19S caps are responsible for the recognition of ubiquitinated substrates and subsequent remove of the ubiquitin moieties from those substrates. The protein subunits present in the 19S cap also play an important role in unfolding the protein substrate and feeding it through the proteolytic chamber of the 20S core (Fernandes et al., 2006).

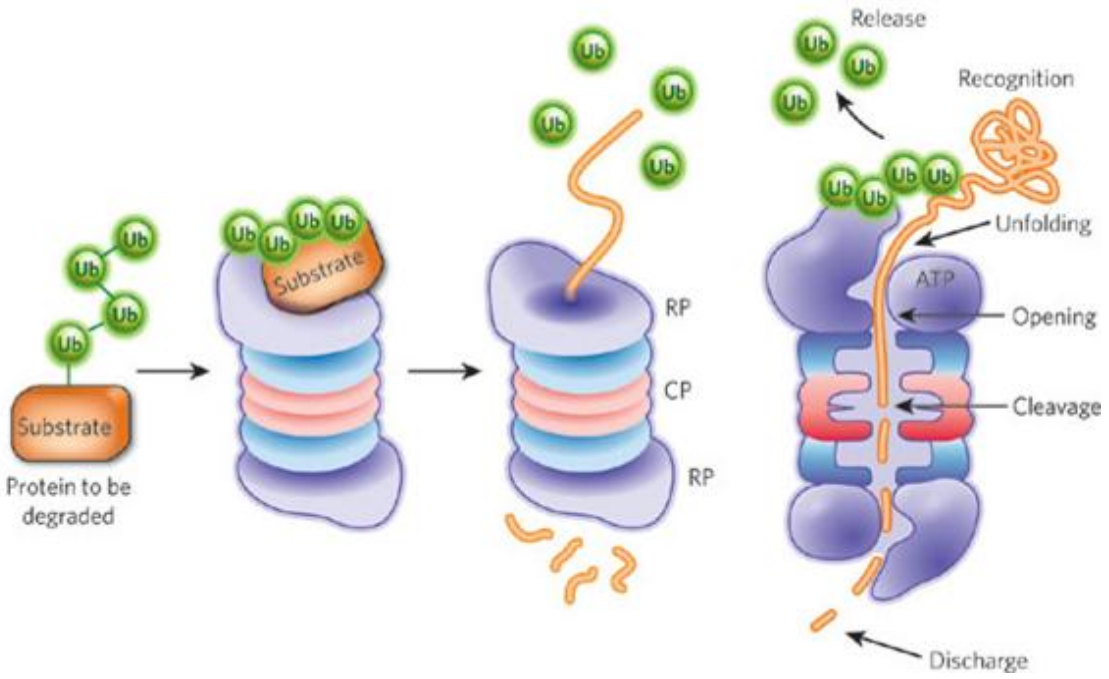

Figure 1.7 – Degradation of ubiquitinated substrates by the proteasome. The 26S proteasome first recognizes the polyubiquitin chain attached to the substrate. The substrate is unfolded and then translocated into the catalytic pore, in an ATP-dependent process. Once a substrate is committed to degradation, it is deubiquitinated, with the release of a free polyubiquitin chain. The substrate is then broken down into smaller peptides that subsequently exit the proteasome. RP, regulatory particle; CP, core particle. (Image taken from http://info.agscientific.com/advancing-biochemical-research/).

The proper function of the UPS allows degradation not only of structural and constitutive proteins, but also of many regulatory proteins, including those which control biosynthetic pathways and cell cycle as well as transcription factors, proteins encoded by oncogenes and immune response proteins. It was, therefore, a matter of time to design and synthesize different groups of chemicals for proteasome inhibition with a potential use in the treatment of cancer and autoimmune and inflammatory diseases (Wojcik, 2013).

A wide variety of both natural and synthetic substances, which inhibit the activity of the proteasome by reversible or irreversible binding to the active site of its 20S catalytic subunit has been discovered (Wu et al., 2010). Of special clinical significance was the introduction into the cancer treatment the dipeptide boronic acid, bortezomib (PS-341), which reversibly and selectively inhibits the proteasome (Kawaguchi et al., 2011; Teicher et al., 1999; Zhang et al., 2014). MG-132 (carbobenzoxy-Leu-Leu-leucinal), a peptide aldehyde that reversibly inhibits proteasomal chymotrypsin- and caspase-like activities is widely used in experimental studies (Ciechanover, 1994; Lee & Goldberg, 1998; Fernandes et al., 2006).

The majority of intracellular proteins are degraded by the UPP. When the proteasome is inhibited, the damaged and misfolded proteins that were marked with ubiquitin for proteasomal degradation cannot be degraded. Instead, they accumulate as ubiquitinated protein conjugates (Ciechanover, 1994). Nowadays it is admitted that ubiquitin conjugates can be stored within the cell or degraded in lysosome by autophagy to avoid cytotoxicity (Bhutto & Lutty, 2012; Wang et al., 2009a) ; however the fate of ubiquitin conjugates is still unclear (Wojcik, 2013).

3.1.1. CDKN1A/p21

Several proteins have been considered as proteasome substrates since they are specifically degraded by the UPP, such as the cyclin-dependent kinase inhibitor 1A (CDKN1A) (Ferreira et al., 2013; Naujokat et al., 2000).

Also known as p21/WAF1 and CDK-interacting protein 1 (CIP1), CDKN1A/p21 is a potent cyclin-dependent kinase (CDK) inhibitor, and thus functions as a regulator of cell cycle progression. CDKN1A/p21 expression is tightly controlled by the tumor suppressor protein p53. Activated p53 binds DNA and activates expression of several genes, including the CDKN1A gene. CDKN1A/p21 mediates growth arrest especially at G1 and S phase, by binding to and inhibiting the activity of several CDKs. When CDKN1A/p21 is complexed with a CDK, the cell cannot continue to the next stage of cell division. This pathway is extremely important, namely considering the p53 function as a tumor suppressor, preventing cancer. CDKN1A/p21 plays also a role as a senescent cell-derived inhibitor (Gartel & Radhakrishnan, 2005).

The exact mechanism by which CDKN1A/p21 suffers proteasomal degradation is not established yet. CDKN1A/p21, as well as several other cell cycle proteins, is ubiquitinated and its degradation is dependent upon the proteasome in vivo (King et al., 1996; Koepp et al., 1999). Pharmacologic inhibition of the proteasome has been shown to increase the half-life of CDKN1A/p21 from less than 30min to more than 2h and results in the accumulation of CDKN1A/p21–ubiquitin conjugates (Sheaff, Singer, & Swanger, 2000). The data indicates that CDKN1A/p21 turnover regulated by the proteasome does not require direct ubiquitination (Sheaff et al., 2000). CDKN1A/p21 is ubiquitinated at the N Terminus in vivo, which is sufficient for proteasomal breakdown. The degradation rate is dependent on the position of the ubiquitin chain (Bloom et al., 2003).

3.2. Autophagy

Autophagy, or autophagocytosis, is a ubiquitous and evolutionarily highly conserved group of mechanisms by which a healthy cell degrades misfolded and long-lived proteins, macromolecules and damaged or old organelles through the use of lysosomes (Marino et al., 2010). First described by Arstila e Trump (Arstila and Trump, 1969), autophagy is a key process in maintenance of cellular homeostasis, and thus it can be stimulated to cope with excessive organelle damage, aggregate removal and pathogen defense (Cuervo, 2008).

In mammalian cells three main types of autophagy have been described: microautophagy, chaperone-mediated autophagy (CMA) and macroautophagy (Peracchio et al., 2012) (Figure 1.8). All three forms of autophagy occur in the cell to assure its homeostasis. Nutrient deprivation, hypoxia, endoplasmic reticulum stress, proteasome malfunction or damage caused by drugs or radiation can decrease autophagy (Benbrook and Long, 2012).

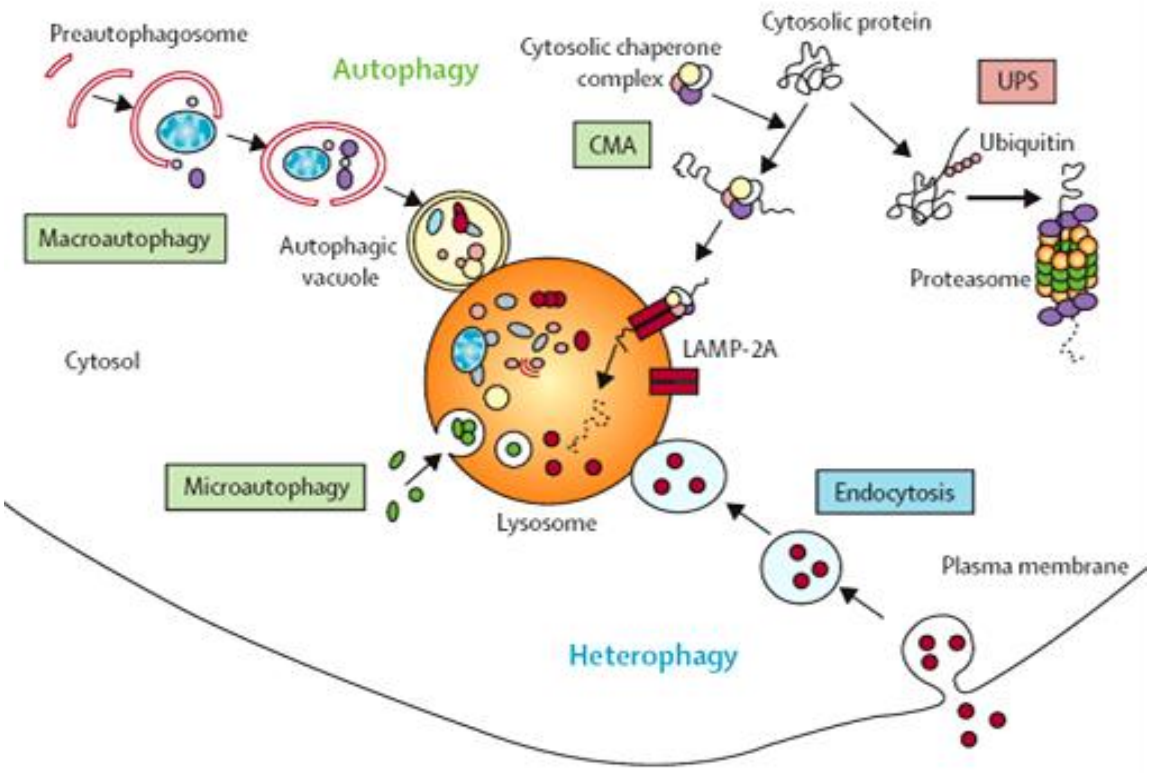

Figure 1.8 – Mechanisms of damaged proteins and organelles by mammalian cells. To maintain its homeostasis, the cells undergo several processes: autophagy (microautophagy, CMA and macroautophagy), heterophagy and the ubiquitin proteasome system (UPS) are represented. (Image taken from https://www.mdc-berlin.de/research_teams/proteomics_and_molecular_mechanisms_of_ neurodegenerative_diseases)

Microautophagy is a process in which defective molecules or organelles are directly engulfed into the lysosomes for degradation and recycling of their components (Li, Li & Bao, 2012).

CMA refers to the chaperone-dependent selection of soluble cytosolic proteins that are targeted to lysosomes and then directly translocated across the lysosome membrane for degradation. In this proteolytic pathway, substrates containing a targeting motif biochemically related to the pentapeptide KFERQ are recognized by HSPA8/HSC70 (heat shock 70 kDa protein 8) and selectively degraded in the lysosome. At the lysosomal membrane, the substrates interact with LAMP2A (lysosomal-associated membrane protein 2A) which acts as a CMA receptor, mediating the translocation of the substrate to the lumen of the lysosome (Cuervo and Dice, 1996; Ferreira et al., 2013).

Macroautophagy (referred here as autophagy, a focus of this work), is a process in which a non-selective sequestration of cytoplasmic material is followed by digestion in lysosomes (Wojcik, 2013), and is the most used for the removal of large aggregates, including organelles (Mitter et al, 2012). Autophagy process begins with the formation of pre-autophagosomal structures (PAS) consisting of isolation membranes. These latter then become elongated and surround portions of cytoplasm containing oligomeric protein complexes and organelles to form a double-membraned vesicles called autophagosomes. The autophagosomes eventually fuse with lysosomes to form autolysosomes where the contents are digested and their components released for recycling within the cells (Benbrook and Long, 2012; Eskelinen and Safting, 2009; Patel et al., 2012). More specifically, the production and processing of autophagic vesicles is divided into 4 steps: 1) initiation, 2) nucleation, 3) maturation and 4) fusion with lysosomes (Figure 1.9). These processes are mediated by a series of proteins encoded by autophagy-related genes (ATGs), which were originally characterized in yeast, and are highly conserved in higher eukaryotes (Klionskly et al., 2003).

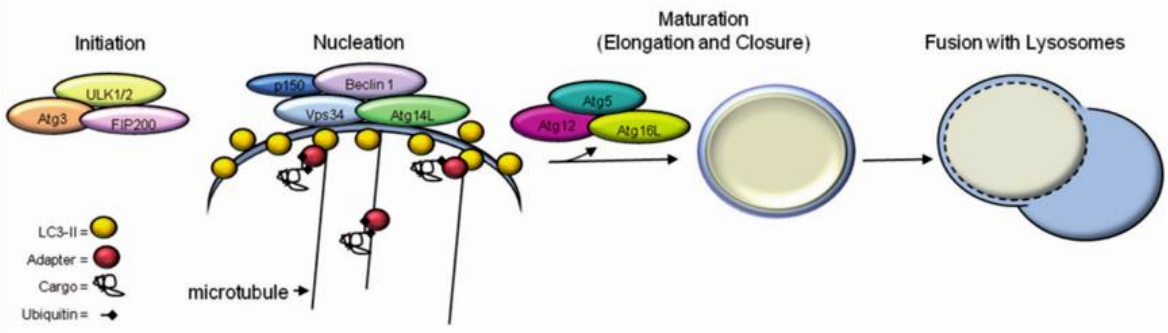

Figure 1.9 – Macroautophagy: a four-step process. Simplified illustration of macroautophagy, showing the protein complexes involved (Benbrook and Long, 2012).

During initiation, *de novo* synthesis of isolation membranes recruits lipids from several organelles depending on the cell type and stimulus. The endoplasmic reticulum appears to be the source of membrane lipids for the *de novo* formation of autophagosomes in the cytoplasm (Hayashi-Nishino et al., 2009). The mitochondrial enzyme, PS (phosphatidylserine) decarboxylase, converts PS to PE (phosphatidylethanolamine), which is needed for autophagosome formation. The complex of proteins that mediate initiation consists of ULK1 (uncoordinated 51-like kinase 1)/Atg1, Atg13 and Atg17/FIP200 (focal adhesion kinase interacting protein of 200 kD).

Nucleation is controlled by a PI3K called Vps34 (vacuolar protein sorting 34) that forms a complex with Beclin 1/Atg6 (Lindmo and Stenmark, 2006). Production of PIP3 (phosphatidylinositol 3,4,5-trisphosphate) by Vps34 recruits Atg18 proteins to the isolation membrane allowing recruitment of LC3 (light chain of the microtubule-associated protein 1/ Atg8) (Polson et al., 2010).

Two interdependent ubiquitin-like conjugation systems mediate the maturation of the autophagosome. In one system, LC3 is first cleaved by the Atg4 serine protease and then conjugated to PE by the Atg7 and Atg3 enzymes (Ichimura et al., 2000). The unmodified and lipidated forms of LC3 are termed LC3-I and LC3-II, respectively, and can be distinguished by Western blot analysis, a well accepted method to monitor autophagy (Klionsky et al., 2012; Mizushima & Yoshimori, 2007; Wang et al., 2009). The second system recruits LC3-II to the isolation membrane by the ubiquitin-like activity of Atg12, which is covalently bound to Atg5 and physically associated with Atg-16L to form a complex (Mizushima et al., 2001). Once the isolation membrane is formed, the Atg-12-5-16L complex is released, which affords its utilization as a marker of isolation membrane formation (Mizushima et al., 2001). On the other hand, LC3-II remains associated with the autophagosome until fusion with the lysosome. Thus the transition of diffuse to punctuate pattern of a transfected LC3-green fluorescent protein (GFP) fusion protein in the cytoplasm is a commonly used marker of autophagosome formation (Klionsky et al., 2012; Tasdemir et al., 2008).

Finally, the fusion step is mediated by dynein transportation of the autophagosomes along microtubules to fuse with lysosomes (Ravikumar et al., 2010). Inhibition of lysosomal acidification by Bafilomycin A1, a specific V-ATPase (vacuolar H+ ATPase) inhibitor, or by other lysosomal function inhibitors, CQ (Chloroquine) and HCQ (hydroxychloroquine), also cause accumulation of autophagosomes and is therefore used

to assess autophagic flux (Klionsky & Abdalla, 2012; Klionsky & Elazar, 2008; Mizushima & Yoshimori, 2007; Yamamoto et al., 1998).

3.2.1. mTOR pathway

Starvation, Hypoxia, depletion on ATP, necessary nutrients or growth factors and increased levels of misfolded /unfolded cytoplasmic proteins can induce autophagy (Wojcik, 2013). The cascade of events linking the variety of autophagy-triggering signals with activation of downstream targets has not been completely elucidated. However, it is known that this process is strongly dependent on mTOR (mammalian target of rapamycin) pathway.

In eukaryotic cells, mTOR is present in the form of at least two distinct multiprotein complexes of different intracellular activity and regulatory capacity. mTOR complex 1 (mTORC1) is responsible for autophagy induction in response to stress, reduced insulin and IGF-1 signaling, and starvation (Jung et al., 2010). During such unfavorable conditions, mTORC1 dissociates from the ULK1 complex allowing it to initiate autophagosome formation. Low glucose levels or high levels of AMP (adenosine 5'-monophosphate), which indicate low cellular energy status or stress, activate AMPK (AMP-activated protein kinase), which inhibits mTORC1 and stimulates autophagy (Jacinto et al., 2004; Wojcik, 2013).

mTOR complex 2 (mTORC2) is a negative regulator of autophagy under conditions of nutrient depletion (Zhao et al., 2007). mTORC2 regulates Akt/PKB (protein kinase B) pathway, since it phosphorylates the serine/threonine protein kinase Akt/PKB at serine residues, which stimulates Akt phosphorylation by 3-phosphoinositide dependent protein kinase-1 (PDPK1) and leads to full Akt activation (Sarbassov et al., 2005). mTORC2 may also play a role in cancer, given its regulation of the widely studied oncogenetic Akt pathway (Guertin et al., 2009).

Chemical inhibitors of mTORC1 currently in clinical use or in clinical trials, including rapamycin and analogs, induce autophagy and are often used as tools to study autophagy (Huang, Bjornsti, & Houghton, 2003; Li et al., 2013; Sahani, Itakura, & Mizushima, 2014). Rapamycin inhibits mTOR by associating with its intracellular receptor FKBP12 (FK-binding protein 12). The FKBP12-rapamycin complex binds directly to the FKBP12-Rapamycin Binding (FRB) domain of mTORC1, inhibiting its activity (Huang, Bjornsti, & Houghton, 2003; Kamada et al., 2000).

3.3. Exosomes

Another process of cell degradation involves exosomes. Exosomes are 40–100 nm membrane vesicles of endocytic origin. Exosome biogenesis occurs within multivesicular bodies (MVBs) in the endosomal system (Bhat and Gangalum, 2011; Ohno, 2012). The endosomal system consists of primary endocytic vesicles, early endosomes, and MVBs. Early endosomes are located near the cell membrane where they act as the first port of call for primary endocytosed vesicles which are either recycled to the plasma membrane or targeted to MVBs. Proteins that are sequestered to the limiting membrane of MVBs can be selectively incorporated into intraluminal vesicles (ILVs) by invagination of the MVB membrane. From here, proteins are either degraded by fusion of the MVB with the lysosomal membrane and release of the ILV's into the lysosome, or alternatively, they can be released into the extracellular environment as exosomes when MVBs fuse with the plasma membrane (Figure 1.10) (Bhat and Gangalum, 2011). Protein sorting and packaging into ILVs occurs in a regulated manner, involving a variety of mechanisms including mono-ubiquitination and the ESCRT (endosomal sorting complex required for transport) machinery (Hicke, 2001; Katzmann et al., 2002).

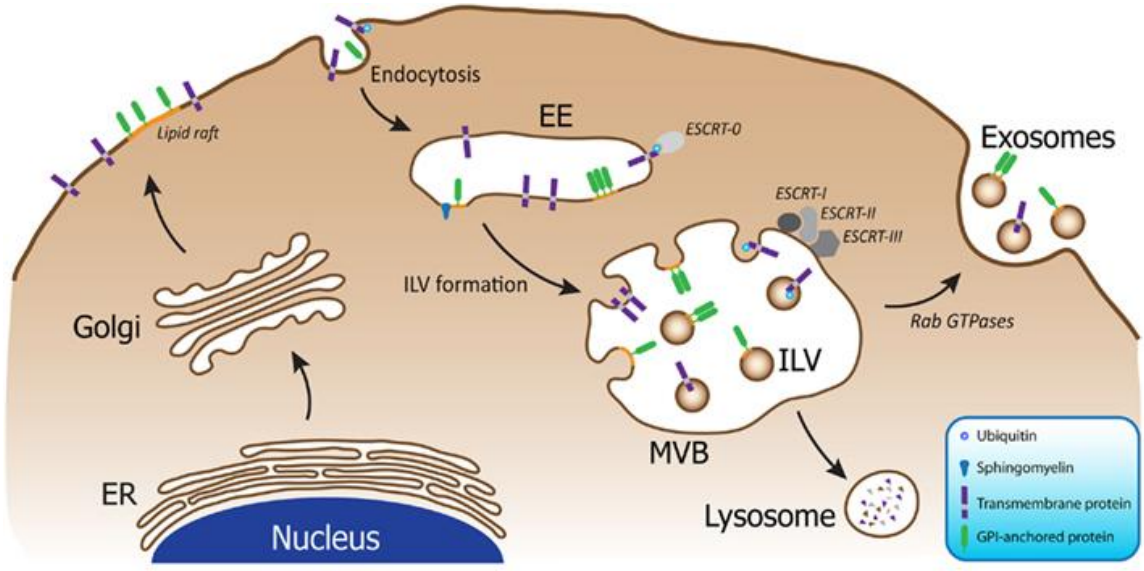

Figure 1.10 - Exosome biogenesis occurs within MVBs of the endosomal system. Following endocytosis into early endosomes (EE), the cargo is packaged into ILVs within MVBs upon inward budding of the membrane. MVBs can then fuse with lysosomes resulting in degradation of the cargo, or alternatively, the MVBs can fuse with the plasma membrane, resulting in release of the ILVs as exosomes, a process which is regulated by Rab GTPases (Bellingham et al., 2012).

Exosomes from different cellular origins contain a common set of molecules: membrane and intracellular proteins, RNA, DNA, and microRNAs (Conde-Vancells et al., 2008; Mathivanan et al., 2010), which are essential for their biogenesis, structure and trafficking, as well as cell type-specific components (Biasutto et al., 2013).

They have been reported in many biological fluids in vivo, including blood, urine, saliva, amniotic fluid, malignant ascites, pleural effusion, bronchoalveolar lavage fluid, synovial fluid, and breast milk (Admyre et al., 2007; Conde-Vancells et al., 2008). Many cells release exosomes into culture medium in vitro (Biasutto et al., 2013). The reported functions of exosomes include the regulation of programmed cell death, angiogenesis, inflammation, coagulation, and the interaction between tumor cells and their environment (Conde-Vancells et al., 2008). Nowadays an increasing ongoing investigation focuses in the potential diagnostic and therapeutic applications of exosomes (Conde-Vancells et al., 2008; Kang et al., 2014).

4. Proteolytic pathways in age-related macular degeneration

4.1. UPP impairment in AMD

Dysfunction of the UPP has been implicated in several age-related diseases, such as Alzheimer's disease (Hope *et al.*, 2003, Ihara et al., 2012), Parkinson's disease (Dawson and Dawson, 2003), diabetic retinopathy (Fernandes *et al.*, 2006) and cataract (Dudek *et al.*, 2005; Shang *et al.*, 2001). Consistent with an age-related decline in proteasome activity in many other tissues, a decline in proteasome activity upon ageing also was reported in the neural retina (Louie et al., 2002; Kapphahn et al., 2007).

Impairment of the UPP may contribute to accumulation and aggregation of various forms of damaged proteins, such as those observed in subretinal deposits. Accumulation of ubiquitin or ubiquitin conjugates is prominent in age-related sub-RPE deposits, i.e. drusen, basal laminar deposits and inclusion bodies in human retinas (Naash et al., 1991, 1997; Mauger et al., 1999), as well as in ganglion cells in rats with chloroquine retinopathy (Yoshida et al., 1997). The presence of ubiquitin in drusen raises the possibility that certain proteins become ubiquitinated within RPE but due UPP impairment its degradation does not occur and then ubiquitinated proteins are expelled from the RPE through exocytosis (Crabb et al., 2002; Leger et al., 2011).

As previously referred, oxidative stress, including photo-oxidation, is often associated with accumulation of ubiquitinated proteins, both in neural retina and RPE (Fernandes et al., 2008, 2009; Zhang et al., 2008). Impairment of the UPP in RPE not only resulted in accumulation of oxidatively modified proteins (Zhang et al., 2008), but also increased the expression and secretion of pro-angiogenesis and pro-inflammation factors (Fernandes et al., 2006, 2008, 2009).

Inflammation has also a role in the development of AMD. Studies conducted in our lab shown that prolonged inhibition of the UPP in RPE triggers the expression of IL-8, a potent pro-inflammation and pro-agiogenesis factor (Fernandes et al., 2008, 2009). Disruption or up-regulation of NF-κB, p38 MAP kinase or PI3K signaling pathways also appears to be involved in the increased expression of IL-8 upon inhibition of the UPP (Fernandes et al., 2008, 2009). The inhibition of NF-κB signaling by proteasome inhibition is also related to the down-regulation of monocyte chemotactic protein 1 (MCP-1) (Fernandes et al., 2006; Uetama et al., 2003). MCP-1 deficiency in mice causes AMD-like lesions, such as accumulation of lipofuscin in RPE, photoreceptor atrophy and

CNV (Ambati et al., 2003). Thus, down-regulation of MCP-1 expression upon proteasome inhibition may be a factor for AMD pathogenesis.

Despite these data, direct evidence for UPP impairment in AMD pathogenesis is still lacking. Ethen et al. compared proteasome activity in retina from donor eyes with different grades of AMD and found that the chymotrypsin-like activity of the proteasome increased in neurosensory retina with disease progression (Ethen et al., 2007).

Taken together, these data imply that age-or stress-related impairment of the UPP may contribute to pathogenesis of AMD via multiple UPP-requiring mechanisms (Shang and Taylor, 2012).

4.2. Autophagy enhancement in AMD

In RPE cells, simultaneously with proteasome inactivation, it has been admitted that occurs the activation of autophagy when in conditions of AMD (Mitter et al., 2012; Wang et al., 2009a and 2009b). Autophagy proteins are strongly expressed in the RPE (Wang et al. 2009a; Krohne et al. 2010; Viiri et al. 2010). Oxidative stress, hypoxia, the unfolded protein response and inflammation can active autophagy and are presented in AMD pathology (Kaarniranta et al., 2013).

Many of the important pathogenic features of the RPE in AMD, e.g. lipofuscin accumulation, susceptibility to oxidative stress, mitochondrial damage and lysosomal dysregulation have an association with autophagy. However, it remains to be determined whether changes in autophagy flux are a cause or consequence of disease and whether autophagy changes reflect alterations in the formation or elimination of autophagosomes.

Autophagy has been reported in photoreceptor cells (Reme and Young, 1977), and is associated with lipofuscin accumulation in rod and cone photoreceptors (Iwasaki and Inomata 1988). Autophagic proteins Atg9 and LC3 were found at high levels in the ganglion cell layer, a subpopulation of cells in the inner nuclear layer, the outer nuclear layer, and the RPE in normal mouse retina (Mitter et al., 2012). Under oxidative stress, a variety of retinal cells undergo autophagic cell death (Kunchithapautham and Rohrer, 2007).

Accordingly with autophagy enhancement in AMD, Wang and collaborators found increased levels of mitochondrial damage in RPE cells and ex vivo AMD donor eyes (Wang et al., 2009a). They also verified an enhanced autophagy and exocytic activity in aged RPE cells, as well as the presence of autophagic and exosome markers (CD63,

CD81 and LAMP2) in drusen in AMD donor eyes (Wang et al., 2009a and 2009b). In this last study several exosome markers (CD63, CD81 e LAMP2) were found between the RPE and the choroid of mice chronically exposed to cigarette smoke, contrary to controls (Wang et al., 2009b). Exosome protein markers appears to be located in BrMb, namely at choroid side (Wang et al., 2009b). The high levels of exosomes make sense, since RPE is responsible for damaged macromolecules removal, whose levels are increased due toxic components from tobacco (Wang et al., 2009). It is admitted that increased autophagy can lead to the release of intracellular proteins via exosomes by the aged RPE, which may contribute to the formation of drusen.

4.3. HIF-1α plays a role in AMD

Hypoxia-Inducible Factor 1 (HIF1) is the most conserved hypoxia-inducible transcriptional complex (Salceda & Caro, 1997). HIF1 is a heterodimer composed of two subunits: hypoxia inducible factor 1, α subunit (basic helix-loop-helix transcription factor) (HIF-1α) and aryl hydrocarbon receptor nuclear translocator (ARNT/HIF-1β) (Arjamaa et al., 2009).

The HIF signalling cascade controls vasculature adaptations to hypoxia (namely the formation of new blood vessels) and is also a key regulator of many other processes, including transcription of pro-angiogenic factors, such as VEGF, TGF-β3, and various components of glucose transport and glycolysis (Arjamaa, 2009; Shang & Taylor, 2012;Lőw et al., 2013).

In oxygen normal conditions (normoxia), HIF-1α is hydroxylated by specific prolyl hydroxylases. Once hydroxylated, HIF-1α is recognized by the von Hippel-Lindau tumor suppressor (VHL) protein (Maxwell et al., 1999), which acts as an ubiquitin ligase complex that targets HIF-1α for polyubiquitination and subsequent degradation by the proteasomal pathway (Bento et al., 2010; Cockman et al., 2000; Kamura et al., 2000). Decreased levels of oxygen lead to stabilization of HIF-1α (its hydroxylation is inhibited) and thus preventing ubiquitination, and consequent degradation. HIF-1α is then translocated into the nucleus, where it dimerizes with ARNT.

Currently, a regulatory role of HIF-1α in the pathogenesis of AMD has been discussed (Arjamaa et al., 2009). Increasing evidences suggests that ROS and HIF-1α are directly involved in stimulating angiogenesis, both in tumours and in the retina (Al-Shabrawey et al., 2008; Ushio-Fukai and Nakamura, 2008). ROS production may lead to

HIF activation and accelerated appearance of age-related diseases (Rapino et al., 2005; Yuan et al., 2008). ROS increases HIF protein expression and prevents the hydroxylation of HIF-1a protein (Yuan et al., 2008). These molecular responses ultimately lead to the increased expression of VEGF that is the major growth factor triggering choroidal neovascularization in the exudative AMD form (Schlingemann, 2004; Arjamaa et al., 2009).

5. Aims

Several recent studies highlight the interplay between UPP and autophagy pathways in several diseases (Pandey et al., 2007; Viiri et al., 2013; Zhang et al., 2014). However the mechanism by which ubiquitinated proteins are shuttled to autophagy lysosomal pathway remains still unclear.

AMD is the leading cause of blindness in elderly people from western countries and its prevalence is rising as a consequence of longevity (Rattner and Nathans, 2006). Increasing data indicates a key role for the proteolytic pathways in the development of this disease (Arjamaa et al., 2009; Kaarniranta et al., 2013; Wang et al., 2009a), making AMD the perfect model to study the link between UPP, autophagy and exosomal removal of proteins.

Thus, the general purpose of this study is to investigate the crosstalk between proteasome and autophagy proteolytic pathways in RPE cells in ageing-associated diseases such as AMD. We expect to identify the mechanisms and key players intrinsically linked to RPE dysfunction in AMD and how UPP and autophagy processes are involved.

The work will focus on three main objectives: (i) to inhibit the proteasome-dependent degradation of RPE cells through the use of MG-132 (ensured by ubiquitin conjugates and CDKN1A/p21 protein levels); (ii) to investigate the effect of proteasomal inhibition on autophagy (analysis of the autophagic markers LC3 (LC3-I e LC3-II), HIF-1α and SQSTM1/p62) and lysosomal activity (by measuring the CatD protein levels); (iii) to establish an AMD cell line model, with RPE cells exhibiting concomitant proteasome impairment and autophagy enhancement, as it happens in AMD.

CAPTER 2

MATERIAL and METHODS

1. Materials

The culture medium Dulbecco's Modified Eagle's Medium/ Ham's F-12 (DMEM:F12; 1:1) was obtained from Sigma-Aldrich (St Louis, MO, USA). Trypan blue (0.4%) solution, Fetal bovine serum (FBS), antibiotics (100 U/mL penicillin and 100 μg/mL streptomycin) and Glutamax for cell culture were purchased from Gibco (Grand Island, NY, USA). Trypsin-EDTA (0.25%) was from Sigma-Aldrich (St Louis, MO, USA).

N-(benzyloxycarbonyl)leucinylleucinylleucinal (MG-132) was obtained from Calbiochem (La Jolla, CA, USA). Bafilomycin A1 (BafA1) and Cycloheximide (CHX) were purchased from Sigma-Aldrich (St Louis, MO, USA). Rapamycin was from Invitrogen (Camarillo, CA, USA).

The *DC* Protein Assay used in total protein quantification was from Bio-Rad (Hercules, CA, USA).

40% Acrylamide/Bis-acrylamide (29:1 solution) was purchased from NZYTech (Lisbon, Portugal). Other SDS-Page reagents and materials were from Bio-Rad Laboratories (Hercules, CA, USA), as well as the nitrocellulose (Nitrocellulose Membrane 0.45 μm, Bio-Rad) and polyvinylidene difluoride (PVDF) (Immun-blot PVDF membrane 0.20 μm, Bio-Rad) membranes. Clarity™ Western ECL substrate for detection of proteins was also from Bio-Rad.

Hydrogen Peroxide (30% H_2O_2) was obtained from Merck Millipore (Darmstadt, Germany). 1x protease inhibitor cocktail was from Roche (Indianapolis, IN, USA) and Glycergel mounting medium from Dako (Carpinteria, CA, USA).

3-(4,5-dimethylthiazol-2-yl)-2,5-diphenyltetrazolium bromide (MTT), bovine serum albumin (BSA) and all other chemicals were purchased to Sigma-Aldrich (St Louis, MO, USA) and were of the highest purity available.

2. Cell culture and treatments

The spontaneously arising human retinal pigment epithelium cell line (ARPE-19) was obtained from LGC Promochem (Teddington, UK). Cultures of ARPE-19 cells were maintained in DMEM-F12 supplemented with 10% FBS, antibiotics (100 U/mL penicillin and 100 μg/mL streptomycin) and 1x Glutamax. The cell line was routinely

maintained at 37°C under 5% CO_2 atmosphere and it was shown to exhibit features characteristic of RPE cells including defined cell borders and a cobblestone appearance.

Upon reach confluency, adherent ARPE-19 cells were washed once with Phosphate-buffered saline (PBS) and then trypsinized. The viable cells were counted using trypan blue, and a specific number of cells was plated.

For Western blot and Immunocytochemistry assays, cells were seeded in 12 multiwell plates (30,000 cells/well). For proteasome inhibition treatment, MG-132 was prepared in DMSO for stock solution at 10mM. One day after seeding, the cells were treated with 0.10 to 1.0μM of MG-132 freshly prepared in regular medium and incubated for 48h.

In autophagic flux studies, a stock solution of BafA1 at 100μM in DMSO was prepared; the epithelial cells were incubated with 50nM of BafA1 for 1h and 6h. When the cells were co-treated with both MG-132 and BafA1, the last one was added in the last 1h or 6h of the incubation with the proteasome inhibitor MG-132. The autophagy was induced with 30nM rapamycin freshly prepared, from a stock solution in DMSO at 500μM, for 6h. Additionally, starvation was performed by removing the cell medium and culturing the cells in DMEM:F12 without FBS from 1h incubation up to 24h. Furthermore CHX, an inhibitor of protein biosynthesis in eukaryotic organisms (produced by the bacterium *Streptomyces griseus*), was prepared in Milli-Q water at 5mg/mL, with the cells being exposed to 1μg/mL or 5μg/mL during the time of MG-132 and BafA1 treatment.

3. Cell metabolic activity

Cell metabolic activity after MG-132 and BafA1 incubation was determined by measuring the ability of ARPE-19 cells to reduce MTT, to a colored insoluble formazan, being this reduction proportional to the mitochondrial enzyme succinate dehydrogenase activity. ARPE-19 cells seeded in a 96 well plate at a density of 10,000 cells /well were grown one day until they reached confluency. Then, the treatments were performed with the same concentrations and times used in the experiments previously described. H_2O_2 was used as a positive control (final concentration of 1mM, for 2h). After the treatments, the medium was removed, the cells were washed twice with PBS and incubated with 0.5 mg/ml MTT in cell medium for 4h at 37°C. Subsequently, supernatants were removed and the precipitated dye was dissolved in 200 μl 0.04 M HCl (in absolute isopropanol)

with agitation at room temperature until all the crystals were dissolved. They were quantified at a wavelength of 570 nm, using 620 nm wavelength as a background in the microplate reader (Synergy HT, Biotek, Winooski, VT, USA). Each experiment was done in quadruplicates of the different conditions. Cytotoxicity was determined by the following formula:

$$\text{Cytotoxicity (\%)} = \frac{\text{Abs (570nm)} - \text{Abs (620nm) treated cells}}{\text{Abs (570nm)} - \text{Abs (620nm) control cells}} \times 100$$

4. Protein Quantification

Total protein concentration was determined using the Bio-Rad *DC* Protein Assay, a colorimetric assay based on the Lowry method. Briefly, BSA was used to generate a standard curve, by preparation of several dilutions of BSA in sample buffer in a range between 62.5 and 2000 μg/mL of BSA. In a 96 multi-well plate, the standard curve was prepared in duplicate, by adding into each well 5μL of the different BSA dilutions, 25μL of reagent A' (49 parts of reagent A mixed with 1 part of reagent S) and 200μL of reagent B. The same procedure was performed for the samples and the blank (sample buffer), also in duplicates. The plate was incubated at 37°C for 30min. Then, the absorbance at 655 nm was measured in the plate reader Biotek Synergy HT spectrophotometer. The protein concentration in the samples was directly obtained by plotting the average of the absorbance at 655 nm for each BSA standard in function of its concentration (μg/mL).

5. Western blotting

The cell lysates were prepared for the Western blot analysis. After treatments, the cells were rinsed twice with PBS, collected immediately in 50μL of 4x Laemmli Buffer (250mM Tris-HCl (pH 6.8), 35% (v/v) glycerol, 20% (v/v) β-mercaptoethanol, 8% (m/v) SDS, 0.03% (m/v) bromophenol blue) and boiled for 5min at 95ºC. In some experiments, namely in CHX assays, cells were collected in Radioimmunoprecipitation assay buffer (RIPA): 150mM NaCl, 50mM Tris-HCl (pH 7.5), 1% (v/v) NP-40, 0.1% (m/v) SDS, supplemented with 2 mM phenylmethylsulfonyl fluoride (PMSF), 10 mM iodoacetamide (IAM), 1 mM sodium orthovanadate and 1x protease inhibitor cocktail. Briefly, the cells in the 12 multi-well plates were rinsed twice with ice-cold PBS and then scraped and collected in 100μL of RIPA buffer after 15min of incubation on ice with agitation. After centrifugation (11,000g for 10min at 4°C) of the cell lysates, supernatants were used to

determine protein concentration and then were denatured with Laemmli buffer. The samples were boiled for 5min at 95°C and frozen at -20°C until use.

For the western blot analysis, 20 to 50 μg of protein were loaded per lane and separated by electrophoresis on 10-15% polyacrylamide gel containing sodium dodecyl sulfate (SDS-PAGE). The electrophoresis was performed using Tris-HCl buffer (pH 8.0-8.5), containing 0.4M Tris, 3.2 M glycine and 0.1% (m/v) SDS, at 140 V.

After electrophoresis, proteins were electro-transferred to nitrocellulose or PVDF membranes. Western blot transfer was performed using 100 mM Tris-HCl (pH 7.5-8.0) containing 25 mM glycine, 20% (v/v) methanol and 0.01% (m/v) SDS, for 75min at 100V, on ice with agitation. After transfer, membranes were blocked with 5% (m/v) nonfat milk in Tris-buffered saline (TBS) (50 mM Tris (pH 7.6) and 150 mM NaCl, containing 0.01% (v/v) Tween-20 (TBS-T)), for at least 30min under agitation, at room temperature.

Membranes were incubated with primary antibodies (Table I) diluted in TBS-T supplemented with 5% non-fat milk, overnight at 4°C. On the following day, membranes were washed with TBS-T (3x10min) and then incubated with adequate horseradish peroxidase (HRP) conjugated secondary antibodies (Table I) with agitation for 1h, at room temperature. After secondary antibody incubation, membranes were washed again with TBS-T (3x 10min) and the immunoreactive bands were visualized with enhanced chemiluminescence (ECL) reagent. To confirm equal protein loading and sample transfer, blots were reprobed with mouse anti-α-tubulin or goat anti-GAPDH antibodies. Immunoreactive bands were revealed by scanning blots using a VersaDoc (Bio-Rad Life Science) imaging system. Exposure times were adjusted so that the band intensity fell within the linear range of detection. Densitometric analyses were performed using the ImageJ 1.47v software.

Table I – Primary and secondary antibodies for Western blot.

Antibody	Host	Type	Dilution	Supplier
anti-Ubiquitin (P4D1)	Mouse	monoclonal	1:1000	Santa Cruz Biotechnology, Inc. (Santa Cruz, CA, USA)
anti-HIF 1-α	Rabbit	polyclonal	1:1000	Santa Cruz Biotechnology, Inc.
anti-p21	Rabbit	polyclonal	1:100	Santa Cruz Biotechnology, Inc.
anti-LC3	Rabbit	polyclonal	1:500	Thermo Fisher Scientific Inc. (Waltham, MA, USA)
anti-SQSTM1/p62	Mouse	monoclonal	1:1000	Santa Cruz Biotechnology, Inc
anti-Cathepsin D	Rabbit	monoclonal	1:1000	GeneTex, Inc. (Irvine, CA, USA)
anti-GAPDH	Goat	polyclonal	1:2500	Sicgen (Coimbra, Portugal)
anti-α-tubulin	Mouse	monoclonal	1:1000	Sigma-Aldrich Co. (St Louis, MO, USA)
HRP secondary anti-mouse	Goat	IgG (H+L)	1:5000	Bio-Rad (Hercules, CA, USA)
HRP secondary anti-rabbit	Goat	IgG (H+L)	1:5000	Bio-Rad
HRP secondary anti-goat	Rabbit	IgG (H+L)	1:5000	Invitrogen (Carlsbad, CA, USA)

6. Immunocytochemistry

As referred above, 30,000cells/well were seeded in a 12 well plate in glass coverslips (2 coverslips per well). The proteasome and lysosome inhibition (with MG-132 and BafA1, respectively) was performed as previously described. After treatment, cells were fixed with paraformaldehyde (PFA) 4% (v/v) in PBS for 10min and then washed with PBS (3x5min). After, cells were permeabilized with 0.2% (v/v) Triton X-100 in PBS for 10min and rinsed again with PBS (3x5min). Next, the cells were blocked for 30min with 2% (m/v) BSA and then incubated with the primary antibodies (Table II) in 0.02% (m/v) BSA for 1h30 at room temperature in a humidified chamber. After this, the cells were rinsed with PBS (3x10min) and incubated with the fluorophore-conjugated secondary antibodies (Table II) and 1µg/mL 4',6-diamidino-2-phenylindole (DAPI), for 1h at room temperature in a humidified chamber in the dark. As negative control, coverslips were incubated only with the secondary antibodies in order to establish background fluorescence and non-specific staining of the antibodies. Finally the cells were washed with PBS (3x10min) and the slides were mounted with Glycergel mouting medium. The slides were stored at 4ºC in the dark until acquisition of images using the confocal fluorescence microscope (LSM 710, Carl Zeiss, Gottingen, Germany).

Table II – Primary and secondary antibodies for Immunocytochemistry

Antibody	Host	Type	Dilution	Supplier
anti-Ubiquitin (P4D1)	Rabbit	polyclonal	1:50	Boston Biochem (Cambridge, MA,USA)
anti-SQSTM1/p62	Mouse	monoclonal	1:100	Santa Cruz Biotechnology, Inc.
Alexa Fluor 488 anti-rabbit	Goat	IgG (H+L)	1:100	Molecular Probes Inc. (OR, USA)
Alexa Fluor 568 anti-mouse	Goat	IgG (H+L)	1:100	Molecular Probes Inc.

7. Statistical analysis

Results were analyzed using GraphPad Prism (GraphPad Prism 5.0 software, La Jolla, CA, USA). They are presented as mean ± standard errors of the mean (S.E.M.) with n indicating the number of experiments. All the results are representative of at least three independent experiments. To test the significance of the difference between two independent groups, a Student's t test followed by Mann-Whitney test was used. The comparison of values between more than two groups was performed using one-way analysis of variance (ANOVA), followed by Tukey's multiple comparison test. A value of $p<0.05$ was considered to represent a significant difference.

CAPTER 3

RESULTS

1. MG-132-induced proteasome inhibition stimulates autophagy and increases lysosomal activity in ARPE-19 cells

1.1. Proteasome inhibition increases ubiquitin and CDKN1A/p21 levels

ARPE-19 (Dunn et al., 1996) is a cell line commonly used as a model of human retinal epithelial cells (Dunn et al., 1998; Philp, 2003; A. L. Wang, Lukas, Yuan, Du, Tso, et al., 2009). This is a spontaneously arising human RPE cell line with normal karyology which forms epithelial stable monolayers, exhibiting morphological and functionally polarity. ARPE-19 has structural and functional properties characteristic of RPE cells in vivo: the cells express the RPE-specific markers CRALBP and RPE-65 (Dunn et al., 1996; Dunn et al., 1998) making them a good model for in vitro studies of retinal pigment epithelium physiology (Ablonczy et al., 2011).

To investigate whether proteasome inhibition affects the RPE, the ARPE-19 cells were treated with MG-132 (carbobenzoxy-Leu-Leu-leucinal), a peptide aldehyde that effectively blocks the proteolytic activity of the 26S proteasome complex (Ciechanover, 1994; Lee & Goldberg, 1998; Fernandes et al., 2006). In order to mimic the chronic UPP inhibition that occurs in AMD (Shang & Taylor, 2012; Kinnunen et al., 2012), cells were exposed to various concentrations of MG-132 (0.1-1μM) for 48h.

MG-132 cytotoxic effect was assessed by the MTT colorimetric assay (Figure 4.1). No significant cytotoxicity was observed when cells were incubated with MG-132 up to 0.20uM. However, there was an increased cytotoxicity in a concentration time dependent manner, for increasing concentrations of MG-132 (0.50 and 1μM). H_2O_2 (1 mM) was used as a positive control in MTT assay, since it is known to be inducer of oxidative stress and thus compromising the cell membrane structure.

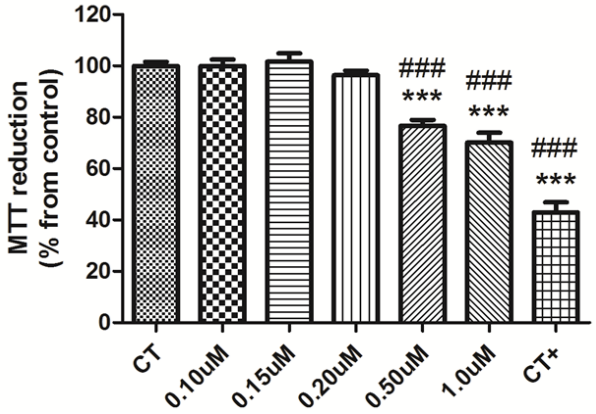

Figure 4.1 – Chronic treatment with MG-132 induces cytototixicy for concentrations higher than 0.20 µM. ARPE-19 cells were treated with 0.10, 0.15, 0.20, 0.50 and 1.0µM of MG132 for 48h. Positive controls were performed adding 1mM hydrogen peroxide (30% H_2O_2) to ARPE-19 cells in the last 2h of the experiments. Cytotoxicity was evaluated by the MTT assay. Data are expressed as percentage of the control and represent the mean ± SEM of three independent experiments (each one was done in quadruplicates). ***p<0.001 significantly different from control, ### p<0.001 significantly different from 0.20µM, 1way ANOVA followed by Tukey's Multiple Comparison Test.

To test whether the concentrations of MG-132 under analysis induce inhibition of the proteasome, western blot was performed to determine the amount of ubiquitinated proteins (Figure 4.2).

There were no significant differences in the levels of the ubiquitin conjugates when cells were incubated with MG-132 up to 0.15 µM. However, there was a concentration-dependent effect of MG-132 on ubiquitin conjugates for concentrations above 0.15 µM. ARPE-19 cells treated during 48h with 0.20µM of the proteasome inhibitor exhibited levels of ubiquitin conjugates significantly higher (3.959±0.547, p=0.0002) compared with control cells (1.000±0.069). For higher concentrations of MG132, the accumulation of ubiquitin conjugates was even greater.

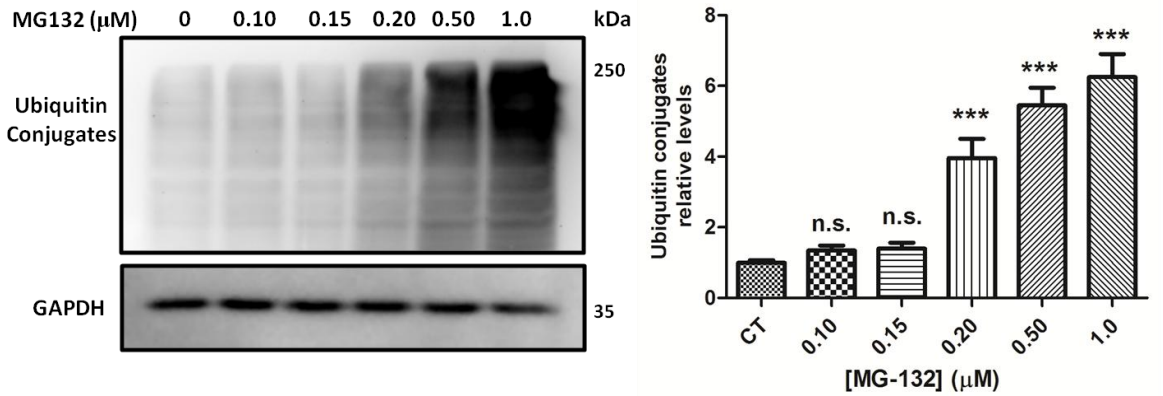

Figure 4.2 – Proteasome inhibition with 0.20µM of MG-132 led to accumulation of ubiquitin conjugates. ARPE-19 cells were treated with 0.10, 0.15, 0.20, 0.50 and 1.0µM of MG-132 for 48h. The protein levels of ubiquitin conjugates were assessed in total cell lysates by Western Blotting using specific antibodies against ubiquitin (P4D1 antibody). GAPDH was used as loading control. Data represent the mean ± SEM (n≥8 for each concentration), ***p<0.001 significantly different from control, Student's t test followed by Mann-Whitney test.

Besides the accumulation of ubiquitin conjugates, we also confirmed the MG132-induced proteasomal inhibition by analyzing the protein levels of the proteasome substrate cyclin-dependent kinase inhibitor 1A (CDKN1A/P21/Cip1) by Western Blotting (Figure 4.3).

According to our hypothesis, proteasome inhibition induced CDKN1A/p21 accumulation. The protein levels of CDKN1A/p21 were about 3 times higher at 0.20μM (3.121±0.666, p=0.0067) comparing with the control (1.000±0.03).

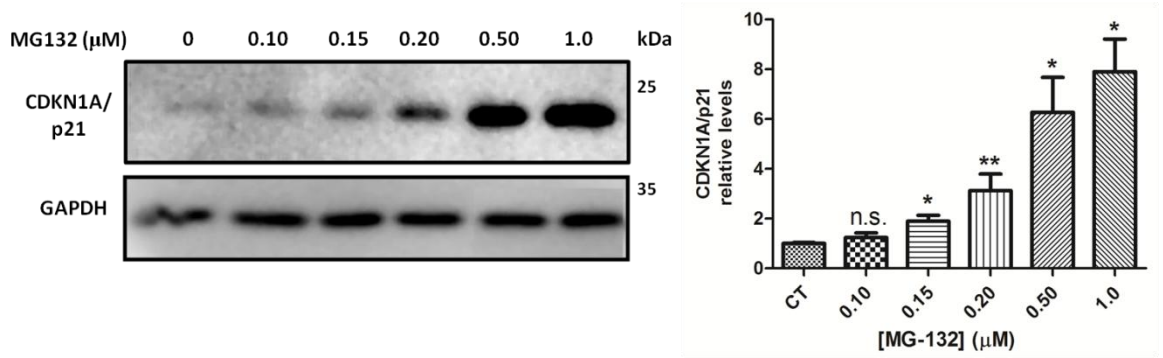

Figure 4.3 – Effects of proteasome inhibition with MG-132 results in increased CDKN1A/p21 protein levels in ARPE-19 cells. ARPE-19 cells were treated with 0.10, 0.15, 0.20, 0.50 and 1.0μM of MG-132 for 48h. The protein levels of CDKN1A/p21 were assessed in total cell lysates by Western Blotting against correspondent antibodies. GAPDH was used as loading control. All the results represent the mean ± SEM of at least four independent experiments. n.s. non-significant; *p < 0.05; **p < 0.01 significantly different from control, Student's t test followed by Mann-Whitney test.

1.2. MG-132-induced proteasomal inhibition leads to increased levels of autophagy markers

Another mechanism for protein degradation is macroautophagy. This pathway usually shares its proteolytic burden with proteasomes during normal cellular homeostasis and protein clearance in response to cellular stress and the aging process (Kaarniranta, Salminen, Eskelinen, & Kopitz, 2009; Viiri et al., 2010). Recently, there has been an increased general interest in understanding the crosstalk between these proteolytic pathways (Kaarniranta et al., 2013;Lőw et al., 2013; Wojcik, 2013).

In order to investigate whether proteasome inhibition could induce macroautophagy, we treated ARPE-19 cells with MG-132 exactly as performed in the previous studies and analyzed the autophagy marker LC3 by Western blot (Figure 4.4). As expected, endogenous LC3 was detected as two bands, one representing LC3-I, which is cytosolic and the other, LC3-II, which is conjugated with phosphatidylethanolamine (PE) and is

present on isolation membranes and autophagosomes, and much less on autolysosomes (Mizushima & Yoshimori, 2007)

Interestingly, we found that when ARPE19 cells were incubated with increasing concentrations of MG-132 the amount of LC3-I decreased and that of LC3-II increased (Figure 4.4). LC3-II protein levels can be used as a measure of autophagy dynamics (Mizushima & Yoshimori, 2007). As shown in Figure 4.4, there was a significant increase in the levels of LC3-II when RPE cells were incubated with MG-132, for concentrations above 0.15μM: when the cells were exposed to 0.20μM of MG-132 (2.041±0.237, p=0.0003) there was a significantly difference comparing with the control (1.000±0.03), which was even more evident when we considered higher concentrations. These results suggest upregulation of autophagosome formation or blockage of autophagic degradation.

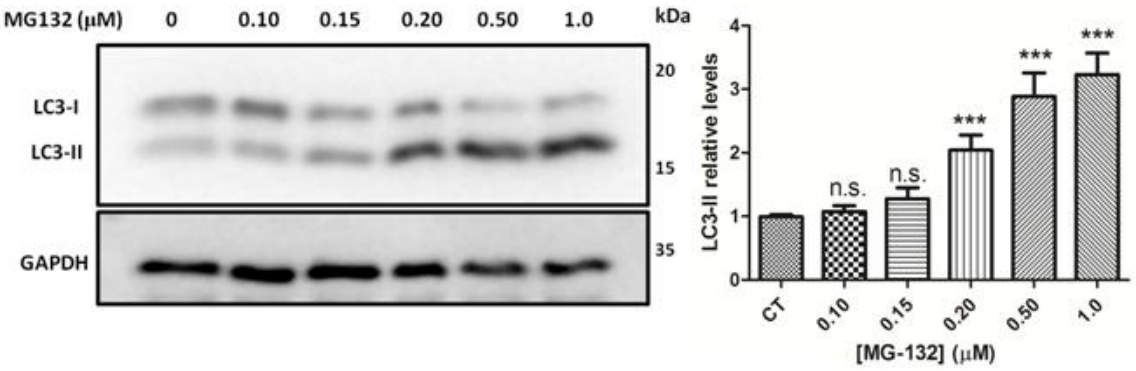

Figure 4.4 – Inhibition of the proteasome with MG-132 leads to increased LC3-II levels in ARPE-19 cells. . ARPE-19 cells were treated with 0.10, 0.15, 0.20, 0.50 and 1.0μM of MG-132 for 48h. The protein levels of LC3 (LC3-I and LC3-II) were assessed in total cell lysates by Western Blotting. GAPDH was used as loading control. All the results represent the mean ± SEM of at least seven independent experiments. n.s. non-significant; ***p < 0.001 significantly different from control, Student's t test followed by Mann-Whitney test.

Our group has recently shown that the HIF-1α is degraded by alternative pathways, by the UPP or in the lysosome through CMA (Ferreira et al., 2013). Lysosomal inhibitors, but not macroautophagy inhibitors induce the accumulation of HIF-1α (Ferreira et al., 2013). STUB1, an ubiquitin ligase, is required for degradation of HIF-1α in the lysosome by CMA (Ferreira et al., 2013).

In this context we measured the HIF-1α protein levels of RPE cells subjected to chronic proteasomal inhibition. Treatment of cells with increasing concentrations of MG-132 for 48h decreased HIF-1α protein levels (Figure 4.5). This reduction was

significantly different above 0.20μM (0.356±0.01, p=0.0112), the same concentration that induced significant accumulation of LC3-II (Figure 4.4). This data suggests that HIF-1α may be degraded by another pathway than the UPP when ARPE-19 cells were incubated with MG-132 for 48h.

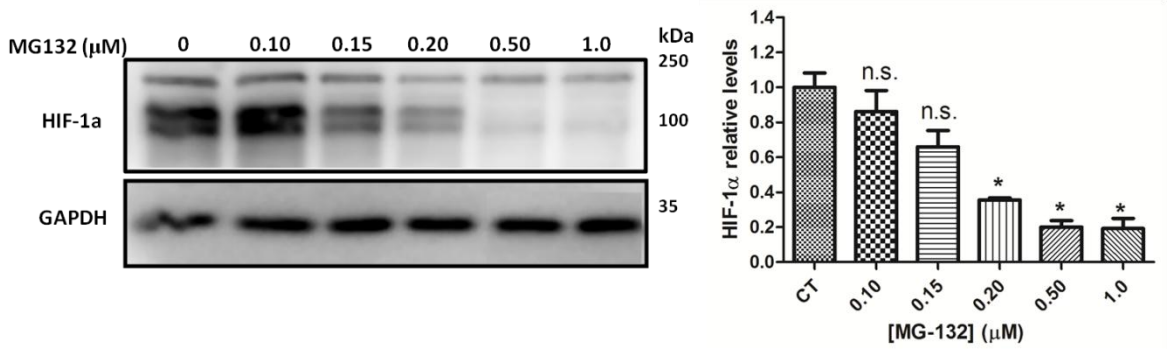

Figure 4.5 – Proteasome inhibition with MG-132 decreases HIF-1α protein levels. ARPE-19 cells were treated with 0.10, 0.15, 0.20, 0.50 and 1.0μM of MG-132 for 48h. The protein levels of HIF-1α were assessed in total cell lysates by Western Blotting against correspondent antibodies. GAPDH was used as loading control. All the results represent the mean ± SEM of at least four independent experiments. n.s. non-significant; *p < 0.05 significantly different from control, Student's t test followed by Mann-Whitney test.

In order to investigate whether the increase in LC3-II and the decrease in HIF-1α observed upon proteasome inhibition is due to macroautophagy activation, we assessed the levels of another autophagy marker, the Sequestosome 1 (SQSTM1/p62). SQSTM1/p62 is one of the best known autophagic substrates and is therefore widely used as an indicator of autophagic degradation (Mizushima & Yoshimori, 2007; Sahani, Itakura, & Mizushima, 2014). It can interact with LC3, through its LC3-interacting region (LIR). SQSTM1/p62 is able to translocate not only to the phagophore membrane but also to the autophagosome formation site. Therefore, it is selectively incorporated into the autophagosome and then degraded (Pankiv et al., 2007; Sahani et al., 2014).

Additionally, SQSTM1/p62 serves as a shuttling factor for the delivery of ubiquitinated substrates to the proteasome through its UBA domain (Seibenhener et al., 2004). SQSTM1/p62 is also the best-characterized and ubiquitously expressed autophagy receptor that connects proteasomal clearance with lysosomes (Korolchuk, Menzies, & Rubinsztein, 2009; Viiri et al., 2013).

In this context we evaluated the SQSTM1/p62 levels by Western blot (Figure 4.6A), as well as the distribution of SQSTM1/p62 and ubiquitin in treated ARPE-19 cells by Immunocytochemistry (Figure 4.6B). In our results, SQSTM1/p62 accumulated due MG-132-induced proteasomal inhibition. The protein levels of SQSTM1/p62 were increased

in more than 10 times at 0.20µM (11.950±5.499, p=0.0117) comparing with non-treated cells (1.000±0.02).

By Immunocytochemistry, we also observed an increased immunoreactivity for SQSTM1/p62, as well as for ubiquitinated proteins in MG-132 treated cells. Furthermore we assessed the localization of ubiquitin and SQSTM1/p62 within the cells, which showed a remarkable co-localization for these two proteins when exposed to 0.20µM of MG-132.

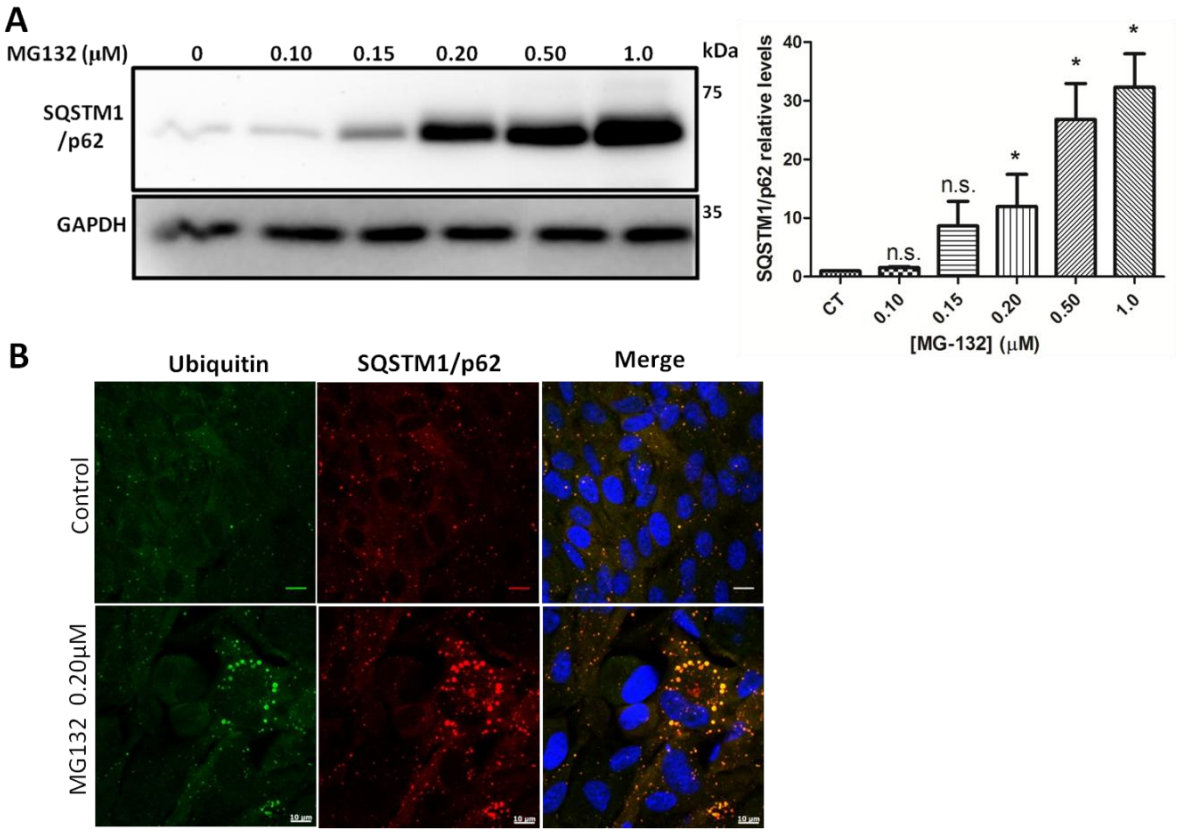

Figure 4.6 – MG-132-induced proteasomal inhibition increases SQSTM1/p62 protein levels, which co-localize with ubiquitin conjugates. ARPE-19 cells were treated with 0.10, 0.15, 0.20, 0.50 and 1.0µM of MG-132 for 48h. **(A)** Protein levels of SQSTM1/p62 were measured in total cell lysates by Western Blotting. GAPDH was used as loading control. All the results represent the mean ± SEM of at least five independent experiments. n.s. non-significant; *$p < 0.05$ significantly different from control, Student's t test followed by Mann-Whitney test. **(B)** Immunofluorescence microscopy analysis of untreated ARPE-19 cells and cells exposed to 0.20µM of MG-132 for 48h. Cells were immunostained with anti-ubiquitin (green) and anti-SQSTM1/p62 (red) antibodies. Nuclei are marked with DAPI. Original magnification 40x. The scale bar equals to 10µm.

1.3. Proteasomal inhibition leads to increased levels of Cathepsin D

Many previous works have proposed that autophagy is associated with CatD (Hah et al., 2012; Wang, Lukas, Yuan, & Du, 2009). Cathepsins are the most studied lysosomal proteases that participate in autophagic degradation; in RPE cells the most abundant is cathepsin D (CatD) (A. L. Wang et al., 2009a). One essential step of autophagy is the fusion of autophagosomes with lysosomes, where CatD plays a key role as the major lysosomal protease in RPE cells. Moreover, it has been suggested that CatD might activate autophagy to enhance cell survival under oxidative stress (Hah et al., 2012). There are several forms of CatD including the precursors (the immature, inactive pre-pro-cathepsin, 52 kDa and the intermediate pro-cathepsin, 48 kDa), and the mature form (mature, active, 34 and 14 kDa dimmer). We next investigated whether MG-132 treatment altered the activity of lysosomal proteases.

Based on Western blotting for CatD, we were able to detect the intermediate form (48 kDa) and the mature form (34 kDa) (Figure 4.7). Interestingly, the precursor forms of CatD increased after the MG-132 exposure in a dose-dependent manner up to 0.20μM (3.532±1.117, p=0.0143), in comparison with control (1.000±0.005). However, concentrations of MG-132 above 0.2μM significantly decreased the protein levels of CatD precursors. The mature form of CatD also exhibited the same tendency, but slightly than the precursor forms. Only at 0.20μM of MG-132 (1.379±0.198, p=0.0473) the mature CatD levels were significantly different than the control (1.000±0.012).

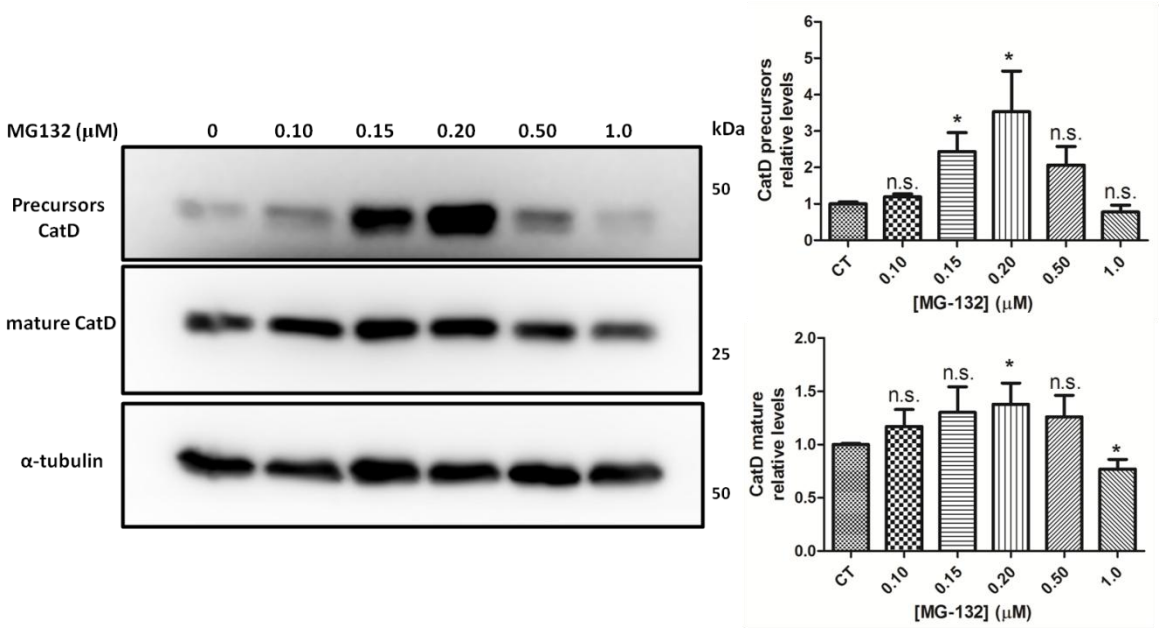

Figure 4.7 –MG-132-induced proteasome inhibition induces increased CatD protein levels. ARPE-19 cells were treated with 0.10, 0.15, 0.20, 0.50 and 1.0μM of MG-132 for 48h. The protein levels of precursor and mature forms were assessed in total cell lysates by Western Blotting against CatD antibody. GAPDH was used as loading control. All the results represent the mean ± SEM of at least six independent experiments. n.s. non-significant; *$p < 0.05$ significantly different from control, Student's t test followed by Mann-Whitney test.

2. The role of autophagy activity in conditions of proteasome inhibition

2.1. BafA1 does not alter MG-132-induced proteasomal inhibition

Our data above strongly indicate that MG-132-induced proteasome inhibition leads to an increase in autophagy and lysosomal activity in ARPE-19 cells. To better understand the contribution of the autophagy-lysosomal pathway, we inhibited lysosomal function using BafA1, a specific inhibitor of vacuolar-type H^+ ATPase. BafA1 blocks autophagic degradation but does not affect autophagosome formation (Yamamoto et al., 1998).

In this context, we exposed ARPE-19 cells to 0.20μM MG-132, since it was the lowest concentration that effectively inhibited proteasome activity and exhibited the most significant results in ubiquitin conjugates, CDKN1A and LC3 reported above studies. We examined the effects of MG-132 in the presence and absence of BafA1, which was added to cells in the last 6h or 1h of the experiment.

As a first approach, we employed the MTT assay to assess cytotoxicity of BafA1 and MG-132 on ARPE-19 cells, as shown in Figure 4.8. The results obtained showed that these treatments did not induce cytotoxicity.

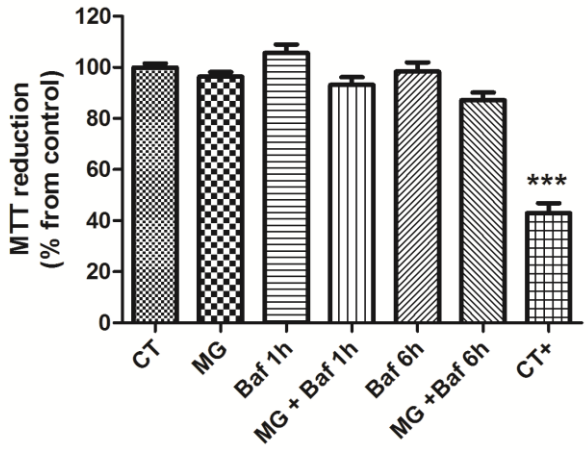

Figure 4.8 –Toxic effects of MG-132 and BafA1 on ARPE-19 cells. ARPE-19 cells were exposed to 0.20μM MG-132 for 48h, in the presence or absence of 50nM BafA1 for 1h or 6h. Positive controls were performed adding 1mM H_2O_2 to non-treated cells in the last 2h of the experiments. Cytotoxicity was determined by MTT assay. Data are expressed as percentage of the control and represent the mean ± SEM of three independent experiments (each one was done in quadruplicates). *$p < 0.05$; ***$p < 0.001$ significantly different from control, 1way ANOVA followed by Bonferroni´s *Post-hoc* test.

Then we wanted to explore the effect of the co-treatment of MG-132 and Baf1 on the ubiquitin conjugates and proteasome substrate CDKN1A/p21 in RPE cells. Therefore, we measured the protein levels of ubiquitin conjugates in ARPE-19 cells by Western blot, as shown in Figure 4.9.

The results confirmed that MG-132 leads to an accumulation of ubiquitin conjugates, as we had previously observed. Moreover, BafA1 did not affect the formation of ubiquitin conjugates, since there were not significant differences between control (1.000±0.043) and BafA1 1h (1.341±0.093) or BafA1 6h (1.477±0.088). As expected, there were no significant differences in the levels of ubiquitin conjugates both when cells were exposed to MG-132+BafA1 for 1h (2.778±0.778) or 6h (2.953±0.678) compared with cells exposed to MG-132 alone (2.935±0.430).

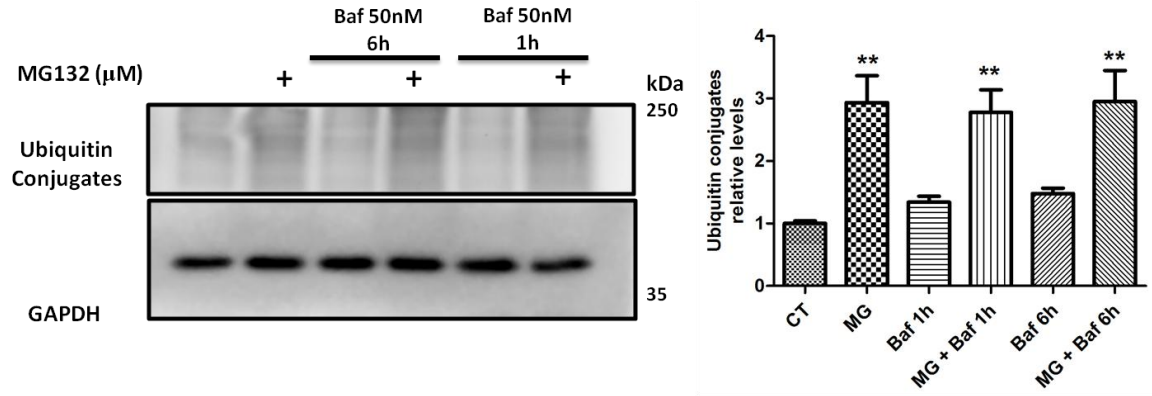

Figure 4.9 –BafA1 does not alter ubiquitin conjugates formation. ARPE-19 cells were exposed to 0.20μM MG-132 for 48h, in the presence or absence of 50nM BafA1 for 1h or 6h. The protein levels of ubiquitin conjugates were assessed in total cell lysates by Western Blotting against ubiquitin (P4D1 antibody). GAPDH was used as loading control. All the results represent the mean ± SEM of at least five independent experiments. *p < 0.05; **p < 0.01 significantly different from control, 1way ANOVA followed by Bonferroni´s *Post-hoc* test.

The protein levels of CDKN1A/p21 were also analyzed (Figure 4.10). As expected, CDKN1A/p21 accumulated when cells were exposed to MG-132, alone (3.284±0.551) or with BafA1 at both 1h (3.205±0.710) and 6h (3.473±0.438). However, there were no significant differences between control (1.000±0.024) and BafA1 1h (1.436±0.152) or BafA1 6h (1.616±0.276), suggesting that CDKN1A/p21 is not degraded by autophagy in ARPE-19 cells.

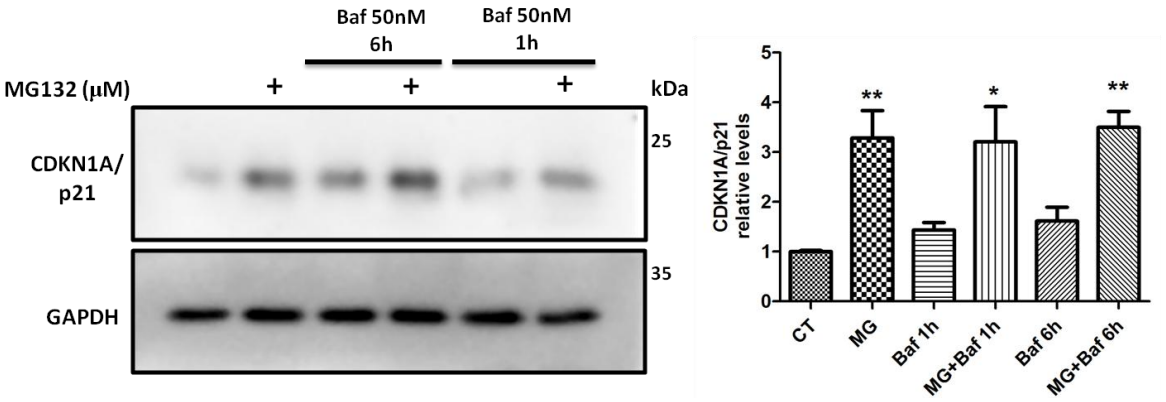

Figure 4.10 –CDKN1A/p21 is degraded by the proteasome in ARPE-19 cells. ARPE-19 cells were exposed to 0.20μM MG-132 for 48h, in the presence or absence of 50nM BafA1 for 1h or 6h. The protein levels of CDKN1A/p21 were assessed in total cell lysates by Western Blotting against correspondent antibodies. GAPDH was used as loading control. All the results represent the mean ± SEM of at least five independent experiments. *p < 0.05; **p < 0.01 significantly different from control, 1way ANOVA followed by Bonferroni´s *Post-hoc* test.

2.2. Enhancement of autophagic flux by exposure of RPE cells to MG-132

Our previous data showed that MG-132 led to an increase in autophagy, as revealed by the results of LC3-II (Figure 4.4), HIF-1α (Figure 4.5) and SQSTM1/p62 (Figure 4.6). In order to evaluate whether autophagy is regulated when the proteasome is inhibited, we exposed the cells both to MG-132 and BafA1 and assessed the levels of autophagic markers LC3-II and SQSTM1/p62, as well as HIF-1α.

By Western blot, we evaluated the protein levels of LC3, as represented in Figure 4.11. LC3-II protein levels, a measure of autophagy dynamics, are shown in the graphic.

Similarly to what previously observed, MG-132 induced autophagy. LC3-II doubled in cells exposed to MG-132 alone (2.103±0.286). Incubation of ARPE-19 cells with BafA1 for 1h (4.258±0.870) caused accumulation of LC3-II, which is even higher in MG + Baf 1h (4.716±1.062). The same happened when the exposure time to BafA1 was extended to 6h, with the protein levels of LC3-II being significantly different from control (Baf 6h (6.720±1.014) and MG+Baf 6h (7.500±1.457)).

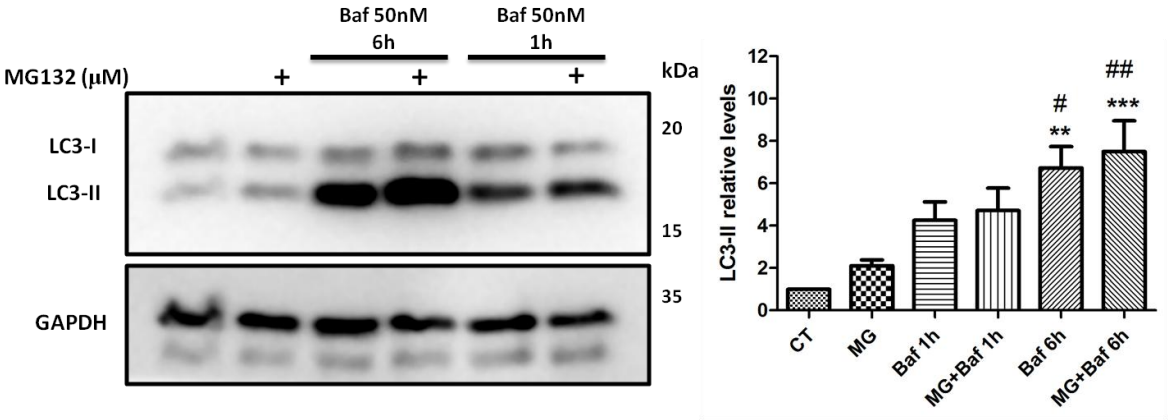

Figure 4.11 – Enhancement of autophagic flux by exposure of RPE cells to MG-132: measuring of autophagic marker LC3-II protein levels. ARPE-19 cells were exposed to 0.20μM MG-132 for 48h, in the presence or absence of 50nM BafA1 for 1h or 6h. The protein levels of LC3 (LC3-I and LC3-II) were assessed in total cell lysates by Western Blotting against the correspondent antibody. GAPDH was used as loading control. All the results represent the mean ± SEM of at least six independent experiments. **p < 0.01; ***p < 0.001 significantly different from control, # p < 0.05; ## p < 0.01 significantly different from 0.20μM MG-132, 1way ANOVA followed by Bonferroni´s *Post-hoc* test.

Accordingly to our previous results, HIF-1α protein levels decreased when ARPE-19 cells were exposed to MG-132 (0.523±0.088), comparing with control (1.000±0.001) (Figure 4.12). Incubation with BafA1 led to a considerable increase at 6h (5.399±1.177), which was diminished when the cell medium contained the proteasome inhibitor (4.443±1.056). For 1h of BafA1 the tendency is the same, but the levels of HIF-1α were not so high (Baf 1h (2.868±0.638) and MG + Baf1h (2.424±0.485)).

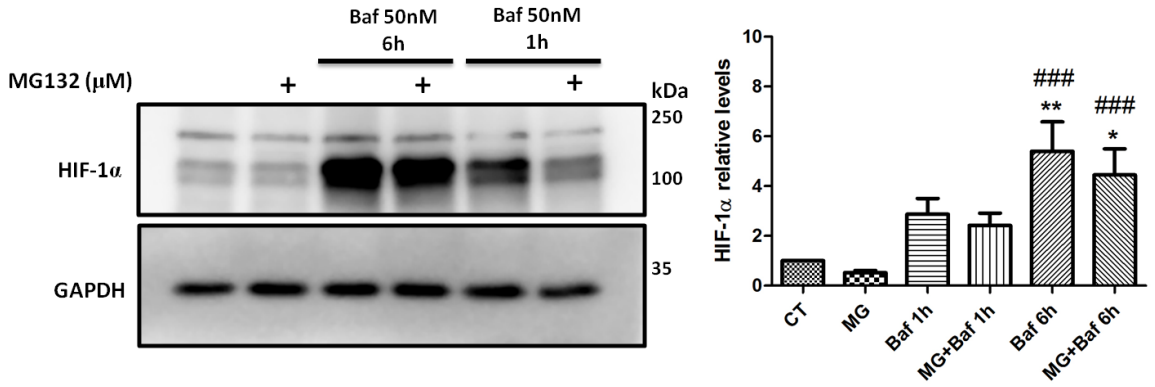

Figure 4.12 – HIF-1α seems to be an autophagic substrate in RPE cells. ARPE-19 cells were exposed to 0.20μM MG-132 for 48h, in the presence or absence of 50nM BafA1 for 1h or 6h. The protein levels of HIF-1α were assessed in total cell lysates by Western Blotting against correspondent antibodies. GAPDH was used as loading control. All the results represent the mean ± SEM of at least five independent experiments. *p < 0.05; **p < 0.01 significantly different from control, ### p < 0.001 significantly different from 0.20μM MG-132, 1way ANOVA followed by Bonferroni´s *Post-hoc* test.

In order to investigate the effect of MG-132 and BafA1 in SQSTM1/p62, its protein levels and distribution in the ARPE-19 cells were evaluated by Western blot and immunocytochemistry, respectively (Figure 4.13A and B).

A significant increase in SQSTM1 levels was observed in RPE cells incubated with MG-132 (Figure 4.13A). The protein levels of SQSTM1/p62 were very similar in the cells were incubated with MG-132 alone (9.074±2.137) or in the presence of BafA1 (MG+Baf1h (8.105±1.810) and MG+Baf6h (8.520±1.621)). The use of BafA1 prevented the autophagic flux, which seems to cause a slightly and probably time-dependent accumulation of SQSTM1/p62.

Immunocytochemistry experiments performed in fixed ARPE-19 cells confirmed the previous results (Figure 4.13B). We observed an increased immunoreactivity for SQSTM1/p62, as well as for ubiquitinated proteins in MG-132 treated cells. In comparison to control cells, MG-132 induced an increased immunoreactivity for SQSTM1/p62 mainly in the nuclear/perinuclear compartment and also in the cytoplasm (Figure 4.13B). The localization of ubiquitin and SQSTM1/p62 showed a remarkable co-localization for these two proteins in both BafA1 and MG-132 treatments, mainly at 0.20μM of MG-132. In this condition the cells exhibit a strong punctate staining.

In its turn, BafA1 led to reduced immunoreactivity for ubiquitin and SQSTM1/p62 comparing with MG-132; however, the staining for these two proteins was higher than in the untreated cells. The use of the autophagy inhibitor caused a more diffuse staining; however the co-localization of the two proteins is still very evident.

Additionally, we observed an intermediate situation when the cells were treated with both proteasome and lysosomal activity inhibitors. In this condition, immunofluorescence of ARPE-19 cells with ubiquitin and SQSTM1/p62 showed a less diffuse staining than when incubated only with BafA1. We identify several distinct bright spots of colocalization for the two proteins, but the intensity of the signal is lower than with MG-132.

To determine whether the observed accumulation in SQSTM1/p62 is due to an increase in the protein synthesis or a decrease in its degradation, we treated ARPE-19 cells with MG-132 and/or BafA1 in the presence of the inhibitor of protein biosynthesis, CHX. SQSTM1/p62 protein levels were assessed by Western Blotting (Figure 4.13C).

As previously observed, MG-132 induced an increase in SQSTM1/p62 protein levels, both in the presence or absence of BafA1. When we added the protein synthesis inhibitor CHX, this increase disappeared, indicating that an enhanced protein synthesis is the cause of MG-132-induced accumulation of SQSTM1/p62. This effect was observed either with 1μg/mL and 5μg/mL of CHX and appears to be CHX-concentration dependent. At 5μg/mL CHX the protein levels of SQSTM1/p62 were very similar to control.

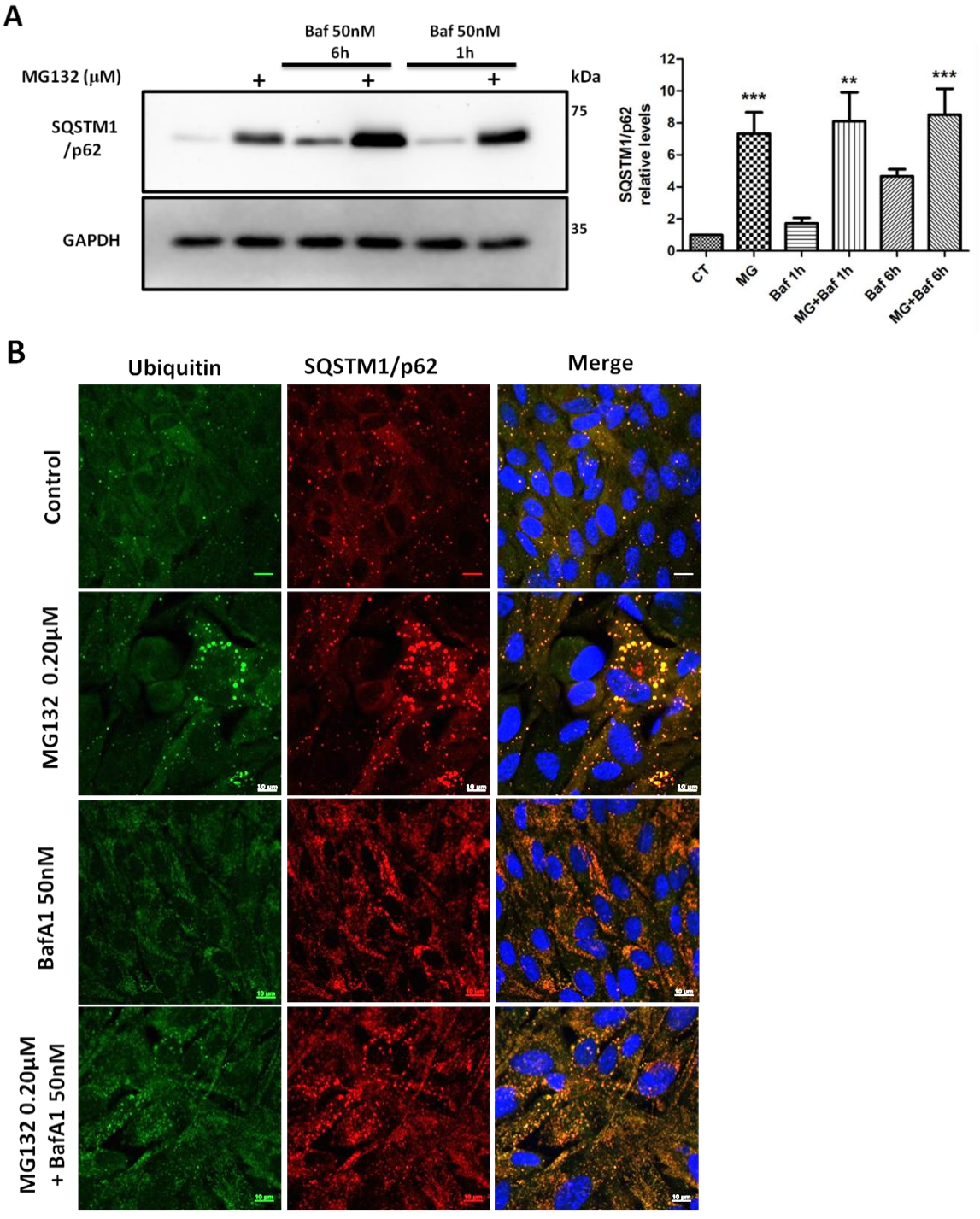
A
Baf 50nM 6h
Baf 50nM 1h
MG132 (μM)
+
+
+
kDa
SQSTM1 /p62
75
GAPDH
35
SQSTM1/p62 relative levels
12
10
8
6
4
2
0
***
**
***
CT
MG
Baf 1h
MG+Baf 1h
Baf 6h
MG+Baf 6h
B
Ubiquitin
SQSTM1/p62
Merge
Control
MG132 0.20μM
BafA1 50nM
MG132 0.20μM + BafA1 50nM
C
SQSTM1/p62 relative levels
7
6
5
4
3
2
1
0
CT
MG 0.20uM
###
###
CHX 1ug/ml
CHX 5ug/ml
CHX 1ug/ml
CHX 5ug/ml
MG 132 0.20uM
BafA1 50nM
kDa
SQSTM1/ p62
75
GAPDH
35

Figure 4.13 – Proteasome inhibition leads to ubiquitin and SQSTM1/p62 perinuclear aggregates and the accumulation of SQSTM1/p62 is due to increased protein synthesis. ARPE-19 cells were exposed to 0.20μM MG-132 for 48h, in the presence or absence of 50nM BafA1 for 1h or 6h. **(A)** Protein levels of SQSTM1/p62 were measured in total cell lysates by Western Blotting. GAPDH was used as loading control. All the results represent the mean ± SEM of at least six independent experiments. **p < 0.01; ***p < 0.001 significantly different from control, 1way ANOVA followed by Bonferroni´s *Post-hoc* test. **(B)** Immunofluorescence microscopy analysis of untreated ARPE-19 cells and cells exposed to 0.20μM MG-132 for 48h, in the presence or absence of 50nM BafA1 for 6h. Cells were immunostained with anti-ubiquitin (green) and anti-SQSTM1/p62 (red) antibodies. Nuclei are marked with DAPI. Original magnification 40x. The scale bar equals to 10μm. **(C)** ARPE-19 cells incubated with 0.20μM MG-132 for 48h and/or 50nM BafA1 for 6h were exposed to 1μg/mL and 5μg/mL of CHX during the time of MG-132 and BafA1 treatment. The protein levels of SQSTM1/p62were assessed in total cell lysates by Western Blotting. GAPDH was used as loading control. All the results represent the mean ± SEM of at least three independent experiments. ### p < 0.001 significantly different from control 0.20μM MG-132, 2way ANOVA followed by Bonferroni´s *Post-hoc* test.

2.3. MG-132 and BafA1 induce increased levels of CatD precursors

Based on our previous results, inhibition of the proteasome with 0.20μM MG-132 led to an increase in both precursor and mature forms of CatD. At this concentration we found raised protein levels of autophagy markers LC3 and SQSTM1/p62. All the results pointed to a concomitant stimulation of autophagy and enhanced lysosomal activity induced by low concentration of the proteasome inhibitor MG-132.

To test this hypothesis, we determined the protein levels of CatD forms when the cells were incubated with MG-132 and/or BafA1 (Figure 4.14). ARPE-19 cells exposed to MG-132 exhibited increased levels of CatD precursor (3.405±0.639) and mature form (1.286±0.123), although in this latter the difference to the control was very small. As expected, BafA1 did not alter CatD protein levels, since lysosome was alkalized and lysosomal activity impaired. Interestingly, co-treatment of cells induced a significant increase of CatD precursors levels in comparison to control cells, but no significant differences were observed when compared with MG-treated cells. In its turn, the mature form of CatD appeared to exhibit the same tendency. However, the differences are so slight that is difficult to ensure the MG-132-induced CatD increase, which may indicate an effort of the cell to enhance active CatD formation and thus improve lysosomal activity.

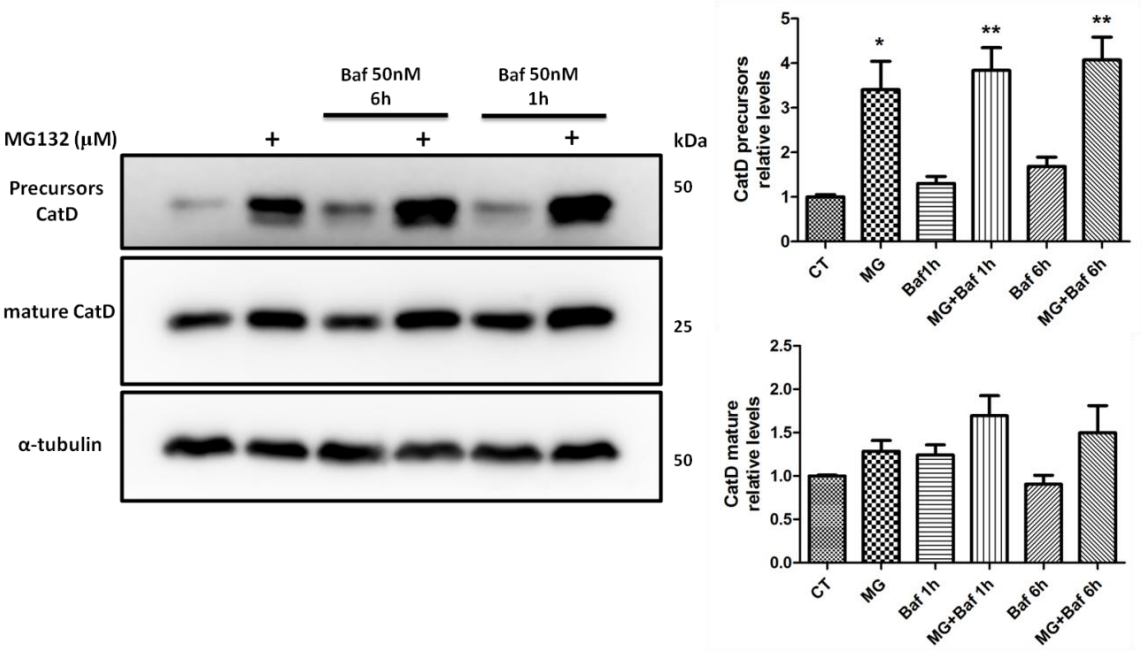

Figure 4.14 – Effect of MG-132 and BafA1 in lysosomal activity in ARPE-19 cells. ARPE-19 cells were exposed to 0.20µM MG-132 for 48h, in the presence or absence of 50nM BafA1 for 1h or 6h. The protein levels of precursor and mature forms were assessed in total cell lysates by Western Blotting against CatD antibody. GAPDH was used as loading control. All the results represent the mean ± SEM of at least six independent experiments **p < 0.01 significantly different from control; 1way ANOVA followed by Bonferroni´s *Post-hoc* test.

3. Concomitant autophagy activation and UPP inhibition in RPE cells as a model of AMD

3.1. Autophagy activation with starvation and rapamycin

In RPE cells, simultaneously with proteasome impairment, activation of autophagy has been described to play an important role in AMD development (A. L. Wang, Lukas, Yuan, Du, Handa, et al., 2009; A. L. Wang, Lukas, Yuan, Du, Tso, et al., 2009). Recent evidences suggest that these events are intrinsically linked with age, where inactivation of the proteasome leads to enhanced autophagy. Moreover, oxidative stress, hypoxia, the unfolded protein response or inflammation can activate autophagy, and are present in AMD pathology (Kaarniranta et al., 2013).

In order to further explore the crosstalk between UPP and autophagy in RPE cells, we first examined the autophagy induced by starvation (by culturing cells in DMEM:F12 without FBS) or rapamycin (a mTOR inhibitor). As a first approach, we determined the optimal conditions of starvation, by culturing the ARPE-19 cells in DMEM:F12 medium without FBS up to 24h. Autophagy markers LC3II and SQSTM1/p62 protein levels were analyzed by Western Blotting (Figure 4.15). Starvation induced LC3-II with a maximal accumulation at 6h, which indicates an activation of autophagy. However, above 6h of starvation (1.266±0.241), autophagy clearance was impaired since LC3-II levels decreased in a time-dependent manner. Accordingly, the autophagic substrate SQSTM1/p62 levels decreased in cells starved up to 6h (0.674±0.049); after this time point, the prolonged nutrient deprivation in RPE cells led to a time-dependent autophagy inhibition and consequent inefficient SQSTM1/p62 degradation.

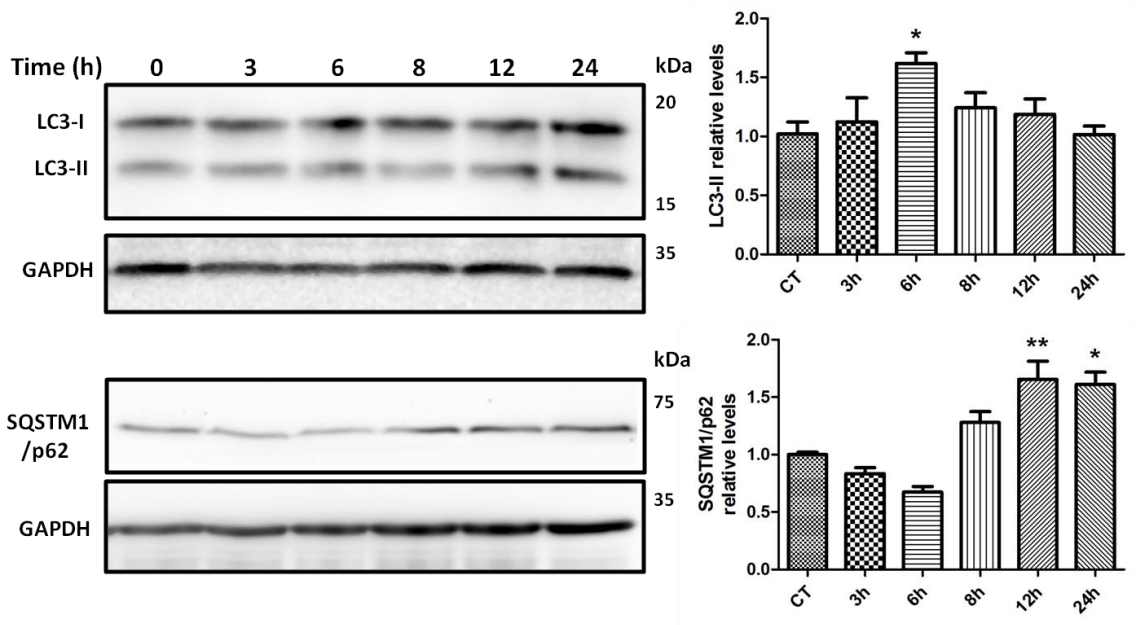

Figure 4.15 – Serum starvation-triggered autophagy: time-course evaluation of autophagy by measuring the autophagic markers LC3-II and SQSTM1/p62 protein levels. ARPE-19 cells were cultured in serum-free medium for 3h, 6h, 8h, 12h and 24h. The protein levels of LC3 (LC3-I and LC3-II) and SQSTM1/p62 were assessed in total cell lysates by Western Blotting against the correspondent antibodies. GAPDH was used as loading control. All the results represent the mean ± SEM of at least three independent experiments, *p < 0.05, **p < 0.01 significantly different from control; 1way ANOVA followed by Bonferroni´s *Post-hoc* test.

Next, we assessed the autophagic flux when cells were starved or incubated with rapamycin, by using BafA1 to block autophagic degradation and thus verify if the autophagy inducers caused enhanced autophagosome formation. Taking into account the previous results, starvation was performed by culture the RPE cells in serum-free medium for 6h. The protein levels of SQSTM1/p62 and LC3-II were measured by Western blotting, as shown in Figure 4.16.

RPE cells treated with autophagy activators exhibited an increase in the autophagic flux. As expected, both starvation and rapamycin decreased the BafA1-induced SQSTM1/p62 accumulation, indicating an enhanced degradation of this protein in the presence of those activation inducers. Furthermore, LC3-II protein levels increased with BafA1, and a concomitant treatment with rapamycin or starvation resulted in even higher LC3-II protein levels. Starvation or rapamycin alone was also able to increase LC3-II levels comparing with the control, strongly indicating that these autophagy inducers effectively enhanced the autophagic flux.

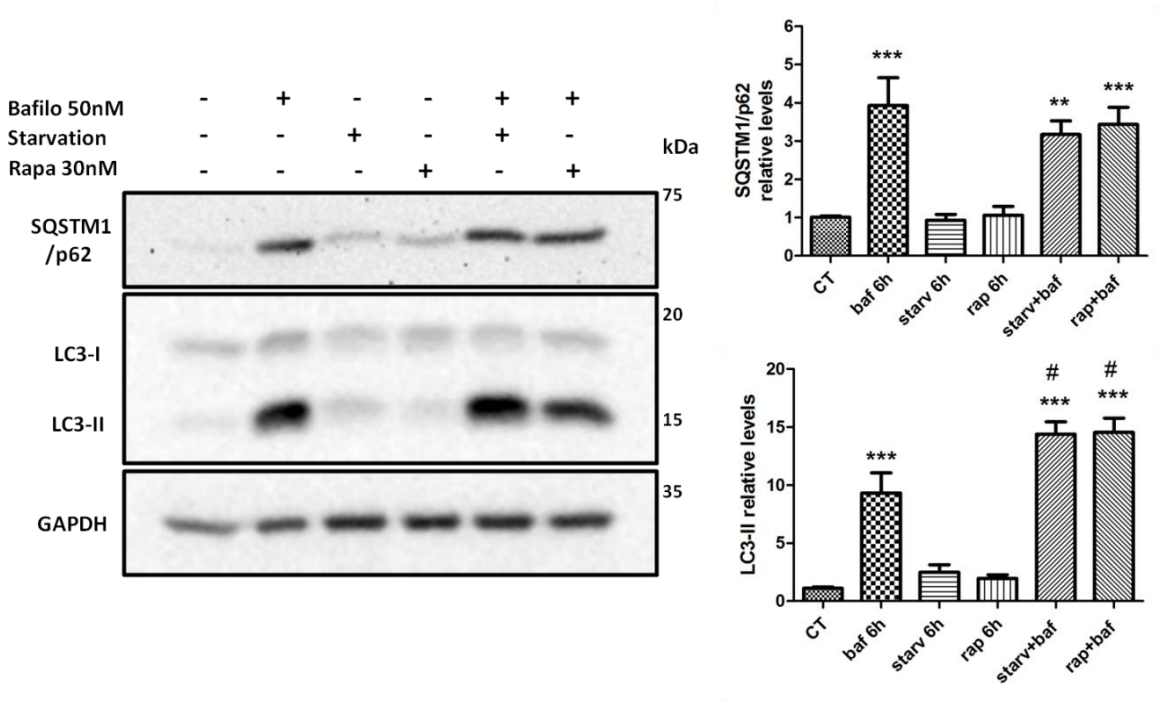

Figure 4.16 – Enhancement of autophagic flux by exposure of RPE cells to starvation and rapamycin: measuring of autophagic markers SQSTM1/p62 and LC3-II protein levels. ARPE-19 cells were exposed to 30nM rapamycin or cultured in serum-free medium for 6h, in the presence or absence of 50nM BafA1. The protein levels of SQSTM1/p62 and LC3 (LC3-I and LC3-II) were assessed in total cell lysates by Western Blotting against correspondent antibodies. GAPDH was used as loading control. All the results represent the mean ± SEM of at least four independent experiments. *p < 0.05; **p < 0.01; ***p < 0.001 significantly different from control, 1way ANOVA followed by Bonferroni´s *Post-hoc* test.

3.2. Simultaneous autophagy stimulation and UPP inhibition increases autophagic clearance but not SQSTM1/p62 degradation in RPE cells

Despite the known decline in autophagy clearance with aging (Cuervo, 2008), growing evidence suggests that RPE cells exhibit an autophagy enhancement in AMD (A. L. Wang et al., 2009a; A. L. Wang et al., 2009b). One possible explanation is the inducible nature of autophagic function and the presence of several compensatory adaptations within the system (Grune, Jung, Merker & Davies, 2004).

One of the mechanisms that is responsible for the autophagy activation in AMD is the proteasomal inhibition. The decreased activity of proteasomal degradation as well as the reduced turnover rates during aging can expose proteins to age-related modifications, such as protein carbonyl formation and aggregation, which can increase the pressure on the autophagic system (Salminen & Kaarniranta, 2009). Moreover, autophagy clearance can be stimulated by oxidative stress, hypoxia and inflammation, all present in the pathophysiology of AMD (Kaarniranta et al., 2013).

In this context we exposed ARPE-19 cells simultaneously to both MG-132 and one of the tested autophagy inducers (rapamycin or starvation). In these conditions, we guarantee proteasomal inhibition and autophagy activation in RPE cells, as it occurs in AMD. SQSTM1/p62 and LC3 protein levels were assessed by Western blot and are represented in Figure 4.17.

As previously observed, MG-132 revealed to induce autophagy. The increase on LC3-II protein levels in cells treated with MG-132 (1.385±0.086) is similar to that induced by rapamycin (1.451±0.152). Starvation was the most effective autophagy inducer (2.352±0.334). Concomitant treatment of RPE cells with MG-132 and starvation led to the highest LC3-II levels, indicating strong autophagy stimulation (3.103±0.381).
As shown in our previous results, proteasomal inhibition with MG-132 led to an accumulation of SQSTM1/p62 (1.262±0.081), which is even more pronounced in RPE cells that were co-treated with autophagy inducers (MG+rap (1.709±0.071) and MG+starv (1.855±0.242)). Once more, the data suggest that although SQSTM1/p62 is an autophagic substrate, this protein is not degraded upon proteasome inhibition, even when autophagy is stimulated.

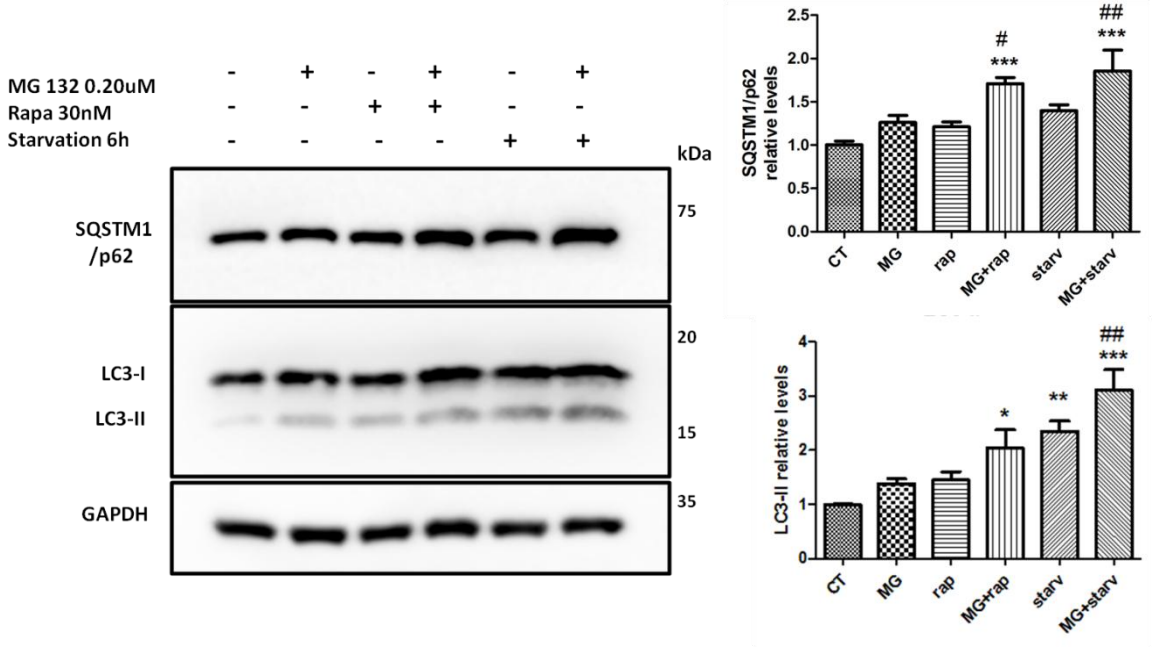

Figure 4.17 – Upregulation of autophagy and accumulation of SQSTM1/p62 by simultaneously inhibiting the UPP and inducing autophagy in RPE cells. ARPE-19 cells were exposed to 0.20μM MG-132 for 48h, in the presence of 30nM rapamycin or cultured in serum-free medium for 6h. The protein levels of SQSTM1/p62 and LC3 (LC3-I and LC3-II) were assessed in total cell lysates by Western Blotting against correspondent antibodies. GAPDH was used as loading control. All the results represent the mean ± SEM of at least three independent experiments. *p < 0.05; **p < 0.01; ***p < 0.001 significantly different from control, # p < 0.05; ## p < 0.01 significantly different from 0.20μM MG-132, 1way ANOVA followed by Bonferroni´s Post-hoc test**.**

CAPTER 4

DISCUSSION

Currently, although there are some therapies available to slow down the progression of the disease, there is no cure for AMD. In the case of geographic atrophy, there are no approved therapies, which is mainly due to the lack of suitable molecular targets. The formation and accumulation of drusens, particularly in the macula, is strongly correlated with the development and progression of the disease (Ambati et al., 2013). Over the past decades a significant effort has been made to understand the mechanisms underlying drusens biogenesis and the involvement of RPE in their formation. Despite the significant knowledge that has been gathered in the last years, the processes that lead to the formation of drusens remain relatively unknown.

Most of the hypotheses have focused on oxidative stress and inflammation. Indeed, previous studies carried out in our lab have suggested that oxidative stress-induced a deregulation (inhibition) of the UPP in the RPE that in turn might contribute to the development of AMD (Fernandes, Ramalho & Pereira, 2006; Fernandes et al., 2008; Fernandes et al., 2009). Since the activity of the proteasome was shown to decrease upon ageing, it is conceivable that impairment of the proteasome-dependent degradation of ubiquitin conjugates leads to increased macroautophagy activity, by diverting UPP substrates to the lysosome.

It is well established that the basal autophagic activity of living cells decreases with age (Marino et al., 2008). There is also an inactivation of the proteasome, probably induced by oxidative stress since the level of proteins modified by oxidation is increased (Louie et al., 2002; Shang and Taylor, 2012). Over the past years, accumulated evidence suggests that UPP decreases in AMD. Our group has shown that inactivation of UPP key mediators in RPE cells led them to acquire the phenotypic alterations associated with AMD, including the neovascular component (Fernandes et al., 2006). The misfolded and damaged proteins are not degraded by UPP, so they aggregate forming the drusen. This study aims to understand the molecular mechanisms and key players intrinsically linked to RPE dysfunction and to evaluate the crosstalk between UPP and autophagy in AMD. In this study, we have used ARPE-19 cells, the most common cell line in human RPE studies (Dunn et al., 1998; Philp, 2003; Wang, Lukas, Yuan, Du, Tso, et al., 2009). As a first approach, proteasomal inhibition was performed by adding to the cells a potent inhibitor of 26S proteasome complex, MG-132 to mimic the chronic UPP inhibition that occurs in AMD (Shang & Taylor, 2012; Kinnunen et al., 2012) Our results showed that treatment with 0.20 uM MG-132 for 48h does not induce any significant cytotoxic effect

and is able to induce significant accumulation of ubiquitin conjugates. MG-132 can therefore block the enzymatic activity of the proteasome without affecting cell viability.

With UPP impairment, the damaged and misfolded proteins that were marked with ubiquitin for proteasomal degradation are not degraded and then accumulate as ubiquitin protein conjugates. Besides the formation of ubiquitin conjugates, proteasome inhibition was also verified by the impaired degradation (and consequent increase in protein levels) of CDKN1A/p21, a known proteasome substrate.

One of the main goals of this work was to investigate the effect of proteasomal inhibition in macroautophagy. LC3-II and Beclin-1, proteins necessary for autophagosome formation are commonly used as markers of autophagy. Bortezomib, a 26S proteasome inhibitor approved for treating multiple myeloma, was shown to increase cellular levels of LC3-II and Beclin-1 proteins in human glioblastoma U251 and U87 cells (Zhang et al., 2014), melanoma cells (Selimovic et al., 2013), several cell lines of head and neck squamous cell carcinoma (Li and Johnson, 2012) and human osteosarcoma (HOS) cells (Lou et al., 2013; Wojcik, 2013). This data indicate that inhibition of proteasomal activities used to induce cell death caused enhanced autophagy. Based on these data, we assessed the LC3-II protein levels of RPE cells subjected to chronic proteasomal inhibition. Our results show that LC3-II accumulates in cells incubated with MG-132, suggesting an MG-132-induced increase in autophagy. LC3 is, in fact, widely used to monitor autophagy, since LC3-II conversion is correlated with the number of autophagosomes. However, one should be very careful in the interpretation of the results of LC3 immunobloting, since there are several factors that affect autophagic activity and LC3 conversion: LC3-II itself is degraded by autophagy; the levels of LC3 –II at a certain time point do not indicate the autophagic flux. Therefore, it is important to measure the amount of LC3-II in the presence and absence of lysosomal protease inhibitors, as well as, the degradation of autophagic substrates.

Recently our group has shown that HIF-1α can be degraded by alternative pathways (Ferreira et al., 2013). Besides being a well-established substrate of the UPP, HIF-1α can also be targeted for degradation in the lysosome through CMA (Ferreira et al., 2013). This targeting is dependent on its interaction with the ubiquitin ligase STUB1 (co-chaperone STIP1 homology and U-box containing protein 1), which mediates the ubiquitinylation and subsequent degradation of HIF-1α in an oxygen-independent manner (Bento et al., 2010). It was found that the human, mouse and rat HIF-1α all have the pentapeptide sequence biochemically related to the KFERQ motif, required for a protein

to be a substrate for CMA. This motif is responsible for direct HIF-1α to CMA by recruitment of HSPA8 and the STUB1, which targets proteins for ubiquitinylation and subsequent proteasomal degradation. The results from our lab show that STUB1 is required for degradation of HIF-1α by CMA, ultimately resulting in an increased interaction of HIF-1α with the CMA receptor LAMP2A (Ferreira et al., 2013). Lysosomal inhibitors, but not macroautophagy inhibitors induce the accumulation of HIF-1α (Ferreira et al., 2013). CMA-mediated degradation of HIF-1α is activated by nutrient deprivation, affecting the cell survival under hypoxic conditions (Ferreira et al., 2013).

Accordingly, we found reduced HIF-1α protein levels in RPE cells due proteasomal inhibition. HIF-1α decreased after the MG-132 exposure in a dose-dependent manner, being this reduction significantly different above 0.20μM. Taking this in account, we admit that HIF-1α may be degraded by another pathway than the UPP in RPE cells, probably by CMA.

To ensure that the increase in LC3-II and reduction of HIF-1α protein levels observed upon proteasome inhibition are caused by macroautophagy activation, we assessed the levels of another autophagy marker, the SQSTM1/p62. SQSTM1/p62 is specifically degraded by autophagy (Komatsu et al., 2007; Pankiv et al., 2007). The protein possesses a short LC3-interacting region (LIR) that facilitates direct interaction with LC3 and GABARAP (Gamma-aminobutyric acid receptor-associated protein) family proteins. Because its degradation is dependent on autophagy, the level of p62 increases in response to inhibition of autophagy (Bjørkøy et al., 2005). Accumulation of SQSTM1/p62 has been used as a marker for autophagy inhibition or defects in autophagic degradation (Bjørkøy, Lamark, & Johansen, 2006; Bjørkøy et al., 2005; Komatsu et al., 2007; Mizushima & Yoshimori, 2007). The protein accumulates in cells and tissues from autophagy-deficient mice (Komatsu et al., 2004; Nakai et al., 2007). SQSTM1/p62 is also used as a marker for autophagy induction (Klionsky & Abdalla, 2012; Mizushima & Yoshimori, 2007; Tasdemir, Galluzzi, & Maiuri, 2008). SQSTM1/p62 contains an N-terminal Phox and Bem1 (PB1) domain for self-oligomerization, where an acidic surface of one p62 PB1 domain binds to a basic surface in the next p62 PB1 domain. The PB1 domain seems to be needed for the autophagic degradation of SQSTM1/p62 (Lamark et al., 2003; Wilson et al., 2003).

Although the proteasome inhibitor MG-132 induced accumulation of LC3-II, we verify that it significantly increased the autophagy-specific substrate SQSTM1/p62

protein levels in RPE cells. Accumulation of SQSTM1/p62 is concentration-dependent on MG-132 loading and was verified by both Western blotting and immunofluorescence.

Interestingly, the protein levels of SQSTM1/p62 were restored when CHX (an inhibitor of protein synthesis) was added to the cells, suggesting that this increase in SQSTM1/p62 protein content was caused by an enhanced protein synthesis. This result is corroborated by Viiri *et al.* (2013) recent study, which reports up-regulation, at both mRNA and protein levels of ELAVL1/HuR (embryonic lethal, abnormal vision, Drosophila)-like 1 (Hu antigen R) under MG-132 treatment in ARPE-19 cells. ELAVL1/HuR protein is a post-transcriptional factor, which acts mainly as a positive regulator of gene expression by binding to specific mRNAs whose corresponding proteins are fundamental for key cellular functions. ELAVL1/HuR binds and post-transcriptionally regulates SQSTM1/p62 mRNA in RPE cells (Viiri et al., 2013).

Our next step was to investigate whether MG-132 treatment altered the activity of lysosomal proteases. We measured the protein levels of the most abundant lysosomal protease that participate in autophagic degradation in RPE cells, cathepsin D. CatD is essential in the fusion of autophagosomes with lysosomes, actively participating in the autophagic degradation within lysosomes. CatD has been characterized in RPE cells (Im & Kazlauskas, 2007), being its main responsibility the degradation of POS and rhodopsin into glycopeptides within the RPE lysosomes (el-Hifnawi, 1995; Kaarniranta et al., 2013). Furthermore, there is evidence indicating that CatD stimulates autophagy activation to inhibit stress-induced cell death in cancer cells (Hah et al., 2012).

As previously referred, there are several forms of cathepsin D including the precursors (the immature pre-pro-cathepsin, 52 kDa and the intermediate pro-cathepsin, 48 kDa), and the mature form (mature, 34 and 14 kDa dimmer). We found increased levels of CatD precursors forms after exposure to growing concentrations of MG-132 up to 0.20μM, concentration from which the CatD precursors start to reduce. The same tendency was verified for CatD mature form. It is difficult to ensure MG-132-induced CatD increase, which may indicate an effort of the cell to enhance active CatD formation and thus improve lysosomal activity. These findings suggest, once more, that MG-132-induced proteasomal inhibition stimulates autophagy lysosomal pathway.

At this point, we observed an increase in endogenous LC3-II protein levels when proteasome was inhibited by MG-132. HIF-1α is reduced in RPE cells upon proteasomal inhibition, suggesting degradation by autophagy. The SQSTM1/p62 protein levels were also greater, in agreement with recent reports (Viiri et al., 2013). Immunocytochemistry analysis revealed that the number of SQSTM1/p62 puncta was substantially higher in ARPE-19 cells exposed with MG-132. Consistent with this, the protein levels of cathepsin D were significantly increased in ARPE-19 cells exposed to 0.20μM MG-132 for 48h. Taken together, this data strongly indicate an enhanced autophagic activity and raised autophagic vacuoles in MG-132 treated cells.

Increases in the prevalence of autophagic vacuoles can be caused by either an increase in autophagosome formation or a decrease in the lysosome-mediated removal. To identity the potential cause, we assessed the autophagic flux, comparing autophagosome prevalence in the presence and absence of lysosomal inhibition by BafA1. Thus, in co-treated cells, the proteasome is inhibited by MG-132 and lysosomes are alkalized due to BafA1 action. The fusion between the autophagosomes and the lysosomes is prevented, making that autophagosomes accumulate, which explains the increase in LC3-II and SQSTM1/p62 usually verified in the presence of BafA1.

The co-treatment of RPE cells with both proteasomal and lysosomal inhibitors did not induce cytotoxicity. As expected, BafA1 did not alter ubiquitin conjugates formation. MG-132 caused similar accumulation of ubiquitin conjugates in the presence and absence of BafA1 in the two times points considered, 1h and 6h. The same occurred with CDKN1A/p21, which indicates that CDKN1A/p21 is not degraded by autophagy in RPE cells.

As widely described (Klionsky & Abdalla, 2012; Mizushima & Yoshimori, 2007; Wang et al., 2009), the autophagic flux was assessed by measuring the LC3-II protein levels in co-treated RPE cells. Previous incubation with MG-132 before BafA1 treatment induced a slight non-significant increase in LC3-II protein levels, comparing with cells only treated with BafA1. This is the measure of autophagic flux (Klionsky & Abdalla, 2012; Klionsky & Elazar, 2008; Mizushima & Yoshimori, 2007) and was observed both at 1h and 6h, when RPE cells exhibit higher LC3-II relative levels. Other studies reported an MG-132-induced increase in LC3-II levels (Viiri et al., 2013).

The BafA1 treatment allowed us to determine that HIF-1α is an autophagic substrate in RPE cells. Incubation with BafA1 led to a considerable increase at 6h which was diminished when the cell medium contained the proteasome inhibitor. This is explained

by the MG-132-induced autophagy, which is responsible for starting the HIF-1α autophagic degradation and thus cause the slight reduce of HIF-1α protein levels in co-treated RPE cells.

To better understand the role of SQSTM1/p62 in the crosstalk between the two proteolytic systems, we analyzed the effect of concomitant treatment with MG-132 and BafA1 in SQSTM1/p62. As Viiri *et* al. previously reported, in our work SQSTM1/p62 protein levels strongly also increases during exposure to MG-132 (Viiri et al., 2013).

Interestingly, by immunocytochemistry, we observed that in comparison to control cells, MG-132 induced an increased immunoreactivity for ubiquitinated proteins mainly in the nuclear/perinuclear compartment and also in the cytoplasm. This result is consist with other studies that described the formation of structures known as 'aggresomes' (Driscoll & Chowdhury, 2012; Tan, Wong, & Dawson, 2008; Wojcik, 2013). Aggresomes are constituted by the accumulation of protein, often polyubiquitinated, which are prone to aggregate due proteasomal inhibition. These structures are predominantly present in perinuclear compartments. They are considered to be a place of selective autophagy of damaged proteins that are isolated from other cytoplasmic components (Kopito, 2000). With MG-132, SQSTM1/p62 and ubiquitinated proteins co-localize almost completely and the immunoreactive puncta were very intense. Furthermore, SQSTM1/p62 exhibits similar staining pattern of the ubiquitin conjugates, both in experiments with different concentrations of MG-132 and co-treatment with MG-132 and BafA1. These results suggest that SQSTM1/p62 binds to ubiquitinated proteins, constituting SQSTM1-ubiquitin aggresomes.

According to our results, SQSTM1/p62 was found to be an ubiquitin-binding scaffold protein that colocalizes with ubiquitinated protein aggregates in many neurodegenerative diseases, liver diseases and myofibrillar myopathies (Kuusisto et al., 2001,2007; Olive et al., 2008). It has been shown to be a missing link combining the functions of the proteasomal and lysosomal clearance systems (Korolchuk et al., 2009). This protein shuttles polyubiquitinated tau for proteasomal degradation (Babu, Geetha, & Wooten, 2005). SQSTM1/p62 can interact with ubiquitinated proteins via the C-terminal ubiquitin-associated (UBA) domain, enabling non-covalent binding to ubiquitin or ubiquitinated substrate proteins (Seibenhener et al., 2004; Viiri et al., 2010). These complexes are then transported for clearance by proteasomes.

The presence of UBA domain enables SQSTM1/p62 to act as a cargo adapter for ubiquitinated proteins that can be degraded by autophagy. Alternatively, ubiquitinated

complexes can be shuttled to lysosomes for autophagocytic degradation when proteasomes are impaired or overwhelmed, (Geetha and Wooten, 2002; Kirkin et al., 2009a). SQSTM1/p62 is an adaptor for selective autophagy of ubiquitinated substrates, since it interacts with LC3 through its LIR region. Mutations in SQSTM1/p62 lacking this region resulted in the formation of inclusion bodies, structures that were also observed during autophagy-deficiency (Pankiv et al., 2007; Ichimura et al., 2008; Viiri et al., 2010). There is emerging evidence that the SQSTM1/p62-ubiquitin protein complexes are being targeted to autophagic degradation (Komatsu et al., 2007; Pankiv et al., 2007). In agreement, both SQSTM1/p62 and LC3 were shown to colocalize with mutant huntingtin aggregates. Such aggregates were recently shown to be degraded by autophagy (Ravikumar et al., 2002, 2004). Studies of conditional knockout mice of Atg7 demonstrated that autophagy is needed for clearance of ubiquitin-positive aggregates (Komatsu et al., 2005).

Our data suggest that SQSTM1/p62 may link poly-ubiquitinated proteins to the autophagic machinery. This function seems be dependent on both the polymerization of SQSTM1/p62 via the NH2 -terminal PB1 domain and polyubiquitin binding via the COOH-terminal UBA domain of SQSTM1/p62 (Bjørkøy et al., 2005; Pankiv et al., 2007).

It is presently unclear whether there is a specific recognition or targeting of polyubiquitinated protein aggregates by the autophagic machinery. In this study, we propose a mechanism of crosstalk between the proteolytic pathways in which SQSTM1/p62 as a key role. Perinuclear ubiquitin aggregates are promoted by MG-132, since the ubiquitin-marked proteins are not degraded when the proteasomal is inhibited. The ubiquitin conjugates bind to SQSTM1/p62, which is sequestered in these SQSTM1-ubiquitin perinuclear aggresomes. In this context, SQSTM1/p62 can recruit ubiquitinated protein aggregates to the autophagosome through the LIR domain. To ensure cell survival, the RPE cells increase SQSTM1/p62 protein synthesis, which explains the accumulation of SQSTM1/p62 due proteasome impairment. Probably SQSTM1 and other transcript factors synthesis is also stimulated, in order to improve autophagy clearance of non-functional and damaged proteins. Others studies have proposed that SQSTM1/p62 regulates the packing and transport of ubiquitinated, misfolded and aggregated proteins, and also non-functional cell organelles for clearance via autophagy in mammalian cells, corroborating our hypothesis (Kirkin et al., 2009b; Kuusisto, Suuronen & Salminen, 2001).

In RPE cells, in parallel with proteasome inactivation occurs the activation of autophagy when in conditions of AMD (Wang, Lukas, Yuan, Du, Handa, et al., 2009; Wang, Lukas, Yuan, Du, Tso, et al., 2009). The evidence of this work suggests that these events are intrinsically linked, where the age-related inactivation of the proteasome leads to the increase of autophagy. During ageing, there is also an accumulation of damaged and non-degraded ubiquitinated proteins which may increase autophagy (Bhutto & Lutty, 2012; Blasiak, Petrovski, & Veréb, 2011; Wang, Lukas, Yuan, Du, Tso, et al., 2009). Nowadays it is admitted that these ubiquitinated proteins can be degraded in lysosome by autophagy, which works as a compensatory mechanism. Despite the known decline in autophagy clearance with aging (Cuervo, 2008), autophagy enhancement in AMD is possible due the inducible nature of autophagic function and the presence of several compensatory adaptations within the system (Grune, Jung, Merker & Davies, 2004). Moreover oxidative stress, hypoxia, the unfolded protein response or inflammation can activate autophagy, and are present in AMD pathology (Kaarniranta et al., 2013).

Taken this in mind, we improved our AMD cell line model by stimulating autophagy. Two different approaches were performed: autophagy induced by starvation or with rapamycin, an mTOR inhibitor. First, we verify by LC3-II and SQSTM1/p62 protein levels that 6h was the time point in which RPE cells exhibits maximal serum starvation-triggered autophagy activation. RPE cells treated with autophagy activators exhibited an increase in the autophagic flux, as both starvation and rapamycin decreased the BafA1-induced SQSTM1/p62 accumulation. As expected, LC3-II accumulated with BafA1 (due impaired degradation caused by late autophagic inhibition) and a concomitant treatment with rapamycin or starvation resulted in increased LC3-II protein levels and thus increased autophagy clearance. Similar results were obtained by other authors with another autophagy activator, AICAR (Viiri et al., 2013).

In order to establish an accurate cell model of AMD, ARPE-19 cells were exposed simultaneously to both MG-132 and one of the tested autophagy inducers (rapamycin or starvation). In these conditions, we guarantee proteasomal inhibition and autophagy activation in RPE cells, as it occurs in AMD (Handa, 2012; Mitter et al., 2012). The increase of LC3-II protein levels in cells treated with MG-132 was similar to that induced by rapamycin, suggesting that MG-132 can be seen as an autophagic activator. Starvation was the most effective autophagy inducer. Concomitant treatment of RPE cells with MG-132 and starvation led to the highest LC3-II levels, indicating strong autophagy

stimulation. MG-132-induced proteasomal inhibition caused SQSTM1/p62 accumulation, which increased in RPE cells that were co-treated with autophagy inducers. Once more, our data suggest that although SQSTM1/p62 is an autophagic substrate (Bjørkøy et al., 2009; Klionsky & Abdalla, 2012), this protein is not degraded upon proteasome inhibition, even when autophagy is stimulated.

These results are supported by studies from other groups. Wang and collaborators verified an increase in autophagy and exocytic activity in aged RPE cells, as well as the presence of autophagic and exosomes markers (CD63, CD81 and LAMP2) in drusen (Wang, Lukas, Yuan, Du, Handa, et al., 2009; Wang, Lukas, Yuan, Du, Tso, et al., 2009). The high levels of exosomes are explained since RPE is responsible for the removal of damaged macromolecules. It is admitted that the aged RPE may increases its exocytic activity through exosomes (Wang, Lukas, Yuan, Du, Handa, et al., 2009; Wang, Lukas, Yuan, Du, Tso, et al., 2009). In this last study, focused in the effect of cigarette smoke in RPE, exosome markers (CD63, CD81 and LAMP2) were localized between RPE and the choroid from mice exposed to chronic cigarette smoke, which did not occur in control mice (Wang, Lukas, Yuan, Du, Handa, et al., 2009). Furthermore, a decline autophagic efficiency in the RPE is associated with the later pathological stages of AMD and cellular dysfunction (Rao et al., 2009).

AlphaB-crystallin (αβ), a small heat shock protein associated with several neurodegenerative diseases, cancer and cardiomyopathies, was discovered to be secreted from ARPE-19 cells via exosomes (Bhat & Gangalum, 2011). Besides the exosome markers CD9 and CD63, ARPE-19 secreted exosomes contain high levels of activated signaling proteins, such as phosphorylated Akt (T308), VEGFR2 (Y951) or PDGFRβ (Y751) (Biasutto, Chiechi, Couch, Liotta, & Espina, 2013). Also in this study, these investigators found that ARPE-19 exosomes are highly rich in TLR3 (Toll-Like Receptor 3), which was reported to be involved in angiogenesis suppression and retinal degeneration. Human choroidal neovascular membranes from AMD patients were shown to express TLR3 exclusively in RPE cells, thus suggesting a possible role of TL3 in AMD (Biasutto et al., 2013). More recently, Kang and collaborators were able to identify several exosomal proteins in the aqueous humor as novel biomarkers in patients with neovascular AMD (Kang et al., 2014).

Overall, we proposed an in vitro model for AMD, in which the crosstalk between the two major proteolytic pathways was analyzed. One of the AMD features is the impairment of proteasomal activity, which results in accumulated polyubiquitinated

proteins in SQSTM1/p62-ubiquitin aggresomes. Proteasomal inhibition induces autophagy activation, through the action of SQSTM1/p62, which triggers polyubiquitinated proteins to autophagy clearance in the lysosome. However, with time lysosome becomes overloaded and signs of lysosomal dysfunction begin to appear, such as accumulation of lipofuscin and decreased activity of lysosomal enzymes. Thus damaged proteins cannot be degraded. We hypothesize that aged RPE releases intracellular proteins via exosomes and, therefore, this event contributes to formation and accumulation of drusen in AMD. Therefore, further studies investigating the mechanisms underlying exosomes release and accumulation of drusen, in particular in conditions of proteasome inhibition and autophagy activation that were used in this work, should aim at clarifying this issue.

CAPTER 5

CONCLUSION

The results presented in this study show that MG-132-induced proteasome inhibition leads to increased autophagy in RPE cells. The autophagic flux is enhanced and the lysosomal activity stimulated upon UPP impairment. Although, we verified a significantly increase in the autophagy-specific substrate SQSTM1/p62 due stimulation of protein synthesis in the presence of MG-132. MG-132 induced the formation of SQSTM1/p62-ubiquitin aggresomes, mainly in the nuclear/perinuclear compartment. Our data strongly indicates a key role for SQSTM1/p62 in the crosstalk between UPP and autophagy. SQSTM1/p62 bind ubiquitinated proteins that delivers to the autophagy lysosomal pathway through its UBA- LIR-domains.

In this work, we propose that impairment of the proteasome-dependent degradation of ubiquitin conjugates leads to increased macroautophagy activity, since SQSTM1/p62 diverts UPP substrates to the lysosome. With time, the increased flux of substrates through macroautophagy would overload the lysosome leading to lysosomal dysfunction and accumulation of subcellular deposits containing unprocessed material, that are eventually expelled by exocytosis, thus forming the drusen. However, these last steps remain unproved and need to be clarified. Moreover, it is not likely that SQSTM1/p62 is the only protein responsible for the UPP-autophagy shuttling and thus other possible players must be investigated.

CAPTER 6

REFERENCES

References

Ablonczy, Z. (2011). A functional profile of gene expression in ARPE-19 cells. *Investigative Ophthalmology & Visual Science*, *52*(12), 8614–20.

Adamis, A.P., Shima, D.T., Yeo, K.T., Yeo, T.K., Brown, L.F., Berse, B., D'Amore, P.A., Folkman, J. (1993). Synthesis and secretion of vascular permeability factor/vascular endothelial growth factor by human retinal pigment epithelial cells. *Biochem. Biophys. Res. Commun. 193* (2), 631–638.

Admyre, C., Johansson, S. M., Qazi, K. R., Filen, J. J., Lahesmaa, R., Norman, M., Neve, E. P., Scheynius, A., Gabrielsson, S. (2007). Exosomes with immune modulatory features are present in human breast milk. *J Immunol. 179*(3), 1969-78.

Al-Shabrawey, M., Rojas, M., Behzadian, A. et al. (2008). Role of NADPH in retinal inflammation. *Invest. Ophthalmol. Vis. Sci. 49*, 3239–3244.

Ambati, J., Ambati, B.K., Yoo, S.H., Ianchulev, S., Adamis, A.P. (2003a). Age-related macular degeneration: etiology, pathogenesis, and therapeutic strategies. *Surv. Ophthalmol. 48*, 257-293.

Ambati, J., Anand, A., Fernandez, S. et al, (2003b). An animal model of age-related macular degeneration in senescent Ccl-2- or Ccr-2-deficient mice. *Nat. Med. 9*(11), 1390–1397.

Ambati, J. and Fowler, B.J. (2012) Mechanisms of Age-Related Macular Degeneration. *Neuron 75*(1), 26-39.

Arjamaa, O., Nikinmaa, M., Salminen, A., & Kaarniranta, K. (2009). Regulatory role of HIF-1alpha in the pathogenesis of age-related macular degeneration (AMD). *Ageing Research Reviews*, *8*(4), 349–58.

Arstila, A.U., Trump, B.F. (1969) Autophagocytosis: origin of membrane and hydrolytic enzymes. *Virchows Arch B Cell Pathol Incl Mol Pathol 2*, 85–90.

Babu, J.R., Geetha, T., Wooten, M.W. (2005). Sequestosome 1/p62 shuttles poly-ubiquitinated tau for proteasomal degradation. *Journal of Neurochemistry 94*, 192–203.

Beatty, S., Koh, H., Phil, M., Henson, D., Boulton, M., (2000). The role of oxidative stress in the pathogenesis of age-related macular degeneration. *Surv. Ophthalmol. 45*, 115–134.

Bellingham, S., Guo, B.B., Coleman, B.M., Hill, A.F. (2012). Exosomes: vehicles for the transfer of toxic proteins associated with neurodegenerative diseases? *Front. Physiol. 3*(124).

Benbrook, D.M., Long, A. (2012). Integration of autophagy, proteasomal degradation, unfolded protein response and apoptosis. *Experimental Oncology 34*(3), 286-297.

Bento, C.F., Fernandes, R., Ramalho, J. et al. (2010). The chaperone-dependent ubiquitin ligase CHIP targets HIF-1α for degrada- tion in the presence of methylglyoxal. *PLoS One 5*(11), e15062.

Bhat, S.P. and Gangalum, R.K. (2011). Secretion of αB-crystallin via exosomes - New clues to the function of human retinal pigment epithelium. *Communicative & Integrative Biology 4*(6), 739-741 (Article Addendum).

Bhutto, I. and Lutty, G. (2012). Understanding age-related macular degeneration (AMD): Relationships between the photoreceptor/retinal pigment epithelium/Bruch's membrane/choriocapillaris complex. *Molecular Aspects of Medicine 33*, 295–317.

Biasutto, L., Chiechi, A., Couch, R., Liotta, L.A., Espina, V. (2013). Retinal pigment epithelium (RPE) exosomes contain signaling phosphoproteins affected by oxidative stress. *Experimental Eye Research 319*(13), 2113-23.

Bjørkøy, G., Lamark, T., Brech, A. (2005). p62/ SQSTM1 forms protein aggregates degraded by autophagy and has a protective effect on huntingtin- induced cell death. *J Cell Biol 171*, 603-14.

Bjørkøy, G., Lamark, T., Johansen, T. (2006). p62/SQSTM1: a missing link between protein aggregates and the autophagy. *Autophagy 2*(2), 138-139 (Article Addendum).

Bjørkøy, G., Lamark, T., Pankiv, S. et al. (2009). Monitoring autophagic degradation of p62/SQSTM1. *Methods of enzymology, 452*(8), 181-197.

Blasiak, J., Petrovski, G., Veréb, Z. et al. (2014). Oxidative stress, hypoxia and autophagy in the neovascular processes of age-related macular degeneration (AMD). Biomed Res Int. 2014(2014), 768026.

Bloom, J., Amador, V.;,Bartolini, F., DeMartino, G., Pagano, M. (2003) Proteasome-Mediated Degradation of p21 via N-Terminal Ubiquitinylation. *Cell* 115, 71–82

Bulteau, A.L., Verbeke, P., Petropoulos, I., Chaffotte, A.F., Friguet, B. (2001). Proteasome inhibition in glyoxal-treated fibroblasts and resistance of glycated glucose-6-phosphate dehydrogenase to 20 S proteasome degradation in vitro. *J Biol Chem 276*, 45662–45668.

Burke, J.M., Hjelmeland, L.M. (2005). Mosaicism of the retinal pigment epithelium: seeing the small picture. *Molecular Interventions. 5*(4), 241-249.

Carrard, G., Bulteau, A.L., Petropoulos, I., Friguet, B. (2002). Impairment of proteasome structure and function in aging. *Int J Biochem Cell Biol 34*, 1461–1474.

Catarino, S., Bento, C.F., Brito, A., Murteira, E., Fernandes, A.F., Pereira, P. (2012) Regulation of the expression of interleukin-8 induced by 25-hydroxycholesterol in retinal pigment epithelium cells. *Acta Ophthalmologica 90*(6), 255-263.

Chen, Y., Zeng, J., Zhao, C., Wang, K., Trood, E., Buehler, J., Weed, M., Kasuga, D., et al. (2011). Assessing susceptibility to age-related macular degeneration with genetic markers and environmental factors. *Arch. Ophthalmol. 129*, 344–351.

Chopdar, A., Chakravarthy, U., Verma, D. (2003). Age related macular degeneration. *BMJ. 326*, 485-488.

Chung, H.Y., Cesari, M., Anton, S., Marzetti, E., Giovannini, S., Seo, A.Y., Carter, C., Yu, B.P., Leeuwenburgh, C. (2009) Molecular inflammation: Underpinnings of aging and age-related diseases. *Ageing Research Reviews 8*, 18–30.

Ciechanover, A. (1994). The ubiquitin-proteasome proteolytic pathway. *Cell, 79*(1), 12–21.

Ciechanover A. (2003). The ubiquitin proteolytic system and pathogenesis of human diseases: a novel platform for mechanism-based drug targeting. *Biochem Soc Trans 31*, 474-81.

Clemons, T.E., Milton, R.C., Klein, R., et al. (2005). Risk factors for the incidence of Advanced Age-Related Macular Degeneration in the Age-Related Eye Disease Study (AREDS) AREDS Report No. 19. *Ophthalmology 112*(4), 533–539.

Cockman, M.E., Masson, N., Mole, D.R. et al. (2000). Hypoxia inducible factor- alpha binding and ubiquitylation by the von Hippel-Lindau tumor suppressor protein. *J. Biol. Chem. 275*, 25733–25741.

Conde-Vancells, J., Rodriguez-Suarez, E., Embade, N., Gil, D., Matthiesen, R., Valle, M., Elortza, F., Lu, S. C., Mato, J. M., Falcon-Perez, J. M. (2008). Characterization and comprehensive proteome profiling of exosomes secreted by hepatocytes. *J Proteome Res. 7*(12), 5157-66.

Cook, H.L., Patel, P.J. and Tufail, A. (2008). Age-related macular degeneration: diagnosis and management. *British Medical Bulletin 85*, 127–149.

Crabb, J.W., Miyagi, M., Gu, X. et al. (2002) Drusen proteome analysis: an approach to the etiology of age-related macular degeneration. *Proc. Natl. Acad. Sci. USA 99*(23), 14682–14687.

Cuervo, A.M. (2008). Autophagy and aging: keeping that old broom working. *Trends Genet. 24*, 604–612

Cuervo, A.M., Dice, J.F. (1996). A receptor for the selective uptake and degradation of proteins by lysosomes. *Science 273*, 501– 503.

Curcio, C.A. (2001). Photoreceptor topography in ageing and age-related maculopathy. *Eye (Lond.) 15*(3), 376–383.

Dawson, T.M., Dawson, V.L., (2003). Molecular pathways of neurodegeneration in Parkinson's disease. *Science 302*, 819-822.

de Jong, P.M. (2006). Age-related macular degeneration. *N. Engl. J. Med. 355*, 1474–1485.

Del Priore, L.V., Kuo, Y.H., Tezel, T.H., (2002). Age-related changes in human RPE cell density and apoptosis proportion in situ. Invest. *Ophthalmol. Vis. Sci. 43*(10), 3312–3318.

Delori, F.C., Goger, D.G., Hammond, B.R., Snodderly, D.M., Burns, S.A. (2001). Macular pigment density measured by autofluorescence spectrometry: comparison with reflectometry and heterochromatic flicker photometry. *J. Opt. Soc. Am. A. Opt. Image Sci. Vis. 18*(6), 1212–1230.

Ding, X., Patel, M., Chan, C.C. (2009). Molecular pathology of age-related macular degeneration. *Prog Retin Eye Res 28*, 1-18.

Donoso, L. A., Kim, D., Frost, A., Callahan, A., and Hageman, G. (2006). The role of inflammation in the pathogenesis of age-related macular degeneration. *Surv. Ophthalmol. 51*, 137–152.

Driscoll, J.J., Chowdhury, R.D. (2012) Molecular crosstalk between the proteasome, aggresomes and autophagy: translational potential and clinical implications. *Cancer Letters 325*(2), 147–154.

Dudek, E. J., Shang, F., Valverde, P., Liu, Q., Hobbs, M., and Taylor, A. (2005). Selectivity of the ubiquitin pathway for oxidatively modified proteins: relevance to protein precipitation diseases. *FASEB J. 19*, 1707–1709.

Dunn, K C; Aotaki-Keen, A E; Putkey, F R; Hjelmeland, L. M. (1996). ARPE-19, A Human Retinal Pigment Epithelial Cell Line with Differentiated Properties. *Experimental Eye Research*, *62*(2), 155–170.

Dunn, K. C., Marmorstein, a D., Bonilha, V. L., et al. (1998). Use of the ARPE-19 cell line as a model of RPE polarity: basolateral secretion of FGF5. *Invest. Ophthalmol. Vis. Sci.*, *39*(13), 2744–9.

el-Hifnawi, E. (1995). Localization of cathepsin D in rat ocular tissues. An immuno-histochemical study. Ann Anat 177(1), 11-17.

Eskelinen, E.L., Saftig, P. (2009) Autophagy: a lysosomal degradation pathway with a central role in health and disease. *Biochim Biophys Acta 1793*, 664-673.

Ethen, C. M., Hussong, S. A., Reilly, C., Feng, X., Olsen, T. W., Ferrington, D. A. (2007). Transformation of the proteasome with age-related macular degeneration. *FEBS Lett. 581*, 885–890.

Evans, J., (2008). Antioxidant supplements to prevent or slow down the progression of AMD: a systematic review and meta-analysis. *Eye (Lond.) 22*(6), 751–760.

Fernandes, A.F., Bian, Q., Jiang, JK., Thomas, C. J., Pereira., P., Shang, F. (2009) Proteasome inactivation promotes mitogen-activated protein kinase-depedent phosphatidylinositol 3-kinase activation and increases interleukin-8 production in retinal pigment epitelial cells. *Molecular Biology of the Cell 20*, 3690–3699.

Fernandes, A. F., Guo, W., Zhang, X. et al. (2006). Proteasome-dependent regulation of signal transduction in retinal pigment epithelial cells. *Experimental Eye Research*, *83*(6), 1472–81.

Fernandes, A.F., Pereira, P. (2007) Oxidative Stress, Inflammation and Age-Related Macular Degeneration: a Bizarre Love Triangle. *Exp. Ophthalmol.33*(1), 1-8.

Fernandes, A. F., Zhou, J., Zhang, X., Bian, Q., Sparrow, J., Taylor, A., Pereira, P., and Shang, F. (2008). Oxidative inactivation of the proteasome in retinal pigment epithelial cells. A potential link between oxidative stress and up- regulation of interleukin-8. *J. Biol. Chem. 283*, 20745–20753

Fernandes, R., Ramalho, J., Pereira, P. (2006). Oxidative stress upregulates the ubiquitin proteasome pathway in retinal endotelial cells. *Molecular Vision 12*, 1526-35

Ferreira, J. V., Fôfo, H., Bejarano, E. et al. (2013). STUB1/CHIP is required for HIF1A degradation by chaperone-mediated autophagy. *Autophagy*, *9*(9), 1349–66.

Friedman, D.S., O'Colmain, B.J. et al. (2004). Prevalence of age-related macular degeneration in the United States. *Arch Ophthalmol 122*, 564-572.

Gamerdinger, M., Hajieva, P., Kaya, A. M. et al. (2009). Protein quality control during aging involves recruitment of the macroautophagy pathway by BAG3. *The EMBO Journal*, *28*(7), 889–901.

Gartel, A.L., Radhakrishnan, S.K. (2005). Lost in transcription: p21 repression, mechanisms, and consequences. *Cancer Res. 65*(10), 3980–5.

Geetha, T., Wooten, M.W. (2002) Structure and functional properties of the ubiquitin binding protein p62. *FEBS Lett 512*, 19-24.

Glickman, M.H., Ciechanover, A., (2002). The ubiquitin-proteasome proteolytic pathway: destruction for the sake of construction. *Physiol. Rev. 82*, 373-428.

Gong, J., Sagiv, O., Cai, H., Tsang, S.H., Del Priore, L.V. (2008). Effects of extracellular matrix and neighboring cells on induction of human embryonic stem cells into retinal or retinal pigment epithelial progenitors. *Exp. Eye Res. 86*(6), 957–965.

Grune, T., Jung, T., Merker, K., Davies, K. J. A. (2004). Decreased proteolysis caused by protein aggregates, inclusion bodies, plaques, lipofuscin, ceroid, and ‘‘aggresomes’’ during oxidative stress, aging, and disease. *Int. J. Biochem. Cell Biol. 36*, 2519–2530.

Gu, S-M., Thompson, D.A., Srikumari, C. et al. (1997). Mutations in RPE65 cause autosomal recessive childhood-onset severe retinal dystrophy. *Nat. Genet. 17*, 194–197.

Guertin, D.A., Stevens, D.M., Saitoh, M. et al. (2009). mTOR complex 2 is required for the development of prostate cancer induced by Pten loss in mice". *Cancer Cell 15*(2), 148–59.

Guyer, D.R., Fine, S.L. et al. (1986). Subfoveal choroidal neovascular membranes in age-related macular degeneration. Visual prognosis in eyes with relatively good initial visual acuity. *Arch. Ophthalmol. 104*, 702–705.

Hageman, G. S, Mullins, R. F., Russell, S. R., Johnson, L. V.Anderson, D. H. (1999). A common haplotype in the complement regulatory gene factor H (HF1/CFH) predisposes individuals to age-related macular degeneration. *FASEB J. 13*, 477–484.

Haglund, K., Dikic, I., (2005). The role of ubiquitylation in receptor endocytosis and endosomal sorting. *J. Cell Sci. 125*(2) 265–275.

Hah, Y-S., Noh, H. S., Ha, J. H. et al. (2012). Cathepsin D inhibits oxidative stress-induced cell death via activation of autophagy in cancer cells. *Cancer Letters, 323*(2), 208–14.

Handa, J.T. (2012). How does the macula protect itself from oxidative stress? *Molecular Aspects of Medicine 33*, 418–435.

Hayashi-Nishino, M., Fujita, N., Noda, T. et al. (2009). A subdomain of the endoplasmic reticulum forms a cradle for autophagosome formation. *Nat Cell Biol 11*, 1433–7.

Hicke, L., (2001). A new ticket for entry into budding vesicles-ubiquitin. *Cell 106*(5), 527–530.

Hicke, L., Dunn, R. (2003). Regulation of membrane protein transport by ubiquitin and ubiquitin-binding proteins. *Annual Review of Cell and Developmental Biology 19*, 141-172.

Hope, A. D., de Silva, R., Fischer, D. F., Hol, E. M., van Leeuwen, F. W., Lees, A. J. (2003). Alzheimer’s associated variant ubiquitin causes inhibition of the 26S proteasome and chaperone expression. *J. Neurochem. 86*, 394–404.

Hu, X., Du, C., Yang, L. (2010). Proteasome inhibitor MG132 suppresses number and function of endothelial progenitor cells: involvement of nitric oxide synthase inhibition. *Internat. Journal of Molecular Medicine, 25*(3) 385–392.

Huang, S., Bjornsti, M., & Houghton, P. J. (2003). Rapamycins: mcehanism of actions and cellular resistance. *Cancer Biology & Therapy*, *2*(June), 222–232.

Ichimura, Y., Kirisako, T., Takao, T. et al. (2000). A ubiquitin-like system mediates protein lipidation. *Nature 408*, 488–92.

Ichimura, Y., Kumanomidou, T., Sou, Y.S. et al. (2008). Structural basis for sorting mechanism of p62 in selective autophagy. *J Biol Chem 283*, 22847-57.

Ihara, Y., Morishima-Kawashima, M., Nixon, R. (2012). The ubiquitin-proteasome system and the autophagic-lysosomal system in Alzheimer disease. Cold Spring Harb Perspect Med. 2(8).

Im, E., Kazlauskas, A. (2007). The role of cathepsins in ocular physiology and pathology. *Exp Eye Res 84*, 383-8.

Iwasaki, M., Inomata, H. (1988). Lipofuscin granules in human photoreceptor cells. *Invest Ophthalmol Vis Sci. 29*, 671–679.

Jacinto, E., Facchinetti, V., Liu, D. et al. (2006). SIN1/MIP1 maintains rictor-mTOR complex integrity and regulates Akt phosphorylation and substrate specificity. *Cell. 127*, 125–137.

Jager, R.D., Mieler, W.F., Miller, J.W. (2008). Age-Related Macular Degeneration. *N Engl J Med. 358*, 2606-2617.

Johnson, L.V., Leitner, W.P., Staples, M.K., Anderson, D.H. (2001). Complement activation and inflammatory processes in drusen formation and age related macular degeneration. *Exp Eye Res 73*, 887–896.

Jung, C.H., Ro, S.H., Cao, J. et al. (2010). mTOR regulation of autophagy. *FEBS Lett. 584*, 1287–1295.

Jung, T., Catalgol, B., Grune, T. (2009). The proteasomal system. *Mol Aspects Med 30*, 191-296.

Kaarniranta, K., Salminen, A., Eskelinen, E.-L., Kopitz, J. (2009). Heat shock proteins as gatekeepers of proteolytic pathways—Implications for age-related macular degeneration (AMD). *Ageing Research Reviews*, *8*(2), 128–139.

Kaarniranta, K., Sinha, D., Blasiak, J. et al. (2013). Autophagy and heterophagy dysregulation leads to retinal pigment epithelium dysfunction and development of age-related macular degeneration. *Autophagy*, *9*(7), 973–84.

Kaarniranta, K., Hyttinen, J., Ryhanen, T. et al. (2014). Mechanisms of protein aggregation in the retinal pigment epithelial cells. *Journal of the Society for Vector Ecology*, *39*(1), ii–iii.

Kamada, Y., Funakoshi, T., Shintani, T. et al. (2000). Tor-mediated induction of autophagy via na Apg1 protein kinase complex. *J Cell Biol. 150*, 1507-13.

Kamura, T., Sato, S., Iwai, K. et al. (2000). Activation of HIF-1alpha ubiquitination by a reconstituted von Hippel- Lindau (VHL) tumor suppressor complex. *Proc. Natl. Acad. Sci. U.S.A. 97*, 10430–10435.

Kang,G., Bang,J.Y., Choi, A.J.,Yoon, J., Lee, W.C., Choi, S.,Yoon, S., Kim, H.C., Baek, J.H., Park, H.S., Lim, H.J., Chung, H. (2014). Exosomal Proteins in the Aqueous Humor as Novel Biomarkers in Patients with Neovascular Age-related Macular Degeneration Journal of Proteome Research 13(2), 581-595.

Kannan, R., Zhang, N., Sreekumar, P.G., Spee, C.K., Rodriguez, A., Barron, E., Hinton, D.R. (2006) Stimulation of apical and basolateral VEGF-A and VEGF-C secretion by oxidative stress in polarized retinal pigment epithelial cells. *Mol Vis. 12*, 1649-1659.

Kapphahn, R. J., Bigelow, E. J., Ferrington, D. A. (2007). Age-dependent inhibition of proteasome chymotrypsin-like activity in the retina. *Exp. Eye Res. 84*, 646–654.

Katzmann, D.J., Odorizzi, G., Emr, S.D. (2002). Receptor down- regulation and multivesicular-body sorting. *Nat Rev Mol Cell Biol 3*, 893-905.

Kawaguchi, T., Miyazawa, K., Moriya, S., et al. (2011). Combined treatment with bortezomib plus bafilomycin A1 enhances the cytocidal effect and induces endoplasmic reticulum stress in U266 myeloma cells: crosstalk among proteasome, autophagy-lysosome and ER stress. *Int J Oncol 38*, 643–54.

King, R.W., Deshaies, R.J., Peters, J-M., Kirschner, M.W. (1996). How proteolysis drives the cell cycle. *Science. 274*, 1652–1658.

Kinnunen, K., Petrovski, G., Moe, M. C., Berta, A., Kaarniranta, K. (2012). Molecular mechanisms of retinal pigment epithelium damage and development of age-related macular degeneration. *Acta Ophthalmologica*, *90*(4), 299–309.

Kirkin, V., McEwan, D.G., Novak, I., Dikic, I. (2009a) A role for ubiquitin in selective autophagy. *Mol Cell 34*, 259-69.

Kirkin, V., Lamark, T., Sou, Y.S. et al. (2009b). A role for NBR1 in autophagosomal degradation of ubiquitinated substrates. *Mol Cell 33*, 505-516.

Klein, R., Klein, B.E., Linton, K.L., (1992). Prevalence of age-related maculopathy. The Beaver Dam Eye Study. *Ophthalmology 99* (6), 933–943.

Klionsky, D.J., Abdalla, F.C., Abeliovich, H. et al. (2012). Guidelines for the use and interpretation of assays for monitoring autophagy. *Autophagy 8*(24), 445-544.

Klionsky, D.J., Cregg, J.M., Dunn, W.A. Jr. et al. (2003). A unified nomenclature for yeast autophagy-related genes. *Dev Cell 5*, 539–45.

Klionsky, D.J., Elazar, Z., Seglen, P.O., Rubinsztein, D.C. (2008). Does bafilomycin A1 block the fusion of autophagosomes with lysosomes? *Autophagy 4*, 849–50.

Kloetzel, P. M. (2004). Generation of major histocompatibility complex class I antigens: functional interplay between proteasomes and TPPII. *Nat. Immunol. 5*, 661–669.

Koepp, D.M., Harper, J.W., Elledge, S.J. (1999). How the cyclin became a cyclin: regulated proteolysis in the cell cycle. *Cell 97*, 431–434.

Komatsu, M., Waguri, S., Koike, M. et al. (2007). Homeostatic levels of p62 control cytoplasmic inclusion body formation in autophagy-deficient mice. *Cell 131*, 1149–1163.

Komatsu, M., Waguri, S., Ueno, T. et al. (2005). Impairment of starvation-induced and constitutive autophagy in Atg7-deficient mice. *J. Cell Biol. 169*, 425– 434.

Kopito, R.R. (2000). Aggresomes, inclusion bodies and protein aggregation. *Trends Cell Biol 10*, 524–530.

Korolchuk, V., Menzies, F., Rubinsztein, D. (2009). A novel link between autophagy and the ubiquitin-proteasome system. *Autophagy*, *5*(6), 862–863.

Korolchuk, V., Menzies, F., Rubinsztein, D. (2010). Mechanisms of cross-talk between the ubiquitin-proteasome and autophagy-lysosome systems. *FEBS Letters*, *584*(7), 1393–8.

Krohne, T.U., Stratmann, N.K., Kopitz, .J, Holz, F.G. (2010). Effects of lipid peroxidation products on lipofuscinogenesis and autophagy in human retinal pigment epithelial cells. *Exp Eye Res 90*, 465–471.

Kunchithapautham, K., Rohrer, B. (2007). Apoptosis and autophagy in photoreceptors exposed to oxidative stress. *Autophagy 3*, 433–441.

Kuusisto, E., Kauppinen, T., Alafuzoff, I. (2008). Use of p62/SQSTM1 antibodies for neuropathological diagnosis. *Neuropathol. Appl. Neurobiol. 34*, 169–180.

Kuusisto, E., Suuronen, T., Salminen, A. (2001). Ubiquitin-binding protein p62 expression is induced during apoptosis and proteasomal inhibition in neuronal cells. *Biochem Biophys Res Commun 280*, 223-228.

Lamark, T., Johansen, T. (2010). Autophagy: links with the proteasome. *Current Opinion in Cell Biology*, *22*(2), 192–8.

Lamark, T., Perander, M., Outzen, H., Kristiansen, K., 1vervatn, A., Michaelsen, E., Bjørkøy, G., and Johansen, T. (2003). Interaction codes within the family of mammalian Phox and Bem1p domain-containing proteins. *J. Biol. Chem. 278*, 34568–34581.

Lee, D. H., Goldberg, A. L. (1998). Proteasome inhibitors: valuable new tools for cell biologists. *Trends in Cell Biology*, *8*(10), 397–403.

Leger, F., Fernagut, P.O., Canron, M.H. et al (2011). Protein aggregation in the aging retina. *J. Neuropathol. Exp. Neurol. 70*(1), 63–68.

Leung, D.W., Cachianes, G., Kuang, W.J., Goeddel, D.V., Ferrara, N. (1989). Vascular endothelial growth factor is a secreted angiogenic mitogen. *Science 246*, 1306–1309.

Li, C., Johnson, D.E. (2012). Bortezomib induces autophagy in head and neck squamous cell carcinoma cells via JNK activation. *Cancer Lett. 314*, 102–107.

Li, M., Khambu, B., Zhang, H, Kang, J.H., Chen, X. et al. (2013). Suppression of lysosome function induces autophagy via a feedback downregulation of mTORC1 activity. J. Biol. Chem. 288(50), 35769-35780.

Li, W.W., Li, J., Bao, J.K. (2012). Microautophagy: lesser-known self-eating. *Cell Mol Life Sci 69*, 1125–36.

Li, Y.,Wang, Y.S., Shen, X.F. et al. (2008). Alterations of activity and intracellular distribution of the 20S proteasome in ageing retinal pigment epithelial cells. *Exp Gerontol 43*, 1114-1122.

Liang, F. Q., and Godley, B. F. (2003). Oxidative stress-induced mitochondrial DNA damage in human retinal pigment epithelial cells: a possible mechanism for RPE aging and age-related macular degeneration. *Exp. Eye Res. 76*, 397–403.

Lindmo, K., Stenmark, H. (2006). Regulation of membrane traffic by phosphoinositide 3-kinases. *J Cell Sci 119*, 605–14.

Lou, Z., Ren, T., Peng, X. et al. (2013). Bortezomib induces apoptosis and autophagy in osteosarcoma cells through mitogen-activated protein kinase pathway in vitro. *J Int Med Res. 41*, 1505–1519.

Louie, J. L., Kapphahn, R. J., Ferrington, D. A. (2002). Proteasome function and protein oxidation in the aged retina. *Exp. Eye Res. 75*, 271–284.

Löw, P., Varga, A., Pircs, K. et al. (2013). Impaired proteasomal degradation enhances autophagy via hypoxia signaling in Drosophila. *BMC Cell Biology*, *14*, 29.

Maeda, H., Ogata, N., Yi, X., Takeuchi, M., Ohkuma, H., Uyama, M., (1998). Apoptosis of photoreceptor cells in ornithine-induced retinopathy. *Graefes Arch. Clin. Exp. Ophthalmol. 236*(3), 207–212.

Marino, G., Madeo, F., Kroemer, G. (2010). Autophagy for tissue homeostasis and neuroprotection. *Curr Opin Cell Biol. 23*(2), 198-206-

Marino, G., Ugalde, A. P., Salvador-Montoliu, N., Varela, I., Quiros, P. M., Cadinanos, J., van der Pluijm, I., Freije, J. M., and Lopez-Otin, C. (2008). Premature aging in mice activates a systemic metabolic response involving autophagy induction. *Hum. Mol. Genet. 17*(14), 2196–2211.

Martin, D.M., Yee, D., and Feldman, E.L. (1992). Gene expression of the insulin-like growth factors and their receptors in cultured human retinal pigment epithelial cells. *Brain Res Mol Brain Res 12*, 181–186.

Mathivanan, S., Lim, J. W., Tauro, B. J., Ji, H., Moritz, R. L., Simpson, R. J. (2010). Proteomics analysis of A33 immunoaffinity-purified exosomes released from the human colon tumor cell line LIM1215 reveals a tissue-specific protein signature. *Mol Cell Proteomics.9*(2), 197-208.

Matsumoto, M., Yoshimura, N., Honda, Y., (1994). Increased production of transforming growth factor-beta 2 from cultured human retinal pigment epithelial cells by photocoagulation. *Invest. Ophthalmol. Vis. Sci. 35* (13), 4245–4252.

Mauger, C., Del-Favero, J., Ceuterick, C. et al. (1999). Identification and localization of ataxin-7 in brain and retina of a patient with cerebellar ataxia type II using anti-peptide antibody. *Brain Res. Mol. Brain Res. 74*(1–2), 35–43.

Maxwell, P.H., Wiesener, M.S, Chang, G.W. et al. (1999). The tumour suppressor protein VHL targets hypoxia-inducible factors for oxygen-dependent proteolysis. *Nature 399*, 271-275.

McGeer, E. G., Klegeris, A. McGeer, P. L. (2005). Inflammation, the complement system and the diseases of aging. Neurobiol. *Aging 26*(1), 94–97.

Miceli, M., Liles, M., Newsome, D. et al. (1994). Evaluation of oxidative processes in human pigment epithelial cells associated with retinal outer segment phagocytosis. *Exp. Cell Res. 214*, 242–249.

Mitter, S.K., Rao, H.V., Qi, X., Cai, J., Sugrue, A., Dunn, W.A., Jr., Grant, M.B., Boulton, M.E. (2012). Autophagy in the retina: a potential role in age-related macular degeneration. *Adv. Exp. Med. Biol. 723*, 83–90.

Mizushima, N., Yamamoto, A., Hatano, M., et al. (2001). Dissection of autophagosome formation using Apg5-deficient mouse embryonic stem cells. *J Cell Biol 152*, 657–68. 87.

Mizushima, N., Yoshimori, T. (2007). How to interpret LC3 immunoblotting. *Autophagy 306*, 542–545.

Mullins, R.F., Russell, S.R., Anderson, D.H., Hageman, G.S., (2000). Drusen associated with aging and age-related macular degeneration contain proteins common to extracellular deposits associated with atherosclerosis, elastosis, amyloidosis, and dense deposit disease. *FASEB J. 14*, 835–846.

Naash, M., Al-Ubaidi, M.R., Anderson, R.E. (1997). Light exposure induces ubiquitin conjugation and degradation activities in the rat retina. *Invest. Ophthalmol. Vis. Sci. 38*(11), 2344–2354.

Naash, M., Izbicka, E., Anderson, R.E. (1991). Rat retina has an active and stable ubiquitin–protein conjugating system. *J. Neurosci. Res. 30*(2), 433–441.

Nakai, A., Yamaguchi, O., Takeda, T. et al. (2007). The role of autophagy in cardiomyocytes in the basal state and in response to hemodynamic stress. *Nat. Med. 13*, 619–624.

Naujokat, C., Sezer, O., Zinke, H. et al. (2000) Proteasome inhibitors induce caspase-dependent apoptosis and accumulation of p21WAF1/Cip1 in human immature leukemic cells. *Eur J Haematol* 65, 221-236.

Nozaki, M., Raisler, B.J., Sakurai, E. et al. (2006). Drusen complement components C3a and C5a promote choroidal neovascularization. *PNAS 103*(7), 2328–2333.

Ohno, S., Ishikawa, A., Kuroda, M. (2012). Roles of exosomes and microvesicles in disease pathogenesis *Advanced Drug Delivery Review 65*(3), 398-401.

Olinski, R., Siomek, A., Rozalski, R., Gackowski, D., Foksinski, M., Guz, J., Dziaman, T., Szpila, A., Tudek, B. (2007). Oxidative damage to DNA and antioxidant status in aging and age-related diseases. *Acta Biochimica Polonica.54*(1), 11–26.

Olive, M., van Leeuwen, F. W., Janue, A. (2008). Expression of mutant ubiquitin (UBBþ1) and p62 in myotilinopathies and desminopathies. *Neuropathol. Appl. Neurobiol. 34*, 76–87.

Owen, C., Jarrar, Z., Wormald, R. et al. (2012). The estimated prevalence and incidence of late stage age related macular degeneration in the UK. *Br J Ophthalmol* e301109

Özkaynak, E., Finley, D., Varshavsky, A. (1984). The yeast ubiquitin gene: head-to-tail repeats encoding a polyubiquitin precursor protein. *Nature, 312*(12), 663-666.

Pandey, U.B., Nie, Z., Batlevi, Y. et al. (2007). HDAC6 rescues neurodegeneration and provides an essential link between autophagy and the UPS. *Nature 447*, 859–863.

Pankiv, S., Clausen, T. H., Lamark, T. et al. (2007). p62/SQSTM1 binds directly to Atg8/LC3 to facilitate degradation of ubiquitinated protein aggregates by autophagy. *The Journal of Biological Chemistry, 282*(33), 24131–45.

Parier, V., Soubrane, G. (2008) Age-related macular degeneration. *La Revue de médecine interne*. 29, 215–223.

Patel, A.S., Lin, L., Geyer, A., Haspel, J. A., Hyeok An, C., Cao, J., Rosas, I.O., Morse, D. (2012). Autophagy in idiopathic pulmonary fibrosis. *PLoS ONE 7*(7): e41394.

Penfold, P.L., Madigan, M.C., Gillies, M.C., Provis, J.M. (2001). Immunological and etiological aspects of macular degeneration. *Prog Retin Eye Res 20*, 385-414.

Peracchio, C., Alabiso, O., Valente, G., Isidoro, C. (2012). Involvement of autophagy in ovarian cancer: a working hypothesis. *J Ovarian Res 5*(22).

Polson, H.E., de Lartigue, J., Rigden, D.J. et al. (2010). Mammalian Atg18 (WIPI2) localizes to omegasome-anchored phago phores and positively regulates LC3 lipidation. *Autophagy 6*, 506–22.

Philp, N. J. (2003). Polarized Expression of Monocarboxylate Transporters in Human Retinal Pigment Epithelium and ARPE-19 Cells. *Investigative Ophthalmology & Visual Science, 44*(4), 1716–1721.

Qin, S. (2007). Oxidative Damage of Retinal Pigment Epithelial Cells and Age-Related Macular Degeneration. *Drug development research. 68*, 213–225.

Qureshi, N., Vogel, S. N., Van Way, C., Papasian, C. J., Qureshi, A. A., Morrison, D. C. (2005). The proteasome: a central regulator of inflammation and macrophage function. *Immunol. Res. 31*, 243–260.

Rapino, C., Bianchi, G., Di Giulio, C. et al. (2005). HIF-1alpha cytoplasmic accumulation is associated with cell death in old rat cerebral cortex exposed to intermittent hypoxia. *Aging Cell 4*, 177–185.

Rattner, A., Nathans, J. (2006). Macular degeneration: recent advances and therapeutic opportunities. *Nature Reviews. Neuroscience*, *7*(11), 860–72.

Ravikumar, B., Duden, R., Rubinsztein, D.C. (2002) Aggregate-prone proteins with polyglutamine and polyalanine expansions are degraded by autophagy. *Hum Mol Genet 11*, 1107-17.

Ravikumar, B., Moreau, K., Jahreiss, L. et al. (2010). Plasma membrane contributes to the formation of pre-autophago- somal structures. *Nat Cell Biol 12*, 747–57.

Ravikumar, B., Vacher, C., Berger, Z. et al. (2004). Inhibition of mTOR induces autophagy and reduces toxicity of polyglutamine expansions in fly and mouse models of Huntington disease. *Nat Genet 36*, 585-95.

Reme, C. E., Young, R. W. (1977). The effects of hibernation on cone visual cells in the ground squirrel. *Investigative ophthalmology & visual science 16*, 815-840.

Sahani, M. H., Itakura, E., Mizushima, N. (2014). Expression of the autophagy substrate SQSTM1/p62 is restored during prolonged starvation depending on transcriptional upregulation and autophagy-derived amino acids. *Autophagy 10*(3), 431–41.

Salceda, S., Caro, J. (1997). Hypoxia-inducible factor 1alpha (HIF-1alpha) protein is rapidly degraded by the ubiquitin-proteasome system under normoxic conditions. Its stabilization by hypoxia depends on redox-induced changes. *J Biol Chem* 272, 22642-7.

Salminen, A., & Kaarniranta, K. (2009). Regulation of the aging process by autophagy. *Trends in Molecular Medicine*, *15*(5), 217–24.

Sarbassov, D.D., Ali, S.M., Kim, D.H. et al. (2004). Rictor, a novel bin- ding partner of mTOR, defines a rapamycin-insensitive and raptor-independent pathway that regulates the cytoskeleton. *Curr Biol. 14*, 1296–1302.

Schlingemann, R.O., (2004). Role of growth factors and the wound healing re- sponse in age-related macular degeneration. *Graefes Arch. Clin. Exp. Ophthalmol. 242*, 91-101.

Seibenhener, M.L., Babu, J.R., Geetha, T. et al. (2004) Sequestosome 1/p62 is a polyubiquitin chain binding protein involved in ubiquitin proteasome degradation. *Mol Cell Biol 24*, 8055-68.

Selimovic, D., Porzig, B.B., El-Khattouti, A. et al. (2013). Bortezomib/ proteasome inhibitor triggers both apoptosis and auto- phagy-dependent pathways in melanoma cells. *Cell Signal. 25*, 308–318.

Shang, F., Nowell, T. R., Jr., Taylor, A. (2001). Removal of oxidatively damaged proteins from lens cells by the ubiquitin-proteasome pathway. *Exp. Eye Res. 73*, 229–238.

Shang, F., Taylor, A. (2004). Function of the ubiquitin proteolytic pathway in the eye. *Experimental Eye Research, 78*(1), 1-14.

Shang, F., Taylor, A. (2012). Roles for the ubiquitin-proteasome pathway in protein quality control and signaling in the retina: implications in the pathogenesis of age-related macular degeneration. *Molecular Aspects of Medicine, 33*(4), 446–66.

Sheaff, R., Singer, J., Swanger, J. (2000). Proteasomal Turnover of p21 Cip1 Does Not Require p21 Cip1 Ubiquitination. *Molecular Cell 5*, 403–410.

Sparrow, J.R., Boulton, M. (2005): RPE lipo- fuscin and its role in retinal pathobiology. *Exp Eye Res 80*, 595–606.

Sternfeld, M.D., Robertson, J.E., Shipley, G.D., Tsai, J., Rosenbaum, J.T., (1989). Cultured human retinal pigment epithelial cells express basic fibroblast growth factor and its receptor. *Curr. Eye Res. 8* (10), 1029–1037.

Strauss, O. (2005) The Retinal Pigment Epithelium in Visual Function. *Physiol Rev.85*, 845-881.

Streilein, J.W., Ma, N., Wenkel, H., Ng, T.F., Zamiri, P., (2002). Immunobiology and privilege of neuronal retina and pigment epithelium transplants. *Vision Res. 42*(4), 487–495.

Swaroop, A., Branham, K.E., Chen, W., Abecasis, G. (2007). Genetc susceptibility to age-related macular degeneration: a paradigm for dissecting complex disease traits. *Human Molecular Genetics 16*(2), 174-182.

Tan, J.M., Wong, E., Dawson, V.L., Dawson, T.M., Kah-Leong, L. (2008). Lysine 63-linked polyubiquitin potentially partners with p62 to promote the clearance of protein inclusions by autophagy. *Autophagy 4*(2), 251-253. (Article Addendum)

Tanihara, H., Yoshida, M., Matsumoto, M., Yoshimura, N., (1993). Identification of transforming growth factor-beta expressed in cultured human retinal pigment epithelial cells. *Invest. Ophthalmol. Vis. Sci. 34* (2), 413–419.

Tasdemir, E., Galluzzi, L., Maiuri, M.C. et al. (2008). Methods for assessing autophagy and autophagic cell death. *Methods Mol Biol 445*, 29–76.

Teicher, B.A., Ara, G., Herbst, R. et al. (1999). The proteasome inhibitor PS-341 in cancer therapy. *Clin Cancer Res. 5*, 2638–2645.

Tezel, T.H., Del Priore, L.V., Kaplan, H.J., (2004). Reengineering of aged Bruch's membrane to enhance retinal pigment epithelium repopulation. *Invest. Ophthalmol. Vis. Sci. 45*(9), 3337–3348.

Thompson, D., McHenry, C., Li, Y. et al. (2002). Retinal Dystrophy Due to Paternal Isodisomy for Chromosome 1 or Chromosome 2, with Homoallelism for Mutations in *RPE65* or *MERTK*, respectively. *AJHG Cell Press 70*(1), 224-229.

Thornton, J., Edwards, R., Mitchell, P., Harrison, R.A., Buchan, I., et al. (2005). Smoking and age-related macular degeneration: a review of association. *Eye 19*, 935–944.

Uchiki, T., Weikel, K.A., Jiao, W. et al. (2012) Glycation-altered proteolysis as a pathobiological mechanism that links dietary glycemic index, aging, and age-related disease (in nondiabetics). *Aging Cell 11*, 1–13.

Uetama, T., Ohno-Matsui, K., Nakahama, K. et al. (2003). Phenotypic change regulates monocyte chemoattractant protein-1 (MCP-1) gene expression in human retinal pigment epithelial cells. *J. Cell. Physiol. 197*(1), 77–85.

Ushio-Fukai, M., Nakamura, Y. (2008). Reactive oxygen species and angiogenesis: NADPH oxidase as target for cancer therapy. *Cancer Lett. 266*, 37–52.

Viiri, J., Amadio, M., Marchesi, N. et al. (2013). Autophagy activation clears ELAVL1/HuR-mediated accumulation of SQSTM1/p62 during proteasomal inhibition in human retinal pigment epithelial cells. *PloS One*, *8*(7), e69563.

Viiri, J., Hyttinen, J. M. T., Ryhänen, T. et al. (2010). P62/Sequestosome 1 As a Regulator of Proteasome Inhibitor-Induced Autophagy in Human Retinal Pigment Epithelial Cells. *Molecular Vision*, *16*(7), 1399–414.

Vingerling, J.R., Klaver, C.C., Hofman, A., de Jong, P.T., (1995). Epidemiology of age-related maculopathy. *Epidemiol. Rev. 17*(2), 347–360.

Vittal Rao H, Cai J, Afzal A. et al. (2009). A decline in autophagic efficiency is associated with AMD and chronic exposure to oxidative stress. *Invest Ophthalmol Vis Sci 2009*(50).

Wang, A., Lukas, T., Yuan, M., Du, N. (2009). Autophagy, exosomes and drusen formation in age-related macular degeneration. *Autophagy* (5), 563–564.

Wang, A. L., Lukas, T. J., Yuan, M. et al. (2009a). Autophagy and exosomes in the aged retinal pigment epithelium: possible relevance to drusen formation and age-related macular degeneration. *PloS One*, *4*(1), e4160.

Wang, A. L., Lukas, T.J., Yuan, M. et al. (2009b) Changes in Retinal Pigment Epithelium Related to Cigarette Smoke: Possible Relevance to Smoking as a Risk Factor for Age-Related Macular Degeneration. PLoS ONE 4(4): e5304.

Wangsa-Wirawan, N.D., Linsenmeier, R.A. (2003). Retinal oxygen. Fundamental and clinical aspects. *Arch. Ophthalmol.* 121, 547–557.

Weikel, K.A., Fitzgerald, P., Shang, F., Caceres, M.A., Bian, Q., Handa, J.T., Stitt, A.W., Taylor, A. (2011). Natural history of age-related retinal lesions that precede AMD in mice fed high or low glycemic index diets. *Invest. Ophthalmol. Vis. Sci.53*(2), 622-632.

Wilson, M. I., Gill, D. J., Perisic, O. et al. (2003). PB1 domain-mediated hetero-dimerization in NADPH oxidase and signaling complexes of atypical protein kinase C with Par6 and p62. *Mol. Cell 12*, 39–50.

Winkler, B.S., Boulton, M.E., Gottsch, J.D., Sternberg, P. (1999). Oxidative damage and age-related macular degeneration. *Mol Vis 5*(32).

Wojcik, S. (2013). Crosstalk between autophagy and proteasome protein degradation systems: possible implications for cancer therapy. *Folia Histochemica et Cytobiologica 51*(4), 249–64.

Wong, T.Y., Liew, G., Mitchell, P. (2007). Clinical update: new treatments for age-related macular degeneration. *Lancet 370*, 204–6.

Wu, W.K., Cho, C.H., Lee, C.W. et al. (2010). Proteasome inhibition: a new therapeutic strategy to cancer treatment. *Cancer Lett. 293*, 15–22.

Yamamoto, A., Tagawa, Y., Yoshimori, T. (1998). Bafilomycin A1 prevents maturation of autophagic vacuoles by inhibiting fusion between autophagosomes and lysosomes in rat hepatoma cell line, H-4-II-E cells. *Cell Struct. Funct. 23*, 33–42.

Yang, Z., Tong, Z., Chen, Y., Zeng, J., Lu, F., et al. (2010) Genetic and Functional Dissection of *HTRA1* and *LOC387715* in Age-Related Macular Degeneration. PLoS Genet 6(2): e1000836.

Yoshida, T., Fukatsu, R., Tsuzuki, K. et al (1997). Amyloid precursor protein, A beta and amyloid-associated proteins involved in chloroquine retinopathy in rats–immunopathological studies. *Brain Res. 764*(1–2), 283–288.

Young, R.W. (1967). The renewal of photoreceptor cell outer segments. *J Cell Biol. 33*(1):61-72.

Yuan, G., Nanduri, J., Khan, S. et al. (2008). Induction of HIF- 1alpha expression by intermittent hypoxia: involvement of NADPH oxidase, Ca2+ signaling, prolyl hydroxylases, and mTOR. *J. Cell. Physiol. 217*, 674–685.

Zhang, X., Li, W., Wang, C. et al. (2014). Inhibition of autophagy enhances apoptosis induced by proteasome inhibitor bortezomib in human glioblastoma U87 and U251 cells. *Mol Cell Biochem 385*, 265–275.

Zhang, X., Zhou, J., Fernandes, A.F., Sparrow, J.R., Pereira, P., Taylor, A., Shang, F. (2008). The proteasome: a target of oxidative damage in cultured human retina pigment epithelial cells. *Invest Ophthalmol Vis Sci. 49*(8), 3622-3630.

Zhao, J., Brault, J.J., Schild, A. et al. (2007). FoxO3 coordinately activates protein degradation by the autophagic/lysosomal and proteasomal pathways in atrophying muscle cells. *Cell Metabolism 6*(6), 472–483.

Zhou, J., Cai, B., Jang, Y.P., Pachydaki, S., Schmidt, A.M., Sparrow, J.R. (2005). Mechanisms for the induction of HNE- MDA- and AGE-adducts, RAGE and VEGF in retinal pigment epithelial cells. *Exp. Eye Res. 80*, 567-580.

Zhou, J., Jang, Y.P., Kim, S.R., Sparrow, J.R. (2006) Complement activation by photooxidation products of A2E, a lipofuscin constituent of the retinal pigment epithelium. *Proc Natl Acad Sci USA 103*, 16182-16187.